"A novel role for myelin-associated inhibitors in modulating microglial motility"

PhD Thesis

in partial fulfilment of the requirements
for the degree "Doctor of Philosophy (PhD)"
in the Molecular Biology Program
at the Georg August University Göttingen,
Faculty of Biology

submitted by

Foteini Orfaniotou

born in

Athens, Greece

2008

Declaration

I hereby declare that the PhD thesis entitled, **"A novel role for myelin-associated inhibitors in modulating microglial motility"**, has been written independently and with no other sources and aids than quoted. I would like to gratefully acknowledge Prof. U.-K. Hanisch and T. Regen (for the ELISA data) and PD. Dr. H. Steffens and Dr. F. Nadrigny (for the two-photon *in vivo* microscopy).

Foteini Orfaniotou

To my family

List of publications

<u>Orfaniotou F</u>, Nadrigny F, Regen T, Werner HB, Kassmann CM, Steffens H, Kelm S, Kirchhoff F, Hanisch UK, Griffiths IR, Nave KA. Myelin-associated glycoprotein modulates the roaming behaviour of microglial cells (in preparation)

<u>Orfaniotou F</u>, Tzamalis P, Thanassoulas A, Stefanidi E, Zees A, Boutou E, Vlassi M, Nounesis G, Vorgias CE. (2008) The stability of the archaeal HU histone-like DNA-binding protein from Thermoplasma volcanium. *Extremophiles* (in press)

Poulopoulou C, Davaki P, Sgouropoulos P, Tsaltas E, Nikolaou C, **<u>Orfanioutou F</u>**, Vassilopoulos D (2008) Reduced RAGE mRNA in mononuclear blood cells of patients with probable Alzheimer's disease. *Neurology*; 70(17)

Werner HB, Kuhlmann K, Shen S, Uecker M, Schardt A, Dimova K, **<u>Orfaniotou F</u>**, Dhaunchak A, Brinkmann BG, Möbius W, Guarente L, Casaccia-Bonnefil P, Jahn O, Nave KA (2007). Proteolipid protein is required for transport of sirtuin 2 into CNS myelin. *JNeurosci;* 27 (29)

Denikus N, **<u>Orfaniotou F</u>**, Wulf G, Lehmann PF, Monod M, Reichard U (2005). Fungal antigens expressed during invasive aspergillosis. *Infec Immun.;* 73 (8)

Acknowledgements

List of figures

Abbreviations

Bp	Base-pairs
cAMP	Cyclic adenosine monophosphate
CHO	Chinese hamster ovary
CNS	Central Nervous System
CSF	Cerebrospinal fluid
CST	Corticospinal tract
^{o}C	Degrees Celsius
DAB	3,3'-Diaminobenzidine
Dapi	4',6-Diamidino-2-phenylindole
dH_2O	Distilled water
ddH_2O	Double distilled water
dMAG	Degraded myelin-associated glycoprotein
DNase	Deoxyribonuclease
d.p.i	Day(s) post-immunization
EAE	Experimental allergic encephalomyelitis
EGFP	Enhanced green fluorescent protein
ELISA	Enzyme-linked immunosorbent assay
EYFP	Enhanced yellow fluorescent protein
FACS	Fluorescent activating cell sorting
FCS	Fetal calf serum
GDP	Guanosine diphosphate
GFAP	Glial fibrillary acidic protein
GPI	Glycosylphosphtidylinositol
GTP	Guanosine triphosphate
GFAP	Glial fibrillary acidic protein
GST	Glutahione-S-transferase
HRP	Horseradish peroxidase
Hrs	Hours
Ig	Immunoglobulin

kD	Kilodalton
k.o	Knock out
L	Liter
LPS	Lipopolysaccharide
M	Molar
M	Months
MAG	Myelin-associated glycoprotein
MBP	Myelin basic protein
Mg	Milligram
μg	Microgram
MHC II	Major histocompatibility complex II
Min	Minutes
μl	Microliter
mM	Millimolar
MMPs	Matrix metalloproteinases
mRNA	Messenger RNA
MS	Multiple sclerosis
NgR	Nogo-66 receptor
nM	Nanomolar
OMgp	Oligodendrocyte-myelin glycoprotein
PAGE	Polyacrylamide gel electrophoresis
PBS	Phosphate buffered saline
PCR	Polymerase chain reaction
PFA	Paraformaldehyde
PKC	Protein kinase C
PLL	Poly-L-lysine
PLP	Proteolipid protein
PNS	Peripheral Nervous System
RhoA	Ras homolog gene family, member A
RI	Ramification index
RNA	Ribonucleic acid
RNase	Ribonuclease
ROCK	Rho-associated coiled-coil containing protein kinase

rpm	Rotations per minute
RT-PCR	Quantitative real time PCR
S	Seconds
SDS	Sodium Dodecyl Sulphate
SEM	Standard error mean
Siglec	Sialic acid binding Ig-like lectins
TBS	Tris buffered saline
Temed	N, N, N', N'-Tetramethylethylene diamine
TLR	Toll-like receptors

1. Abstract

In the central nervous system of mammals, the regeneration of axons after injury is limited. The reduced ability of neurite outgrowth can be attributed, in part, to the presence of inhibitor proteins enriched in myelin. The three major axon growth-inhibitory molecules include Nogo, the myelin-associated glycoprotein (MAG) and the oligodendrocyte-myelin glycoprotein (OMgp).

Over the last three decades, a considerable amount of research has been devoted to investigating the signalling cascades involved in myelin-associated inhibition as well as the strategies to overcome this inhibition. Nevertheless, little is known about the physiological function of these inhibitors. In evolution, the myelin-associated inhibition of regenerating axons coincides with the refinement of the innate and adaptive immune system of higher vertebrates. We hypothesized that also the motile processes of microglia and astrocytes in the CNS white matter might be responsive to myelin inhibitors that are well positioned to provide a protective shield for the critical axon-glia junctions.

In this study, it was shown that microglia and astrocytes purified from post-natal mouse brains express the receptor NgR1 and its co-receptors known to bind the myelin-associated inhibitors. Furthermore, MAG, when presented by heterologous cells, led to microglial and astrocytic process outgrowth inhibition, while microglial processes also avoided recombinant MAG in stripe assays. The repelling effect of MAG was observed in the absence of the MAG Ig domains 4/5, was partially reversed in microglial cells lacking NgR1, and was fully reversed in the presence of the Rho-associated kinase inhibitor Y27632. By using *in vivo* two-photon confocal microscopy to image the spinal cord of anaesthetized mice, the motility and roaming behaviour of fluorescently labelled microglia at the paranodes and their processes was modulated by the presence of MAG. In the Plp1 null mouse, a model of Wallerian degeneration, the absence of MAG led to the formation of foamy microglial cells, indicating abnormal myelin phagocytosis. In two models of neuroinflammation (the experimental allergic encephalomyelitis and the response of lipopolysaccharide injection), the absence of MAG resulted in altered microglial behaviour. Surprisingly, soluble MAG, which is physiologically associated with myelin breakdown, induces a strong inflammatory microglial response in culture. These findings support a model in which MAG protects intact paranodal junctions from perturbation by motile glial processes, and directly or indirectly modulates the microglial response under pathological conditions.

2. Introduction

2.1 Myelination

Rapid nerve conduction is important for the function of the nervous system. The increase in the body size of vertebrates, along with the increasing complexity of their nervous system required an adaptation that would facilitate the fast action potential propagation. The evolutionary acquisition of myelin in vertebrates, along with the confinement of voltage-dependent sodium channels to the small gap — the node of Ranvier - allowed the fast "saltatory" conduction of action potentials (Hartline and Colman, 2007). Myelin is a highly specialized, compacted, multi-layered plasma membrane that enwraps axons with little or no cytoplasm between adjacent wraps. The cells that produce myelin with their cellular processes are Schwann cells in the peripheral nervous system (PNS) and oligodendrocytes in the central nervous system (CNS) (Arroyo and Scherer, 2000) (Fig.1).
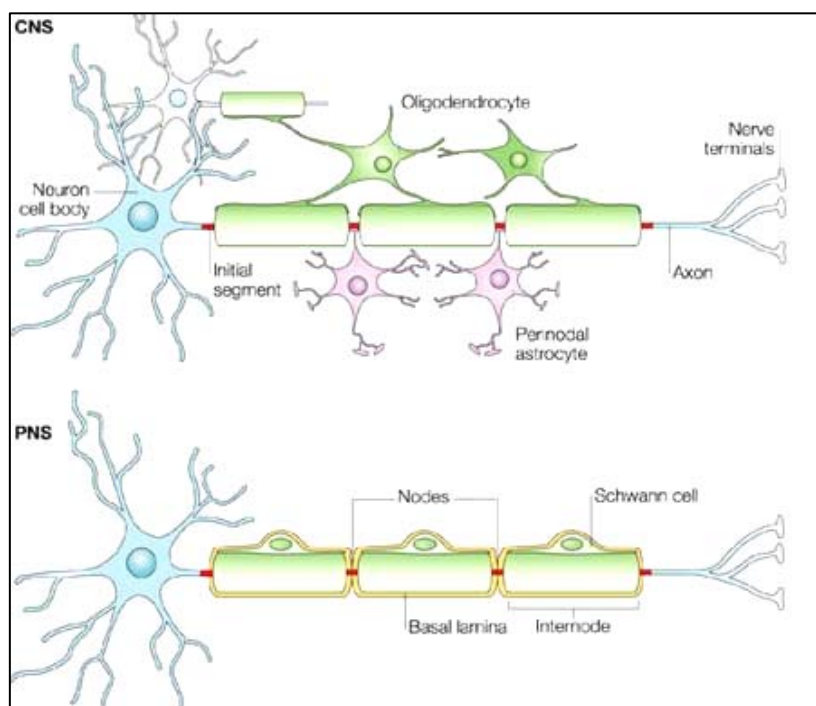
Figure 1. Myelination in the central and peripheral nervous system
Oligodendrocytes in the central nervous system (CNS) and Schwann cells in the peripheral nervous system (PNS) form the myelin sheath that enwraps the axons. Between the multi-layered myelin sheaths, there are gaps, the nodes of Ranvier. Oligodendrocytes myelinate more than one axon, while Schwann cells are in a 1:1 ratio with the axons. Note the presence of astrocytic processes around the nodes in the CNS (adapted from Poliak and Peles, 2003).

The myelin composition is particularly unique; in contrast to other plasma membranes, myelin is a lipid-enriched membrane composed of 70% lipids and 30% proteins (Morell and Ousley, 1994). The major proteins in CNS myelin are the myelin basic protein MBP and the proteolipid protein PLP/DM20 (Krämer et al., 2001). The distribution of the myelin proteins is not uniform, but specialized in distinct domains. The nodes are flanked on either side by the paranodal domains where myelin loops form septate-like junctions with the adjacent axonal membrane. Next to the paranodes are the juxtaparanodal domains residing underneath the compact myelin and finally the internodes extending beneath the compact myelin. These domains have a distinct protein composition that serves their function (Poliak and Peles, 2003) (Fig.2). The myelin sheath itself can also be divided into categories, the internodal compact and the non-compact one with the compact myelin being the dominant type (Scherer and Arroyo, 2002).
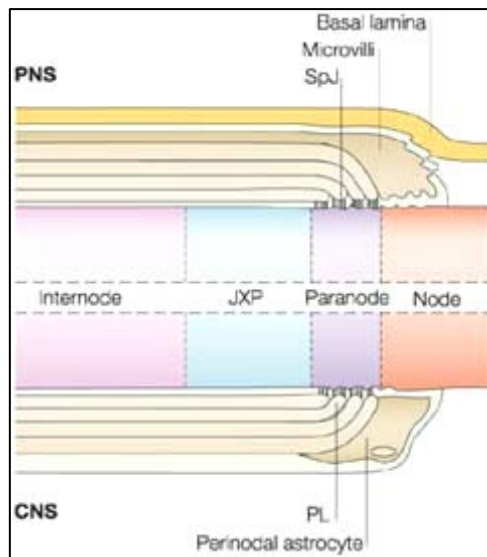
Figure 2. Myelin compartments
Schematic representation of a longitudinal section of a myelinated axon around the node of Ranvier. The node, the paranode, the juxta-paranode and the internode are depicted. In the PNS (upper half), the Schwann cell microvilli contact the node, whereas in the CNS (lower half), perinodal astrocytic processes are in close proximity to the node. Septate-like junctions (SpJ) are formed between the paranodal loops (PL) and the axon. The juxtaparanode lies underneath the compact myelin and next to the paranode (adapted from Poliak and Peles, 2003).

Myelin is not only essential for the fast conduction of the action potential but also for the maintenance of axonal integrity, protection, survival and function (Griffiths et al., 1998; Lappe-Siefke et al., 2003; Yin et al., 2006). Several mouse lines deficient in oligodendroglial proteins show normal myelination, but secondarily develop axonal loss, highlighting the importance of myelinating glia in the maintenance of axons (Nave and Trapp, 2008).

2.2 Myelin-associated inhibition of axonal outgrowth

Although myelin evolved as an advantage for the vertebrates, in higher vertebrates its presence in the injured central nervous system constitutes one of the major impediments for axonal regeneration along with the glial scar and the invading immune cells from the periphery (Zurn and Bandtlow, 2006). Cajal was among the first to observe that the capability of axonal regeneration in the CNS is restricted (Ramon y Cajal, 1928).

"Once development was ended, the founts of growth and regeneration of the axons and dendrites dried up irrevocably. In adult centers, the nerve paths are something fixed, ended, immutable. Everything may die. Nothing may be regenerated."

It took almost 60 years to prove that it is the CNS environment and not axon-intrinsic factors that is the source of axonal outgrowth inhibition (David and Aguayo, 1981; Schwab and Thoenen, 1985). It was hypothesized that breakdown products of myelin are responsible for the inhibition (Berry, 1982). Eventually, specific myelin proteins were described to be inhibitory for neurite outgrowth *in vitro* (Caroni and Schwab, 1988a). The proof that these proteins are inhibitory *in vivo* came when Schwab and colleagues showed that an antibody, i.e. IN-1, raised against CNS myelin fractions that contain the 35kD and 250kD inhibitory proteins, could neutralize the non-permissiveness of CNS myelin and promote axonal outgrowth *in vivo* (Schnell and Schwab, 1990). From this early stage onwards, a lot of research was conducted to identify the proteins that make myelin inhibitory for axonal outgrowth and the underlying mechanisms. The major myelin-associated inhibitors include Nogo, the myelin-associated glycoprotein (MAG) and the oligodendrocyte-myelin glycoprotein (OMgp) (Xie and Zheng, 2008).

2.3 Myelin-derived inhibitors

2.3.1 Nogo

Historically, the first myelin protein fraction identified as having an inhibitory role, termed NI-35/250, was discovered 20 years ago (Caroni and Schwab, 1988). However, it would be another 10 years before the cDNA encoding NI-250 could be identified and named Nogo-A (Chen et al., 2000; GrandPre et al., 2000; Prinjiha et al., 2000). There are three Nogo splice isoforms, i.e. Nogo-A, -B and –C, which share the same C-terminal

region, while Nogo-A has a unique N-terminal domain. These proteins belong to the Reticulon protein family based on sequence homology. They have an ER-retention motif and are mainly associated with the endoplasmic reticulum. The expression of Nogo-A (200 kDa) is mainly restricted to oligodendrocytes in adulthood, while there is also a neuronal expression during development. Nogo-B (55 kDa) is expressed in various tissues, while Nogo-C (25 kDa) is mainly expressed in muscle (Huber et al., 2002; Wang et al., 2002). All three isoforms contain two hydrophobic domains with the loop in between termed Nogo-66, which has axon outgrowth-inhibitory properties (Grandpre et al, 2000; Prinjha et al., 2000) (Fig.3). The amino-terminal domain of Nogo-A is also inhibitory for axonal outgrowth but does not involve the Nogo-66 receptor (Fournier et al., 2001; Oertle et al., 2003). The topology of the amino terminal of Nogo-A has been controversial. There have been two main proposals: one supporting the intracellular localization of the amino-terminal domain and the other an extracellular localization. We now know, however, that both orientations at least occur in cultured oligodendrocytes (Oertle et al., 2003).
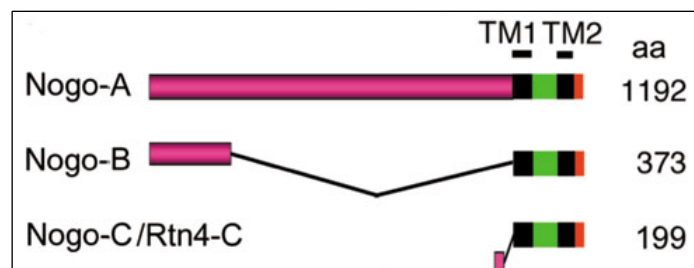
Figure 3. Schematic representation of Nogo-A, -B and –C

All three isoforms share a common C-terminal domain that contains the two hydrophobic transmembrane domains (black), which are separated by a 66-amino acid-loop (green). These 66-amino acids are responsible for the neurite outgrowth inhibition. All Nogo isoforms also share also a common ER retention motif (orange). Nogo-A has an additional long N-terminal domain, which independently can also inhibit the outgrowth of neurites (amino-Nogo) (adapted from Grandpre et al., 2000).

Since the discovery of Nogo and its inhibitory properties, a number of studies have revealed that Nogo-deficient myelin has reduced inhibitory properties *in vitro* (Kim et al., 2003; Simonen et al., 2003; Zheng et al., 2003). However, the findings of the *in vivo* spinal cord injury studies of these mutants were less consistent and inconclusive. One group showed significant corticospinal tract (CST) fiber regeneration in the Nogo A/B deficient mice after spinal cord injury (Kim et al., 2003), while a second group showed a

tendency towards the regeneration of corticospinal axons with considerable variability between the mice analyzed (Simonen et al., 2003). However, a third group did not observe any enhanced CST axon sprouting or regeneration in neither the Nogo A/B nor the Nogo A/B/C mutant mice (Zheng et al., 2003). These differences between the results gained by the three groups failed to provide sufficient evidence of the predominant importance of Nogo in axonal regeneration, and the differences were mainly attributed to the different genetic backgrounds of the mice used in the different studies, the surgical techniques, the axonal tracing methods and the presence of additional inhibitors. Nevertheless, a number of studies using neutralizing agents, such as the IN-1 antibody and the NEP1-40 peptide, revealed recovery after spinal cord injury (GrandPre et al., 2002; Li and Strittmatter, 2003; Liebscher et al., 2005). This discrepancy between the Nogo neutralizing agents and the knockout mice could be attributed to the general effect of the agents on more than one inhibitor and the time limitations for the emergence of compensatory mechanisms.

2.3.2 Myelin-associated glycoprotein (MAG)

MAG, also known as Siglec-4, was isolated as a CNS myelin constituent earlier than Nogo (Quarles et al., 1972; Arquint et al., 1987). It is expressed both by CNS and PNS-myelinating glia with an approximately 10-fold higher abundance in CNS myelin and is localized in periaxonal regions (Quarles, 2007). MAG belongs to the superfamily of proteins with an Immunoglobulin-like domain and, more specifically, the siglec subgroup; it is a single transmembrane domain protein with a large extracellular fragment that contains five immunoglobulin-like domains and binds to sialic acid-containing oligosaccharides. This domain consists of eight glycosylation sites that are mostly complex and negatively charged because of sialic acid (Georgiou et al., 2004). There are two MAG splice isoforms, the short (S-MAG) and the long (L-MAG), which differ in their cytoplasmic domain (Tropak et al., 1988). The longer cytoplasmic domain of L-MAG has been associated with intracellular signalling in the oligodendrocytes via the action of Fyn tyrosine kinase and phospholipase Cγ (PLCγ) (Jaramillo et al., 1994; Umemori et al., 1994) (Fig.4).

Despite the availability of knockout mice (Li et al., 1994; Montag et al., 1994), the physiological role of MAG is still under debate. The localization of MAG in the

periaxonal membrane led to the suggestion that MAG is implicated in axon-glial communication. In the absence of MAG, the mice exhibited subtle structural abnormalities in the periaxonal region, and the formation of compact CNS myelin was normal but slightly delayed (Montag et al., 1994). The phenotype was more severe in the PNS, where axonopathy proceeded with age (Yin et al., 1998). Overall, despite the subtle phenotype of the MAG-deficient mice possibly due to compensatory mechanisms, MAG was suggested to participate in a signalling system that is necessary for the maintenance and survival of some axons (Quarles, 2007). Further investigations are needed to fully understand the relative physiological importance of MAG, while a number of studies have focused on the axonal outgrowth inhibition properties of MAG in the CNS.
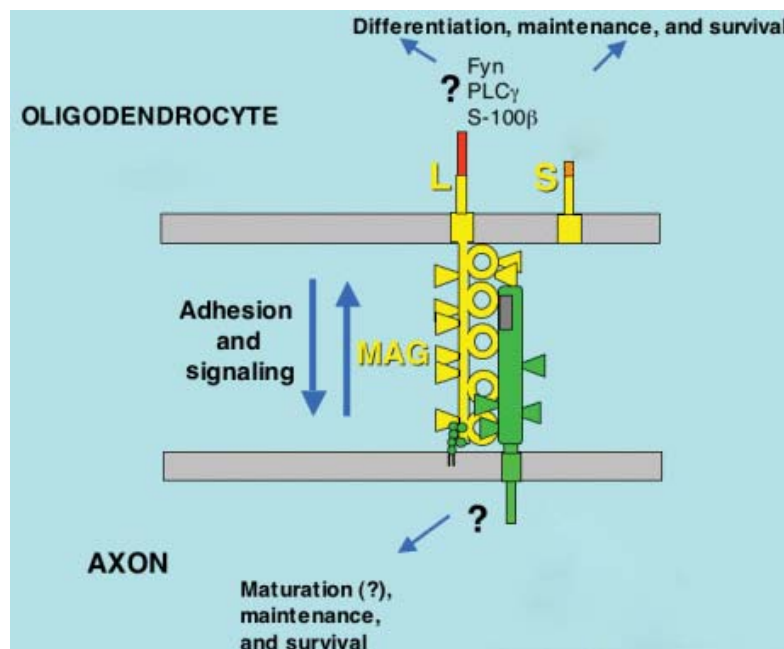
Figure 4. Structure of MAG

MAG (yellow) has five extracellular immunoglobulin-like domains (circles), eight N-linked oligosaccharides (triangles), a single transmembrane domain and two alternative cytoplasmic domains (red for L-MAG and orange for S-MAG). MAG has been suggested to be involved in bidirectional signaling between oligodendrocytes and neurons, though little is known about the pathways involved. The extracellular domain may bind to neuronal gangliosides (green circular structures) or receptors, such as NgR1 and others (adapted from Quarles, 2007).

The ability of MAG to inhibit axonal outgrowth is attributed to its extracellular domain and was discovered using myelin fractionation assays different than those used for Nogo (McKerracher et al., 1994; Mukhopadhyay et al., 1994). Dependent on the developmental stage of the neurons, MAG can be a permissive (embryonic and neonatal) or inhibitory

(adulthood) substrate for axonal outgrowth. It exerts its inhibitory activity by binding to the Nogo-66 receptor (NgR1) (Domeniconi et al., 2002; Liu et al., 2002). Interestingly, it was shown that it additionally binds to Nogo receptor 2 (NgR2) and with a higher affinity than to NgR1 (Venkatesh et al., 2005). MAG, as a siglec protein, binds also to neuronal gangliosides and especially to GD1a and GT1b (Yang et al., 1996). Most of the research regarding the MAG receptor has concentrated on the NgRs, and the involvement of gangliosides in inhibition had been controversial (Vinson et al., 2001; Vyas et al., 2002). However, a recent study revealed that different neuronal cell types could be inhibited by MAG via gangliosides and/or NgRs (Mehta et al., 2007). Although the MAG Ig domain 1 is important for the sialic acid binding, this is not the domain that elucidates the inhibitory activity (Tang et al., 1997a,b), since the neurite outgrowth inhibitory domain was recently mapped to the Ig domain 5 (Cao et al., 2007). Interestingly, a proteolytic derivative of MAG consisting of its extracellular domain, namely dMAG, was detected in purified myelin (Sato et al., 1982; Stebbins et al., 1997) and the CSF of control and patients with neurological diseases (Yanagisawa et al., 1985). Interestingly, this MAG derivative has been shown to maintain its neurite outgrowth inhibitory properties *in vitro* (Tang et al., 1997a; 2001).

2.3.3 Oligodendrocyte-Myelin glycoprotein (OMgp)

OMgp is a glycosylphosphotidylinositol (GPI)-anchored protein that contains five leucine-rich repeat (LRR) domains. However, OMgp is not only expressed in oligodendrocytes but also in neurons (Habib et al., 1998). Later on, it was shown that OMgp also inhibits neurite outgrowth and binds to the same receptor as MAG and Nogo, the Nogo-66 receptor (Wang et al., 2002). Although it was previously believed to be present in compact myelin, it was more recently shown that it is localized in the membrane surrounding the nodes of Ranvier (Huang et al., 2005). Interestingly, OMgp-deficient mice exhibited elevated axonal sprouting both in grey and white matter, suggesting a general role of OMgp in restricting axonal sprouting (Huang et al., 2005). Using an *in vivo* model of spinal cord injury, there was improved regeneration in OMgp-deficient mice and less neurite outgrowth inhibition when myelin from OMgp-deficient mice was used as a neuronal substrate *in vitro* (Ji et al., 2008).

2.3.4 Receptors for myelin inhibitors and downstream signalling

All three main myelin-associated inhibitors, Nogo-A, MAG and OMgp, bind to the same Nogo-66 receptor (NgR1) despite the lack of sequence similarity (Fournier et al., 2001; Domeniconi et al., 2002; Liu et al., 2002; Wang et al., 2002).
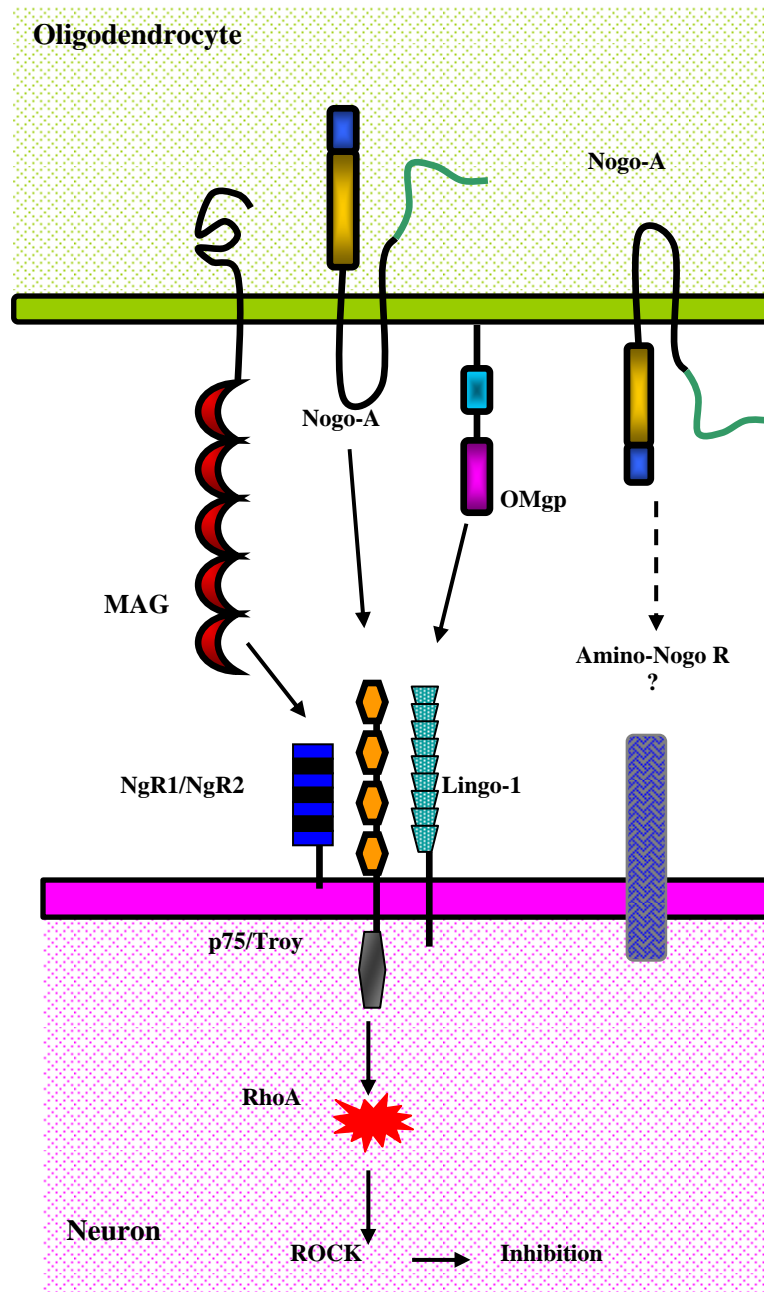
Figure 5. Schematic representation of the myelin-associated inhibitors in the CNS

MAG, Nogo-A and OMgp are the three major inhibitors associated with the CNS myelin. They all bind to the same GPI-anchored NgR1 receptor, which recruits the co-receptors p75 neurotrophin receptor or Troy and additionally Lingo-1, to form a receptor complex that transduces the inhibitory signals downstream in neurons. MAG also binds to NgR2, the co-receptors of which have not been identified. In neurons, the NgR1 receptor complex leads to RhoA activation and the involvement of the Rho-associated kinase

(ROCK), which will lead to further cytoskeletal rearrangements and neurite outgrowth inhibition. Nogo-A has two inhibitory domains: the Nogo-66 loop that binds to NgR1 and the amino-Nogo domain, which binds to an as yet unidentified receptor.

NgR1 is a GPI-anchored protein, so it does not transduce the signal downstream unless it interacts with a transmembrane protein. Indeed, NgR1 recruits the p75 neurotrophin receptor (Wang et al., 2002; Wong et al., 2002) or alternatively Troy/Taj (Park et al., 2005; Shao et al., 2005) and Lingo-1 (Mi et al., 2004) (Fig.5). More recently, the epidermal growth factor receptor (EGFR) has also been linked to the NgR1-ligand signalling but without any direct association with the NgR or the myelin-associated inhibitors (Koprivica et al., 2005).

The intracellular pathway further involves RhoA, a small GTPase that alternates between a GDP-bound inactive form and a GTP-bound active form. This leads to Rho-associated kinase (ROCK) activation, further cytoskeletal rearrangements and finally neurite outgrowth inhibition (Liu et al., 2006) (Fig.5). The involvement of RhoA in myelin-mediated inhibition was known before the discovery of the NgRs. It was shown that blocking Rho activation could eliminate the myelin-elicited inhibition *in vitro* (Lehmann et al., 1999) and *in vivo* (Dergham et al., 2002; Fournier et al., 2003). Another intracellular molecule involved is the protein kinase C (PKC) (Sivasankaran et al., 2004). Interestingly, elevated cyclic adenosine monophosphate (cAMP) was shown to overcome myelin-elicited inhibition and promote regeneration *in vitro* (Song et al., 1998; Cai et al., 1999) and *in vivo* (Qiu et al., 2002).

Although NgR1 was the first receptor discovered to bind the myelin-associated inhibitors, two homologues were identified later, the NgR2 and the NgR3 (Lauren et al., 2003; Pignot et al., 2003). Additionally, it was shown that MAG binds to NgR1 and NgR2, but not NgR3 (Venkatesh et al., 2005). However, the involvement of NgR1 in the myelin-associated inhibition is dependent on the form in which these inhibitors are presented. For example, the acute exposure of MAG leads to NgR1-dependent neurite outgrowth inhibition, while chronic exposure is NgR1-independent (Chivatakarn et al., 2007).

The importance of the NgR1 in the myelin-associated inhibition was assessed *in vitro* by blocking the ligand-receptor interaction with an anti-NgR1 antibody or truncated NgR1

protein and there was an increased neurite outgrowth in the presence of the myelin-associated inhibitors (Li et al., 2004b; Fournier et al., 2002). To investigate the significance of NgR1 *in vivo*, different approaches were followed. On the one hand, the presence of NgR1 ectodomain acted as antagonist to the myelin inhibitory ligands and resulted in enhanced CST regeneration in rats and mice (Li et al., 2004a; 2005), while in an optic nerve crush model the effect was not the same (Fischer et al., 2004). The second line of research included the generation of NgR1-deficient mice (Kim et al., 2004; Zheng et al., 2005). The *in vitro* results of the two groups were contradictory regarding the improvement of neurite outgrowth from NgR1-deficient mice on myelin substrates. Additionally, both groups failed to show enhanced CST regeneration in a spinal cord injury model *in vivo*. Various reasons could account for the discrepancy between the two groups regarding the *in vitro* results, such as the different myelin preparation protocols or the ways it is presented as a substrate or the type of neurons tested (Mehta et al., 2007). Regarding the differences in regeneration for the antagonist approach and the genetic manipulation of the ligand-receptor interaction, it can be that compensatory mechanisms have the time to counteract during development, which is not the case when a substance is applied acutely. However, one important point is that other receptors, such as NgR2 and PirB, might as well be involved in the myelin-associated inhibition (Venkatesh et al., 2005; Mehta et al., 2007; Atwal et al., 2008). Nevertheless, at this point we may conclude that NgR1 is at least partially involved in the myelin inhibition of axonal outgrowth.

2.3.5 Is there a physiological function of the myelin-associated inhibitors?

The emergence of the myelin-associated inhibition of axonal outgrowth remains functionally unexplained, as poor regeneration offers no obvious evolutionary advantage. It has been hypothesized that the CNS, when expressing myelin-associated inhibitors in white matter tracts, may be protected from the effects of abnormal axonal sprouting (Raisman, 2004; Huang et al., 2005; Quarles, 2008). However, the mammalian peripheral nervous system, which regenerates, would not function well if abnormal sprouting was a persistent feature either. I am also unaware as to whether the abnormal sprouting of CNS axons is a tolerated feature of lower vertebrates in which the CNS axons can regenerate. Instead, it was noted that the occurrence of reduced regeneration in higher vertebrates coincides with the refinement of the innate and adaptive immune system (Popovich and Longbrake, 2008). We thus hypothesized that a myelin-mediated "inhibition" may target

the resident glial cells of the CNS, such as the microglia and the astrocytes. The word "glia" originates from the Greek word meaning glue, so these cell types were regarded as the glue that holds the CNS together.

2.4 Microglia

Microglial cells are the resident immune cells of the central nervous system (Kreutzberg, 1996). Microglial research has been conducted for over 50 years and several review articles summarize the current knowledge regarding their function in the healthy CNS and under pathology (Perry and Gordon, 1988; Streit, 2001; 2002; van Rossum and Hanisch, 2004; Schwartz et al., 2006; Hanisch and Kettenmann, 2007). Here, I will only highlight the cell characteristics of microglia that are more relevant to the hypothesis of this work.

Although the microglial origin has long been debated, it is currently believed that mesodermal glial cells invade the CNS parenchyma during embryonic development followed by the second entrance of bone marrow-derived monocytes during the postnatal period (Rock et al., 2004; Chan et al., 2007). Traditionally microglia were classified into two groups based on their morphology and status; the "resting" and the "activated" microglia (Fig.6A). The "resting" microglia have a ramified morphology with many and thin processes extending from the cell soma, while the "activated" ones have a round, amoeboid morphology and properties that make them acquire a phagocytic function, which in turn renders them indistinguishable from macrophages. The amoeboid phase is evident in early development during plasticity, while later on in adulthood microglia are in "resting" mode. Under any kind of pathology, the microglia react and become "activated", not only by changing their morphology but also biochemically and metabolically so that they can cope with the homeostatic changes (van Rossum and Hanisch, 2004). However, a number of recent studies resulted in new terms, "resting" microglia are referred to as "surveying" and, upon receiving activation signals, microglia may acquire a diverse response phenotype and be termed "effector" microglia (Hanisch and Kettenmann, 2007) (Fig.6B).
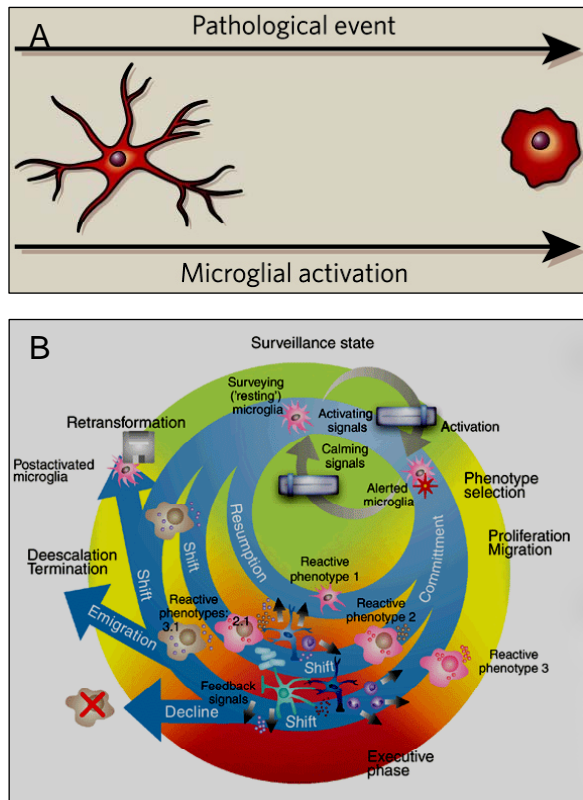
Figure 6. Microglial morphology

Microglia are ramified in the "resting" state and, upon receiving pathological signals, they become "activated". This change coincides with a change in their morphology; microglia become amoeboid. A number of recent studies have changed the simplistic view of microglia between the two main stages (A) into a more complex scheme (B). In the latter case, cells have distinct reactive phenotypes constituted by transcriptional and non-transcriptional changes. The reactive behaviour may change as the activating signals fade. The outcome can vary from cell death to retransformation to the "resting" phenotype (adapted from Kettenmann, 2007; Hanisch and Kettenmann, 2007).

The distinction of the microglial morphologies and the activating signals is more complicated. The microglial morphology and density varies in the different regions of the CNS; in the grey matter, microglial cells have a more stellate morphology while in white-matter areas their processes are arranged more linearly. The number and nature of the molecules and conditions that can trigger the microglial activation is also variable. These signals could be termed as "on" and "off", but in both cases this would lead to the microglial transformation in order to protect the CNS tissue (van Rossum and Hanisch, 2004). The appearance of factors that are not usually present (such as microbial structures, viral proteins, serum components) or changes in their concentration (intracellular components) or in their presentation format (soluble factors, aggregates), signal the emergence of "danger" or damage. That would be the "on" signal for the microglial activation. On the other hand, there is a constitutive calming ("off") system, such as the CD200-CD200R and CX3CR1-CX3CL1 pairs or the neurotransmitter release, the disruption of which would signal and lead to microglial activation (Hoek et al., 2000; Cardona et al., 2006; Pocock and Kettenmann, 2007). Upon activation, as their origin dictates, microglia express a variety of molecules, such as the major histocompatibility complex II (MHC II), complement receptors, multiple receptors for cyto- and

chemokines and others. Furthermore, microglial activation is crucial for the involvement of the adaptive immune system, as microglia are the key components for the recruitment of neutrophils, leukocytes and macrophages (Aloisi, 2001). Nevertheless, microglial activation is a double-edged sword, as it is generally beneficial and acts in a protective way, but chronic microglial activation leads to neuronal damage and accounts for the injury observed in certain neurodegenerative diseases, such as Parkinson's disease and multiple sclerosis (MS) (Gao and Hong, 2008; Lassmann, 2008).

The "resting" microglia were previously regarded as dormant cells. However, recent *in vivo* two-photon microscopy of transgenic mice expressing the enhanced green fluorescent protein (EGFP) under the CX3CR1 promoter revealed that microglia have highly motile processes that roam the intercellular space, extending and retracting in a highly dynamic way (Nimmerjahn et al., 2005; Davalos et al., 2005; 2008). Their somata remain stationary, while their processes constantly retract and rebuild, enabling the microglial surveillance of the brain parenchyma without perturbing the already glial-neuronal structures. Upon activation, such as after a laser-induced lesion, the microglial process outgrowth targets the lesion site. One of the substances that seemed to "guide" the microglial process outgrowth was the release of adenosine triphosphate (ATP) at the site of the local injury (Davalos et al., 2005; Raivich, 2005). Nonetheless, little is known about what controls and restricts this microglial activity in the healthy CNS. If, as discussed above, the myelin-associated inhibitors/NgR signalling pathway plays a role in restricting neurite process outgrowth in a pathological situation post-developmentally, it is equally feasible that it plays a similar role in restricting microglial process outgrowth. Strikingly, the expression of NgR and some of the co-receptors is not restricted to neuronal cells, but is also present in microglial cells (Satoh et al., 2005, 2007).

2.5 Astrocytes

Astrocytes were first described by Camillio Golgi in 1871 as a novel cell type in the CNS characterized by long, numerous, star-like processes. Astrocytes originate from neuroepithelial cells that form the ventricular zone; these proliferate and give rise to astrocytes, neurons and oligodendrocytes (Horner and Palmer, 2003). The abundance of astrocytes in the mammalian CNS is high, reaching approximately 90% of the cells in the

human brain (He and Sun, 2007). In the course of vertebrate evolution, there is evidence of a relative expansion of astrocytes in comparison to neurons, implying an evolutionary advantage of animals with a greater number of astrocytes (Needergard et al., 2003).

One of the markers commonly used to stain astrocytes is the intermediate filament glial fibrillary acidic protein (GFAP). The function of this protein remains unknown, while GFAP-deficient mice display abnormal white matter architecture and the blood-brain barrier integrity is disturbed (Liedtke et al., 1996). Astrocytes in mammals can be distinguished into two types: the fibrous and the protoplasmic. Fibrous astrocytes contain many filaments, have long and thin processes, and are mainly localized in the white matter. Protoplasmic astrocytes, on the other hand, are found in the grey matter, have shorter and thicker processes and are mainly associated with synapses. Despite the evident morphological and structural differences between protoplasmic and fibrous astrocytes, both types of cells share similar functions.

Astrocytic processes contact the blood capillaries with the "end-feet", playing a nutritional role in the CNS. Another major astrocytic function is the support of neuronal function by maintaining local ion concentrations, storing CNS glycogen, clearing neuronal waste and mediating in the uptake of neurotransmitters (Nair et al., 2008). Moreover, astrocytes support neurons by supplying neurotrophic factors (Dreyfus et al., 1999). However, another interesting role of astrocytes is their involvement in the CNS immune responses. Although their origin is not linked to the hematopoietic cells, they exhibit immune functions. They express toll-like receptors (TLRs), act as antigen-presenting cells (APCs) and produce a variety of cytokines and chemokines. Astrocytes are also important for the signalling to the periphery as they secrete chemokines and cytokines and their end-feet contact the blood vessels (Dong and Benveniste, 2001).

Upon activation, astrocytes up-regulate their expression of GFAP in a process termed "astrogliosis", a term that has commonly been used as a marker for pathology in CNS diseases. The role of astrocytes in pathology can be dual. In MS, astrocytes are responsible for the breakdown of the blood-brain barrier (BBB), the recruitment of T cells, along with the axonal damage and the oligodendrocytic death through the secretion of cytokines. On the other hand, astrocytes promote remyelination by helping to clear debris, secreting chemo-attractants for OPCs and supporting the OPC survival,

proliferation and maturation (Williams et al., 2007). Astrocytes also have a beneficial and a detrimental role in the CNS after injury. They form a glial scar, which is thought to protect the fragile brain tissue from further destruction (Myer et al., 2006). On the other hand, the formation of a mechanically obstructive glial scar composed of astrocytes and connective tissue elements is partially responsible for the failure of neuronal regeneration within the CNS after injury (Fitch and Silver, 2008).

Taken together, these studies suggest that the astrocytic morphology reflects and supports the astrocytic function or reaction in the healthy CNS and in pathology. Strikingly, astrocytes express the NgR and some of the co-receptors known to bind the myelin-associated inhibitors in neurons (Satoh et al., 2005; 2007) and, in addition, their morphology and migration is regulated by the small GTPase Rho (Holtje et al., 2005). Therefore, we wanted to assess the possible role of the myelin-associated inhibitors in regulating the astrocytic behaviour.

2.5 Aim of the study

While the ability of myelin-associated inhibitors, including Nogo, MAG and OMgp, to cause neuronal growth cone collapse has been studied in detail, the physiological role of these myelin inhibitors has remained obscure. We hypothesized that the highly motile cellular processes of microglia and astrocytes might also be responsive to myelin inhibitors. These proteins are ideally localized to provide a protective shield around myelin and the critical axon-myelin junctions in CNS white matter tracts. The aim of this thesis was to assess the response of microglia and astrocytes to myelin-associated inhibitors *in vitro* and *in vivo*, focusing on MAG, a well known myelin protein, and the nogo-66 receptor as its binding partner, because for both proteins mutant mice are available as experimental tools.

3. Materials and Methods

3.1 Materials

3.1.1 Kits, chemicals and protocol source

All chemicals used were purchased from the Sigma-Aldrich and Merck unless stated otherwise. All molecular biology kits were purchased from Qiagen, Promega and Sigma-Aldrich, while cell culture and general laboratory material were purchased from Falcon, Nunc and Eppendorf.

Websites for online protocols:

http://mrw.interscience.wiley.com/emrw/9780471142720/home/ (Molecular biology)

http://mrw.interscience.wiley.com/emrw/9780471140863/home/ (Protein Science)

http://mrw.interscience.wiley.com/emrw/9780471142300/home/ (Neuroscience)

3.1.2 Molecular biology buffers

DNA-sample buffer (6x)

20 % (w/v) Glycerol in TAE buffer

0.025 % (w/v) Orange G or bromophenol blue

dNTP-stock solutions (100 mM)

25 mM each dATP, dCTP, dGTP, dTTP (Boehringer, Mannheim)

Ethidiumbromide

1-1.5 µg/ml for agarose gels in 1x TAE

TAE (50x, 1000ml)

2 M Tris-Acetate, pH 8.0

50 mM EDTA

57.1 ml Glacial acetic acid

Add dH_2O up to 1000ml

TE (1x)

10 mM Tris-HCl, pH 8.0

1 mM EDTA

Modified Gitschier buffer (MGB, 10x)

6.7 ml 1 M Tris-HCl (pH 8.8)

1.66 ml 1 M $(NH4)_2SO_4$

650 μl 1 M $MgCl_2$

Add dH_2O up to 10ml

MGB buffer (1x, working solution)

1 ml 10x MGB

100 μl β-Mercaptoethanol

500 μl 10 % Triton X-100

8.4 ml dH_2O

3.1.3 Protein biochemistry buffers

3.1.3.1 Lysis buffers

Lysis buffer I (for brain)

50 mM Tris-HCl, pH 7.5

150 mM NaCl

1 mM EDTA

1 % Triton X-100

1 mM PMSF (add before use)

1 tablet Complete Mini protease inhibitor (Roche)/ 10 ml of lysis buffer

* protease inhibitors are added freshly to the lysis buffer before use

Lysis buffer II (for microglia)

50 mM Tris-HCl, pH 7.5

150 mM NaCl

1 mM EDTA

1 % Triton X-100

1 % Nonidet P40

0.1 % SDS

1 tablet Complete Mini protease inhibitor (Roche)/ 10 ml of lysis buffer

* protease inhibitors are added freshly to the lysis buffer before use

3.1.3.2 Protein purification buffers

Wash buffer I (WB I)

10 mM Tris, pH 7.5

150 mM NaCl

0.05 % Tween-20

10 mM EDTA

Adjust pH to 7.5

Wash buffer II (WB II)

50 mM Tris, pH 7.5

Elution buffer I (EB I)

0.1 M Glycine, pH 3.0

Elution buffer II (EB II)

0.1 M Glycine, pH 2.5

Neutralization buffer (NB)

1 M Tris, pH 8.0

3.1.4 SDS PAGE and Western Blotting

Separating SDS gel (12 %, 4 gels, 1.5 mm thickness)

13 ml dH$_2$O

15 ml 30 % Acrylamide (BioRad, 29.1)

9.4 ml 1.5 M Tris-HCl (pH 8.8)

370 μl 10 % SDS

125 μl 10 % APS (Ammonium persulfate)

30 μl TEMED (BioRad)

Stacking SDS gel (4 gels)

6.1 ml dH$_2$O

1.3 ml 30 % Acrylamide (BioRad, 29.1)

2.5 ml 0.5 M Tris-HCl (pH 6.8)

100 μl 10 % SDS

50 μl 10 % APS (Ammonium persulfate)

10 μl TEMED

SDS running buffer (Laemmli buffer, 1x)

25 mM Tris-HCl

192 mM Glycine

1 % (w/v) SDS

SDS sample buffer (6x)

7 ml 0.5M Tris-HCl buffer (pH 6.8)

3 ml Glycerol (30 % final concentration)

1 g SDS

1.2 ml 1 % Bromophenol blue

0.2 - 2 % β-Mercaptoethanol (add fresh)

Transfer buffer (1x)

48 mM Tris base

39 mM Glycine

10-20 % Methanol

Blocking Buffer

5 % non-fat dry milk powder in TBS or PBS (1x)

Western blot stripping buffer

0.2 M Glycine-HCl, pH 2.5

0.1 % Tween-20

Coomassie blue (Staining solution)

2 g Coomassie brilliant blue (R-250)

1 l Methanol

200 ml Acetic acid

800 ml dH$_2$O

Stir overnight and filter through Whatmann paper.

Destaining solution

50 ml Methanol

10 ml Acetic acid

40 ml dH$_2$O

Tris buffered saline (TBS, 20x)

1 M Tris base

3 M NaCl

Adjust pH 7.4 (with HCl)

TBS with Tween-20 (TBST, 1x)

50 mM Tris-HCl (pH 7.4-7.6)

150 mM NaCl

0.05 % - 0.15 % Tween-20

3.1.5 DNA and Protein markers

GeneRuler 1 kb DNA ladder (Fermentas)

GeneRuler 100 bp DNA ladder (Fermentas)

Precision Plus prestained protein standard (BioRad)

3.1.6 Immunocytochemistry buffers

Phosphate buffered saline (PBS) (1x cell culture, 1000 ml)

136 mM NaCl

2.6 mM KCl

10 mM Na$_2$HPO$_4$ x2 H$_2$O

1.4 mM KH$_2$PO$_4$

Set pH to 7.2 with 10 N NaOH

Add dH$_2$O up to 1000 ml

4 % Paraformaldehyde in PBS/TBS

100 ml 0.2 M NaH$_2$PO$_4$ (Sodiumdihydrogenphosphate)

400 ml 0.2 M Na$_2$HPO$_4$ (di-Sodiumhydrogenphosphate)

108 ml 37 % Formalin

392 ml dH$_2$O

Filtered with a 500 ml Nalgene sterile filter unit

Blocking Buffer

2 % BSA (Fraction V)

2 % Goat serum

0.02 % Biotin

0.1 % Porcine skin gelatine

0.01 % Saponin

Dissolved in TBS or PBS

Mounting Agent

Aqua polymount (Polysciences)

3.1.7 Immunohistochemistry buffers

Phosphate buffer (stock solution)

0.2 M NaH_2PO_4

0.2 M Na_2HPO_4

Phosphate buffer (working solution, pH 7.4)

20 ml 0.2 M NaH_2PO_4

80 ml 0.2 M Na_2HPO_4

100 ml dH_2O

Bovine Serum Albumin (PBS/BSA)

20 ml 0.2 M NaH_2PO_4

80 ml 0.2 M Na_2HPO_4

1.8 g NaCl

1 g BSA

100 ml dH_2O

Karlsson-Schultz (fixative solution for electron microscopy)

20 ml 0.2 M NaH_2PO_4

80 ml 0.2 M Na_2HPO_4

1 g NaCl (0.5 % final concentration)

50 ml 16 % PFA (4 % final concentration)

20 ml 25 % Glutaraldehyde (2.5 % final concentration)

Add up to 200 ml dH$_2$O

Filter with a 500 ml Nalgene sterile filter unit

Citrate Buffer (stock solution)*

0.1 M Citric acid (C$_6$H$_8$O$_7$*H$_2$O)

0.1 M Sodium citrate (C$_6$H$_5$O$_7$Na$_3$*2H$_2$O)

*Stored at 4°C

Citrate Buffer (working solution, 0.01 M, pH 6.0)*

9 ml 0.1 M Citric acid (C$_6$H$_8$O$_7$*H$_2$O)

41 ml 0.1 M Sodium citrate (C$_6$H$_5$O$_7$Na$_3$*2H$_2$O)

450 ml dH$_2$O

*Always freshly prepared

Tris Buffer (stock solution)*

0.5 M Tris base

Adjust pH 7.6 with HCl

*Store at 4°C

Tris Buffer (working solution)*

100 ml 0.5M Tris base (pH 7.6)

9 g NaCl

Add up to 1000 ml with dH$_2$O

*Always freshly prepared

Blocking buffer (2 % milk powder in Tris Buffer)

20 g of non-fat milk powder

Add up to 1000 ml with Tris buffer

3.1.8 Histological stains and reagents

Mayer's Haematoxylin solution

1 g Haematoxylin (Merck) was dissolved in 1000 ml dH$_2$O and 0.2 g sodium iodate and 50 g potassium aluminium sulphate (K$_2$Al$_2$(SO$_4$)$_4$*24H$_2$O) was added under constant shaking. Finally, 50 g chloralhydrate and 1 g citric acid were added and the solution was filtered before use.

Eosin solution

Stock solution (10x)

10 g of Eosin were dissolved in 100 ml of dH$_2$O and left to mature.

Working solution

2.5 ml stock solution

250 ml dH$_2$O

12 drops glacial acetic

Scott's solution

2 g KHCO$_3$ (potassiumhydrogencarbonate)

20 g MgSO$_4$ (magnesium sulphate)

Add up to 1000 ml with dH$_2$O

HCl- Alcohol

1.25 ml HCl

350 ml Ethanol

150 ml dH$_2$O

May-Giemsa

Staining solution

0.1g Eosin was dissolved in 100 ml dH$_2$O and 0.1 g methylene blue in 100 ml dH$_2$O. The two solutions were mixed and left for 3-4 days to mature. The solutions were filtered through Whatmann paper, let to dry over night and then dissolved in 10 ml pure methanol. The solution was stored at 4°C.

Giemsa solution

10 ml Giemsa and 20 ml dH$_2$O

Luxol-Fast-Blue

Staining solution

Dissolve 1 g of Luxol blue (1B, MBS from Chroma) in 1000 ml 96 % ethanol while stirring and warming. Let the solution cool down at room temperature and filter though Whatmann paper. Before use, for every 100 ml of staining solution add 50 µl of concentrated acetic acid (CH$_3$COOH).

'Nuclear fast red' solution

Dissolve 0.2 g of 'nuclear fast red' in 200 ml of boiling 5 % aluminium sulfate solution and boil for an additional 5-10 min. Let it cool down at room temperature and filter with Whatmann paper.

3.1.9 Cell culture media

DMEM for mammalian cell culture was purchased from GIBCO or BioWhittaker.

3.1.9.1 Buffers and media for Primary Cell Culture

Mixed glial and microglial culture medium

DMEM, High glucose (4500mg/l)

10 % heat-inactivated FBS

1 % Penicillin/Streptomycin (Lonza)

Hank's Balanced Salt Solution (HBSS) for preparation of brains

500 ml HBSS

7.5 ml 10 % MgSO$_4$

Trypsin in HBSS

Dilute stock trypsin 1:100 in HBSS

Freeze aliquots at -20°C

DNAse in HBSS (0.05 %)

Dilute 100 mg in 200 ml HBSS, Freeze aliquots at -20°C

3.1.9.2 Buffers and media for Cell lines

CHO medium

DMEM, High glucose (4500 mg/l) and with 4 mM L-Glutamine

10 % heat-inactivated dialyzed FBS

34.8 mM L-Proline

300 nM Thymidine

10 mM Glycine

3T3 Fibroblasts medium

DMEM, High glucose (4500mg/l)

10 % heat-inactivated FBS

1 % Penicillin/Streptomycin

Freezing Medium for CHO and 3T3 cells

70 % DMEM, high glucose

20 % FCS

10 % DMSO

3.1.10 Cell lines

Mammalian cell lines

CHO (Chinese Hamster Ovary cells) (gift from M.Filbin, Mukhopadhyay et al., 1994)

- MAG-expressing CHO cells
- Control-CHO cells

3T3 Fibroblasts (kindly provided by M.Schwab, Dodd et al., 2005)

3.1.11 Mouse lines

MAG knock out (Montag et al., 1994)

PLP knock out (Klugmann et al., 1997)

NgR1 knock out (kindly provided by M. Tessier-Lavigne, Genentech, Zheng et al., 2005)

CX3CR1-EGFP (Jung et al., 2000)

Thy1-EYFP (Winter et al., 2007)

GFAP-EGFP (kindly provided by F.Kirchhoff, MPIem, Goettingen)

3.1.12 Oligonucleotides

Oligonucleotides were synthesized in the Max Planck Institute of Experimental Medicine.

3.1.12.1 Genotyping primers for various mouse lines

MAG

Forward: 5'-ACCCTGCCGCTGTTTTGGAT-3'

Reverse: 5'-ACGGCAGGGAATGGAGACAC-3'

Neo: 5'-TTGGCGGCGAATGGGCTGAC-3'

Amplification product: 600 bp for mutant and 300 bp for wild-type

PLP

Forward: 5'- GGAGAGGAGGAGGGAAACGAG -3'

Reverse: 5'- TCT GTT TTG CGG CTG ACT TTG -3'

Neo: 5'-TTGGCGGCGAATGGGCTGAC-3'

Amplification product: 300 bp for mutant and 150 bp for wild-type

NgR1

Forward: 5'- TCGGCACATCAATGACTCTCC-3'

Reverse: 5'- TATGTACACACACCTGGTGGC-3'

Neo: 5'-TGGGCTCTATGGCTTCTGAG -3'

Amplification product: 300 bp for mutant and 150 bp for wild-type

3.1.12.2 Quantitative real-time PCR primers

beta-actin

Forward: 5'-CTTCCTCCCTGGAGAAGAGC-3'   Reverse: 5'-ATGCCACAGGATTCCATACC-3'

EGFR

Forward: 5'-TCCATCCTAGAGAAAGGAGAGC-3'   Reverse:5'-TCAGCATCTATCATCCAGCACT3'

GFAP

Forward: 5'-AGGGTGACAGCATTCTCTGC-3'   Reverse: 5'-CCGGTGGCTTGTTTCTCTTA-3'

Lingo-1

Forward: 5'-AAGTGGCCAGTTCATCAGGT-3'   Reverse: 5'-TGGGCATGCTTCTCATACC-3'

Mac-1

Forward: 5'-GAGCACCTCGGTATCAGCAT-3'   Reverse: 5'-CCCCAAAATAAGAGCCAATCT3'

NgR1

Forward: 5'-CGACCCCGAAGATGAAGAG-3'   Reverse: 5'-TGTAGCCATAACACCCATGC-3'

NgR2

Forward: 5'-GAGGCTTGGTCAGCCTACAGT-3'   Reverse: 5'-CGCGAACAAGTCATCCTGT-3'

NgR3

Forward: 5'-GCCCAGGGATTTGAATCT-3'   Reverse: 5'-AGCAGCAATTCCACACAG-3'

p75

Forward: 5'-ACTGAGCGCCAGTTACGC-3'   Reverse: 5'-CGTAGACCTTGTGATCCATCG-3'

Troy

Forward: 5'-AGGAGAGAAACCCGGCTTCTGT-3'   Reverse:5'AGAGGATTCTGCATCAGAGGCC3'

3.1.13 Antibodies

Primary antibodies directed against

Antibody	Species	Company	Dilution	Purpose
Fcγ I R	Rat	R&D systems	Series	Block
Fcγ III/II R	Rat	BD Pharmingen	Series	Block
GAPDH	Mouse	Assaydesigns	1:1000	WB
GFAP	Rabbit	Dako	1:400, 1:200	ICC, IHC
GST	Mouse	Sigma	1:1000	WB
Mac-1	Rat	BD Pharmingen	1:1000	ICC
Mac-3	Rat	BD Pharmingen	1:500	ICC
MAG	Mouse	Provided by J. Trotter	1:50	ICC
MAG	Sheep	Provided by S. Kelm	1:500	ICC
NgR1	Sheep	Provided by S. Kelm	1:500	WB

Secondary antibodies

Antibody	Species	Company	Dilution
Alexa488-coupled anti rabbit/rat IgG	Goat	M.probes	1:400
Alexa568-coupled anti rabbit/rat IgG	Goat	M.probes	1:400
Cy™3-coupled anti-mouse IgG	Goat	Dianova	1:1000
Cy™3-coupled anti-rabbit IgG	Goat	Dianova	1:1000
Cy™2-coupled anti-rabbit/mouse IgG	Goat	Dianova	1:100
Cy™3-coupled anti-sheep IgG	Donkey	Dianova	1:750
FITC-conjugated streptavidin	Goat	Linaris	1:100
HRP-conjugated anti-IgG-anti-mouse	Goat	Dianova	1:5000
HRP-conjugated anti-sheep IgG	Goat	Dianova	1:5000
HRP-conjugated anti-goat IgG	Mouse	Sigma	1:50000

3.1.14 Enzymes

RedTaq DNA polymerase (Sigma)

GST-3C PreScission protease (GE Healthcare

3.2 Methods

3.2.1 RNA isolation and quantification

3.2.1.1 Small scale RNA purification ('RNeasy mini prep')

Small-scale 'RNeasy mini preps' (Qiagen) were used to purify the total RNA from FACS-sorted microglia and astrocytes and primary microglia after LPS induction. The RNAs were purified following the manufacturer's instructions. In brief, microglia in culture and FACS sorted microglia and astrocytes were lysed in RLT buffer and kept at -20°C until further use. The samples were thawed quickly by incubating them at 37°C in a water bath and further homogenized by vigorous vortexing for 1 min. Ethanol was then added to provide the appropriate binding conditions, and the homogenates were applied to RNeasy mini columns where the total RNA binds to the membrane and the contaminants are efficiently washed away. An additional step of DNAase incubation was included to digest the genomic DNA contaminations. The RNAs were eluted from the column with 50 µl of RNase-free ddH$_2$O.

3.2.1.2 RNA precipitation

2 µl of coloured DNA carrier were added to the 50 µl of RNA to bind to the RNA pellet and enable later visualization. After vortexing, 25 µl of 7.5 M NH$_4$Ac were added and then 187.5 µl of 100 % pure ethanol was included in the RNA mixture. The RNA solution was centrifuged for 30 min at maximum speed with a table microcentrifuge. After discarding the supernatant, the pellet was washed with 100 µl of 70 % ethanol and the pellet was left to dry. All the steps were carried out at room temperature. 4 µl of RNase-free ddH$_2$O was added to the pellet and put on ice for a further 15 min to dissolve.

3.2.1.3 cDNA synthesis

cDNA synthesis is based on the characteristic feature of eukaryotic messenger RNAs to harbour the defined polyadenylated tail on the 3′ end. First-strand cDNA was synthesized for quantitative RT-PCR. Total RNA was mixed with 2 µl of random 9amer (0.55 pmol/µl) and 2 µl of oligo-dT (110 pmol/µl) primers. The mixture was heated to 70°C for

5 min and then incubated on ice for 2 min. 4 μl of 5x First-Strand buffer, 2 μl of 0.1 M DTT and 1 μl of 10 mM dNTPs were added to the mixture and the final volume was adjusted with dH$_2$O to 19 μl. Finally 1μl of SuperScript™ III RT (200 units/μl) was added to complete the synthesis reaction mixture. This mixture was incubated in the thermocycler at 25°C for 10 min, then 50°C for 30 min, 55°C for 30 min and finally the reaction was terminated by heating at 70°C for 15 min and incubating it further on ice. The cDNA was used later as a template for amplification in PCR.

3.2.1.4 Quantitative real-time PCR for mRNA expression

For each gene expression assay, 5 μl of SYBR green master mix, 1 pmol of each forward and reverse primer pair, 1 μl of dH$_2$O and 4 μl of cDNA mixture were mixed in a 96-well plate. Real-time PCR was carried out using the ABI Prism 7700 Sequence Detection System and SYBR Green Master Mix according to the manufacturer's instructions (Applied Biosystems). The PCR reaction was carried out for 40 cycles in the following temperature conditions: 10 sec -95ºC, 25 sec - 60ºC and 35 sec -72ºC. The SYBR green fluorescence was read at the 72ºC stage. All reactions were carried out in triplicates. The relative quantity (RQ) of RNA with respect to the housekeeping genes (β-actin and DNA methylase I) was calculated using 7500 Fast System SDS software Ver1.3 (Applied Biosystems) and the Excel-based RT-PCR analysis software qBase (Hellemans et al., 2007). The results were depicted as histograms of normalized RQ values with RQ value lower than 1.

3.2.2 Protein biochemical methods

3.2.2.1 Lysis of microglial cells

Microglial cells were harvested in 300 μl Lysis buffer II 24 hrs after plating. The cell lysate was then incubated at 4ºC in a tilt rotator for 30 min and centrifuged at 4ºC for a further 15 min at maximum speed. The supernatant was collected, the protein concentration was measured and the protein solution was further precipitated.

3.2.2.2 Lysis of brains

3-4 month old NgR1 wild type and knockout mice were sacrificed by spinal cord dislocation and decapitated. The brains were removed and collected in 14 ml falcon tubes in Lysis buffer I. These were further homogenized using an Ultraturrax (T8) on the highest settings (20-30s). The brain lysates were incubated 20-30 min on ice, the

insoluble cellular debris were pelleted by centrifugation at 2000 rpm at 4ºC for 10 min and the supernatant was used for further analysis or stored at -70°C.

3.2.2.3 Protein precipitation (Wessel and Fluge)

150 µl of microglial protein solution was precipitated by adding 450 µl methanol and vortexing. After the addition of 150 µl $CHCl_3$ and 300 µl dH_2O, the protein solution was vortexed and centrifuged for 5 min at 9000 rpm. The protein pellet precipitates were present in the interphase between $CHCl_3$/methanol+dH_2O. The interphase was removed and 300 µl of methanol were added and mixed. The protein solution was further centrifuged at maximum speed for 10 min. The supernatant was removed and the pellet was air dried and further resuspended in the desired volume of sample buffer.

3.2.2.4 Purification of recombinant MAG proteins

The plasmids encoding the Fc chimera with the five N-terminal domains of MAG or the three N-terminal domains, MAG d1-5 and MAG d1-3 respectively, have been previously described (Kelm et al., 1994). These were stably transfected into CHO (Chinese hamster ovary) K1 or CHO Lec1 cells. Stable cell lines were established using selection with hygromycin B. Culture supernatants (kindly provided by S. Kelm) were collected and the protein chimeras were purified on a protein-A membrane absorber (Sartobind, Sartorius). All the steps were carried out at 4ºC. First, the pH of the tissue culture supernatants was stabilized through the addition of 1 M Tris (pH 7.5) at a final concentration of 10 mM. EDTA was then added to a final concentration of 10 mM to prevent iron precipitation, and finally sodium azide was added to a final concentration of 0.02 % to prevent bacterial growth. The tissue supernatants were then centrifuged for 15 min at 7800 rpm at 4ºC in a TI-45 rotor (Beckman Coulter Optima LE-80K) and another 45 min at 40.000 rpm. The supernatants were collected and further centrifuged in a fixed angle rotor (Eppendorf 5804R, F34-6-38 rotor) at 11.000 rpm for 15 min. They were then filtered through a 0.22 mm bottle-top filter to remove fine debris. The protein-A membrane absorber was equilibrated with 100 ml WB I. After passing through the supernatants, the absorber was washed with 100 ml WB I, followed by 100 ml WB II to remove any unbound proteins. The Fc-chimeras were eluted and collected as 0.5 ml fractions by applying EB I with a 20 ml syringe. 75 µl of NB was immediately added in every fraction to neutralize the pH. The fractions with $OD_{280} > 0.05$ were then pooled and the buffer was exchanged by using PD10 columns (Sephadex 25, GE Healthcare). Briefly, the columns were washed with 2

volumes of dH$_2$O, then 0.1 N NaOH / 1 % SDS, a further 0.1 N HCl and finally dH$_2$O and TBS. The protein solution was then applied to the column and another 3 volumes of TBS were used for washing. Fractions of 0.5 ml were collected and the procedure was repeated three times. The protein concentration was measured and the fractions of interest were pooled. The Fc portion was then cleaved by adding 50 µg of GST-3C protease (PreScission Protease, GE) and 2 mM of DTT. The digest was carried out over night at 4ºC. Following the same procedure through the protein-A membrane absorber where the Fc portions were bound, the recombinant MAG proteins/3C protease mixture was purified. Furthermore, using a GSH column (Amersham), the GST chimera of the 3C protease was bound to the column while the flow-through contained the recombinant MAG proteins. The buffer of the protein solution was then exchanged following the procedure mentioned above and the samples were further concentrated using the centricon microconcentrators (Sartorius, M-50). The protein solutions were finally sterilized through 0.22 µm filters (Costar Spin).

3.2.2.5 Quantification of protein concentration by Lowry assay

The protein concentrations were determined using the Bio-Rad *DC* Protein Assay kit according to the manufacturer's 'microplate assay' protocol. The working principle of the kit is similar to the Lowry assay (Lowry et al., 1951). The absorbance was measured at 650 nm in a microtitre plate reader. The assay is based on the reaction of proteins with an alkaline copper tertrate solution and folin reagent, which leads to the loss of 1, 2, or 3 oxygen atoms, producing one or several reduced species that have a characteristic blue colour with maximum absorbance at 750 nm. The colour development is primarily due to the amino acids tyrosine and tryptophan, and, to a lesser extent, cystine, cysteine and histidine (Lowry et al., 1951).

3.2.2.6 SDS polyacrylamide gel electrophoresis

The proteins were separated using the discontinuous SDS polyacrylamide gel electrophoresis (SDS-PAGE) described by Laemmli (Laemmli, 1970). The glass plates and the 1 mm spacers were assembled according to the Bio-Rad instructions. The 12 % separating gel solution of acrylamide was prepared freshly and poured between the assembled glass plates. The top of the gel was covered with a layer of dH$_2$O-saturated isobutyl alcohol and left to polymerize for 30 min at room temperature. After rinsing the isobutyl alcohol twice with dH$_2$O, the freshly prepared stacking gel solution was added

and a 1 mm Teflon comb (10 or 15 teeth) was inserted into the layer of the stacking gel solution and left to polymerize. The chamber and the gels were assembled based on the manufacturer's protocol. The protein lysates were diluted in 6x SDS sample buffer containing 1 % β-mercaptoethanol and heated for 5 min to 90°C. 5 μl of pre-stained Precision-plus (BioRad) was loaded on a well as a molecular weight standard. The gels run at 10 mA/gel of constant current until the bromophenol blue tracking dye entered the separating gel and increased to 15 mA/gel. The electrophoresis was terminated once the bromophenol blue had reached the lower end of the gel. The gel was removed and preceded for Coomassie staining or protein blotting.

3.2.2.7 Coomassie staining

The gels were fixed for 15 min in 25 % isopropanol / 10 % acetic acid and then briefly washed with dH_2O. After incubation in the coomassie blue staining buffer overnight, the gels were incubated with the destaining solution and scanned with an UMAX Astra47000 scanner.

3.2.2.8 Western blotting (WB)

Electrophoretic transfer

Proteins were transferred from the SDS-gel onto a PVDF membrane (Amersham/Millipore, pore size 0.45 μm) by electrophoresis, as originally described with modification (Towbin et al., 1979). PVDF membranes were activated for 30 sec in 100 % methanol and further incubated in transfer buffer for 15 min. The gels, the Whatmann paper and the blotting pads were pre-soaked in transfer buffer for 15-30 min and further assembled according to the manufacturer's protocol. Proteins were transferred at a constant voltage of 38 V and a maximum current of 275 mA for a 1.5 mm gel and for 1.5-2 hrs at room temperature.

Immunological detection of proteins on PVDF membranes

After electrophoretic transfer, the membranes were blocked for 1 hr at room temperature in blocking buffer (5 % non-fat dry milk in TBS). The primary antibody diluted in blocking buffer was applied overnight at 4°C with constant gentle shaking. After three 10-min washes in TBST (0.05 % Tween-20 in TBS), HRP-conjugated secondary antibodies were applied for at least 1 hr in blocking buffer, followed by three 10-min washes with TBST. The membranes were washed once with TBS before being exposed

using the Enhanced Chemiluminescence Detection kit (PerkinElmer) according to the manufacturer's instructions (Western Lightning™, Western Blot Chemiluminescence Reagent Plus, PerkinElmer Life Sciences, Inc.). ECL photographic film (Hyperfilm™, Amersham Biosciences) was used to expose the membranes. The time of exposure varied depending on the signal intensity. To reprobe the same membrane with a second antibody, the membrane was incubated with stripping buffer for 1 hr at 60°C with rigorous shaking. After one wash with TBST, the membrane was incubated in blocking buffer for 30 min before probing with the second primary antibody.

3.2.3 Cell cultures

3.2.3.1 Primary microglial and astrocytic cultures

Primary microglia and astrocytes were obtained from primary mixed glial cultures. Glial cell cultures were prepared from the total brains of newborn P0-P2 C57Bl/6 mice or NgR1-deficient mice (kindly provided by M. Tessier-Lavigne, Genentech, South San Fransisco; Zheng et al., 2005) as described previously (Giulian and Baker, 1986) with adaptations. In brief, the brains were removed under sterile conditions and the brain tissue carefully stripped of meninges and trypsinized (1x in HBSS, Lonza) for 5 min at 37°C. The cell suspension was then triturated with a fire-polished Pasteur pipette in the presence of 0.05 % DNAase (Roche). The cell pellet was resuspended in 10 ml glial culture medium and plated onto poly-L-Lysine coated 75-cm^2 tissue culture flasks (Nunc) at a density of three brains per flask. Cultures were incubated at 37°C in a humidified incubator containing 5% CO_2 and 95% air with medium changes every 2-3 days. Microglial cells were harvested from these primary mixed glial cell cultures after 10-12 days. The microglial cells were purified from the initial mixed culture by gentle manual shaking, taking advantage of their differential adhesive properties. Supernatants were collected and centrifuged at 800 rpm for 5 min and the microglial cell pellet was resuspended in microglial culture medium or DMEM only and plated on 6-well plates (1-2 × 10^5 cells/well, RNA), 16-well tissue culture slides (Lab-Tek, Nunc) (1 ×10^4 cells/well, microglia-CHO co-culture), 96-well plates (1.5 × 10^4 cells/well, ELISA), 13-mm coverslips (3 × 10^4/coverslip, stripe assay) and 6 cm plates (0.5 × 10^6 cells, WB). The purity of these cultures was >95% as determined by Mac-1 and Dapi co-staining. After shaking the microglia, the flasks were washed with HBSS and incubated with trypsin for 15 min at 37°C. After shaking, the detached cells were collected and the

enzyme was inactivated by adding the FCS-containing glial medium. The cell suspension was centrifuged at 800 rpm for 5 min and the astrocytic pellet was then resuspended in glial culture medium and plated on 8-well tissue culture slides (Lab-Tek, Nunc) (2×10^4 cells/well,).

3.2.3.2 CHO and 3T3 cell culture

CHO cells (control and MAG expressing, kindly provided by M. Filbin) were maintained in CHO medium containing 10 % FCS on 10 cm tissue culture dishes (Falcon). Cells were grown at 37°C in a 5 % CO_2 atmosphere. For passaging, confluent plates were trypsinized (1x in PBS) shortly and centrifuged at 800 rpm for min. The pellet was diluted in 10 ml CHO medium and 1 ml of the cell suspension was added to 9 ml of medium and further plated. Cells were passaged once or twice a week depending on the experiments. The 3T3 cells (kindly provided by M. Schwab) were passaged and maintained as mentioned above for the CHO cells, but in the 3T3 medium. These cells needed to be more confluent when plated, so they were diluted 1:4 in every passage.

3.2.3.3 Fluorescent-activated cell sorting (FACS) of microglia and astrocytes

To increase the purity of microglia and astrocytes, brain microglia and astrocytes were sorted using transgenic animals that express EGFP under a cell type specific promoter. More specific, heterozygous CX3CR1-EGFP ('green microglia') and GFAP-EGFP ('green astrocytes') mice were used for FACS. The brains of newborn mice were prepared as previously described (section 3.2.3.1) until trypsin was added. The brains were incubated with 2 ml HBSS (containing Mg^{2+}), 1 ml trypsin and 1 ml 0.05 % DNAase at 37°C for 10 min. The cell suspension was then triturated with a 10 ml pipette and incubated at 37°C for another 10 min. The same step was repeated with a 5 ml pipette and a glass Pasteur pipette. The cell suspension was then centrifuged for 10 min at 800 rpm and the cell pellet was resuspended with 3 ml Mg^{2+}-containing HBSS. After filtration through a nylon 40 μm cell filter (BD Falcon), the cell suspension was incubated with 80 μl of PI (stock 1 mg/ml, Sigma) and 4 μl Hoechst (stock 5 mg/ml, Sigma) at 37°C for 20-30 min. Propidium iodide (PI) intercalates into double-stranded nucleic acids; it is excluded by viable cells but can penetrate the cell membranes of dying or dead cells. Hoechst 33342 is also a non-toxic membrane-permeable dye that intercalates in the DNA and is used to stain living cells. 5 ml of HBSS were then added and the pellet resuspended in 10 ml of glial culture medium. The cell suspension was kept

on ice until it could be sorted in a BD FACSAria™ cell sorter with the right filters and based on the manufacturer's instructions (BD Biosciences).

3.2.3.4 Microglial and astrocytic process outgrowth assay

To assess the MAG-mediated or Nogo-mediated inhibition of microglial and astrocytic processes, primary microglial cells and astrocytes were cultured on confluent monolayers of CHO cells that express recombinant MAG on their surface, on control-CHO cells (Mukhoparadhyay et al., 1994), or on 3T3 cells that express Nogo-A at the surface (Dodd et al., 2005). Briefly, 8- or 16-well Lab-Tek chambers were coated with poly-L-lysine for 1 hr at 37°C and then with 25 μg/ml fibronectin (only for the CHO cells) for 2 hrs at 37°C. Confluent dishes of CHO and 3T3 cells were split and 300 μl or 150 μl of $25*10^3$ cell suspensions were plated in the 8- and 16-well chambers respectively. Monolayers of cells were established over a 24-hr period. Microglia and astrocytes were plated onto the CHO cell and 3T3 monolayers and cultured in DMEM. The Rho kinase inhibitor (20 μM, Y27632; Calbiochem) was directly added to the culture medium at the time of plating. Microglial supernatants were collected for ELISA and the co-cultures were fixed after 4 hrs or 24 hrs for 10 min with 4% PFA. The microglial co-cultures were stained for the microglial marker Mac-1 and the astrocytic co-cultures were stained for GFAP following the procedure in the section 3.2.5. The expression of MAG in the CHO cells was regularly checked by staining with a MAG antibody.

3.2.3.5 Quantitative analysis of microglial morphology

In order to quantitatively assess the microglial process inhibition, microglial cells were imaged with a fluorescence microscope (Leica DMRXA) equipped with a water immersion 40x objective and a ProgResC14 camera system (Jenoptic, Jena, Germany). For each group, at least 100 microglial cells from 3 different wells were analyzed using the ImageJ software. The ramification index (=forming factor) was calculated using the following formula (Wilms et al., 1997):

$$RI = 4\pi \, (\text{cell area}) / (\text{cell perimeter})^2,$$

where RI is the ramification index. The ramification index is 1 when the cell is perfectly circular (no processes), whereas extremely ramified cells have a ramification index of 0. Cells with more processes have a value close to 0, whereas cells with fewer processes and more circular morphology have a value close to 1. The mean and SEM of the ramification index was determined from three independent experiments. The statistical significance of

the differences between experimental groups was assessed by applying the Student's t-test using the GraphPad Prism software package.

3.2.3.6 Stripe assay

Silicon matrices (exclusively distributed by M. Bastmeyer, Zoology Institute, University of Karlsruhe, Germany) were used to produce stripe patterns of purified proteins as previously described (Vielmetter et al., 1990). Briefly, the matrices were placed onto 13mm poly-L-Lysine coated coverslips and 100 µl of recombinant MAG protein solution or FITC-conjugated streptavidin (Linaris) with a concentration of 10 µg/ml was filled into the channel. After an incubation period of 1 hr at 37°C, the unbound protein was removed by washing it twice with HBSS. Microglia were plated at a density of 3×10^4 cells/coverslip and left to settle for 30 min before the medium was replaced with new one. After 20-24 hrs, the cultures were fixed and stained for MAG and Mac-1 following the steps mentioned in the section 3.2.5. The experiments were analyzed based on section 3.2.7. More than 150 microglial cells growing on PLL, MAG or streptavidin stripes were measured per experiment and the percentage of the total cell number growing on PLL, MAG or both was calculated. All experiments were carried out with a minimum of 2-3 coverslips per condition and a minimum of three independent experiments. The mean ± SEM of the total cell percentage is presented and the statistical significance was assessed using a Student's t-test.

3.2.3.7 MAG as substrate and TLR agonists

The TLR agonist experiments were performed to check whether the MAG-mediated microglial response interferes with the TLR-mediated response. For that reason, the MAG-expressing CHO cells and coverslips coated with recombinant MAG were used. The microglia-CHO co-cultures were prepared as described in section 3.2.3.4 and the TLR agonists were added simultaneously to the cell suspension as described below. The 13 mm coverslips were pre-coated with PLL for 1 hr at 37°C. After a short washing step with dH_2O, 100 µl of recombinant MAG protein (10 µg/ml in HBSS) was applied to the coverslip and left to dry at 37°C for 1 hr. The solution was removed and the coverslips were washed with HBSS to remove any unbound protein. The microglial cells were plated at a density of $2-3*10^4$ cells/coverslip and fixed after 24 hrs. Different TLR agonists, such as MALP-2 (10 ng/ml, Alexis) as a TLR 2/6 agonist, Pam3SK4 (10 ng/ml, Alexis) as a TLR 1/2 agonist and LPS (1 ng/ml, Alexis) as a TLR 4 agonist, were diluted

in microglial culture medium and added at the time of plating. All experiments were carried out three times.

3.2.3.8 Soluble MAG microglial assay and ELISA

3.2.3.8.1 Soluble MAG microglial assay

Microglial cells were cultured on 96-well plates in microglial culture medium for 24 hrs. The medium was then changed and 10 ng/ml, 100 ng/ml, 1 μg/ml and 10 μg/ml of soluble recombinant MAG proteins were added. Cytokine and chemokine release was assessed in the supernatants 20 h after stimulation. The Fc blockage experiment was carried out as mentioned above by pre-incubating the cells with 1 ng/ml, 100 ng/ml, and 10 μg/ml of anti-CD16/CD32 and anti-CD64 antibodies for 30 min prior to the addition of 1 μg/ml of recombinant protein and the respective anti-Fc dilution. The supernatants were collected after 18 hrs stimulation and analyzed by ELISA.

3.2.3.8.2 ELISA (Enzyme-linked Immunosorbent assay)

Tumor necrosis factor-α (TNF-α), interleukin-6 (IL-6), KC (mouse equivalent of growth regulatory oncogene-α (GROα-CXCL1) and macrophage inflammatory protein-1α (MIP-1α) were analyzed using mouse-specific antibody pairs and mouse protein standards designed for ELISA application in accordance with the manufacturer's instructions (R & D Systems, Minneapolis, USA). Briefly, the captured antibody was diluted to the working concentration in PBS without carrier protein. 100 μl of the diluted antibody were applied on a 96-well plate and incubated overnight at room temperature. After three washes with PBS / 0.05 % Tween-20, any residual washing buffer was removed by inverting the plate against clean paper towels. The wells were then blocked with 1% BSA in PBS for 1 hr at room temperature and then washed twice as mentioned above. The culture supernatants were then diluted and 100 μl of the diluted sample or standard was added to the well and incubated for 2 hrs at room temperature. The plate was washed as mentioned above and 100 μl of diluted detection antibody was added to each well and incubated for another 2 hrs at r.t. The wells were then washed twice with PBST and 100 μl of diluted HRP-conjugated streptavidin was added to the well and incubated for 20 min at room temperature in the dark. After two washes with PBST, 100 μl of substrate solution was added in each well and incubated for another 20 min in the dark. Finally, the reaction was stopped by adding 50 μl of stopping solution to each well and reading the plate at 450 nm. Stimulation with lipopolysaccharide (LPS) (1 ng/ml, Alexis) served as a

positive control. Cytokine amounts were normalized to LPS stimulation. All the experiments were carried out with a minimum of 6 wells per condition (n ≥ 6) and a minimum of three independent experiments.

3.2.4 Animal handling

3.2.4.1 Animal breedings

MAG-deficient mice and PLP-deficient mice were bred into the C57BL/6 background using mice from the breeding colony of the Max Planck Institute of Experimental Medicine. From these breeding pairs, MAG*PLP double mutants and littermate control animals were obtained from the same colony. As previously shown, there were no differences between mag+/- and mag-/- mice (Fujita et al., 1998). Consequently, we used mag -/-, mag+/-plp-/Y and mag-/-plp-/Y mutants at the age of 13 months for our study. Transgenic CX3CR1-EGFP mice (Jung et al., 2000) were bred with transgenic Thy1-EYFP (Winter et al., 2007) and MAG-deficient mice for two-photon laser scanning *in vivo* imaging. The CX3CR1*Thy1*mag+/+ and CX3CR1*Thy1*mag-/- mice were 3-4 months old. Astrocytes were isolated for FACS analysis from transgenic GFAP-EGFP mice (Nolte et al., 2001). All experiments were in compliance with the animal policies of the Max Planck Institute of Experimental Medicine, approved by the German Federal State of Lower Saxony.

3.2.4.2 Preparation of mouse genomic DNA for genotyping

For the preparation of mouse genomic DNA for genotyping, 2-3 mm of tail were cut and placed in microcentrifuge tubes. 180 µl of 1x MGB and 20 µl of proteinase K (10 mg/ml) were added to each tube and incubated at 52ºC overnight with vigorous shaking. Once the tails were dissolved, proteinase K was heat-inactivated by incubating the DNA lysate at 95ºC for 10 min. Then, the DNA lysate was centrifuged at 13.000g for 1 min to pellet all the undigested material and the supernatant was collected in fresh tube. 1-2 µl of this diluted DNA preparation was used for genotyping PCR amplification.

3.2.4.3 Genotyping polymerase chain reaction

PCR	MAG k.o	PLP k.o	NgR1 k.o
Tail DNA	1 µl	1 µl	1 µl
Primer neo (10 pmol/µl)	1 µl	0.5 µl	0.4 µl

Primer forward (10 pmol/µl)	0.25 µl	0.5 µl	0.4 µl
Primer reverse (10 pmol/µl)	1 µl	0.5 µl	0.4 µl
dNTPs (2 mM)	2 µl	2 µl	2 µl
Red Taq Buffer (10x)	2 µl	2 µl	2 µl
Red Taq (Sigma)	1 µl	1 µl	1 µl
dH$_2$O	11.75 µl	12.5 µl	12.8 µl

PCR-program	MAG k.o	PLP k.o	NgR1 k.o
95°C	3 min	3 min	3 min
66°C / 56°C / 62°C	66°C, 30 s	56°C, 30 s	62°C, 45 s
72°C	60 s	60 s	60 s
95°C	30 s	30 s	30 s
Cycles	36	36	39
66°C	60 s	60 s	60 s
72°C	10 min	10 min	5 min
4°C	Pause	Pause	Pause

3.2.4.4 LPS injections and EAE

Wild type and MAG-deficient mice aged 2.5-3.5 months old were weighed and 15 mg of LPS (serotype 055:B5, Sigma) per kg of mouse weight was injected intraperitoneally. The mice were processed following the procedures in the sections 3.2.6.1 and 3.2.6.2. Experimental allergic encephalomyelitis (EAE) served as model of multiple sclerosis in rodents. The induction of EAE in wild type and MAG-deficient mice, the clinical scoring, the perfusion of the animals, as well as the embedding of the tissue were performed in the lab of P.Calabresi (Johns Hopkins University, USA).

3.2.5 Immunocytochemistry

Immunostainings were carried out at the time mentioned in the experiment. All steps were performed at room temperature. Microglia and astrocytes grown on CHO and 3T3 monolayers and in the stripe assay were fixed for 10 min in 4 % PFA. The cells were then washed three times for 10 min with PBS and blocked in blocking buffer for at least 30-60 min. Primary antibodies diluted in blocking buffer were applied for at least 1.5-2 hrs at room temperature. After three 10-min washes with PBS, fluorochrome-conjugated

secondary antibodies were applied for at least 45-60 min. After washing once with PBS, the cells were briefly incubated with 4',6-diamidino-2-phenylindole (Dapi) and further washed twice with PBS. The cells were finally rinsed in dH_2O and mounted in AquaPolyMount (Polysciences, Warrington, PA) on glass slides.

3.2.6 Histology and immunohistochemistry

3.2.6.1 Perfusion and fixation of mouse tissue

The mice were deeply anaesthetized by injecting 2.5 % avertin (0.017 ml per g of mouse body weight) intraperitoneally. After anaesthesia, the mice were washed with 70 % ethanol in the stomach and the skin was removed from the ventral side. A transversal cut was made just below the diaphragm and slowly opened until the heart was visible. A new needle (27 gage) was inserted into the left ventricle and, immediately after starting the perfusion, a small incision was made in the right auricle to allow the blood to flow out of the body. Perfusion was carried out with HBSS and changed from HBBS to fixative (4 % PFA in PB for paraffin embedded tissue or Karlsson-Schultz for electron microscopy). The perfusion was carried out with 30-50 ml of fixation solution. The brain and the spinal cord were removed carefully and collected into vials with cold perfusion buffer. The tissue samples were stored in 4 % PFA overnight at 4°C and then in 1 % PFA until further use.

3.2.6.2 Paraplast impregnation and embedding of the tissue

After post-fixation, the tissue was washed 3-4 times with PBS. The brains were cut into half and pieces of different regions of the spinal cord were transferred into plastic chambers for dehydration and paraplast impregnation. The following steps were carried out before tissue embedding: 50 % ethanol for 1 hr, twice in 70 % ethanol for 2 hrs, twice in 96 % ethanol for 1 hr and twice in 100 % ethanol for 1 hr each. Then, the 100 % ethanol was replaced by isopropanol for 1 hr, twice in xylene for 2 hrs and the tissues were impregnated with paraplast at 60ºC for 2 hrs. Finally, the tissue was embedded in molten paraplast and left to harden.

3.2.6.3 Haematoxylin-Eosin (HE) staining

5-7 μm thick sections were cut from the paraffinized block using a microtome. The sections were floated on a warm water bath (42°C), placed on positively charged glass slides and then dried overnight at 37°C. The sections were then incubated at 60°C for 10

min before being deparaffinized and rehydrated in the following steps: twice in xylol and once in xylol/isopropanol (1:1) for 10 min, 100 %- 90 %- 70 %- 50 % alcohol for 5 min and finally dH_2O. The sections were incubated with 0.1 % haematoxylin for 5 min staining the basic cell nuclear compartment blue. Following a wash with dH_2O, the sections were dipped in HCl-alcohol solution once for 5-10 sec and then in Scott's solution for 5 min. They were briefly rinsed with dH_2O, counterstained with 0.1 % eosin for 3-5 min and then rinsed with dH_2O. Sections were dehydrated by incubating them in an increasing alcohol concentration (50 %, 70 %, 90 %, and 100 %) for 2 min, then in xylol/isopropanol (1:1) and twice in xylol for 5 min. Finally, they were mounted with 'Eukitt' (Kindler GmbH).

3.2.6.4 DAB-based immunodetection on paraffin sections

The sections were processed as above (section 3.2.6.3) until rehydration. The sections were then incubated for 5 min in citrate buffer before being 'cooked' for 10 min in boiling citrate buffer (at 650 watts in microwave oven). After this, the sections were left in the citrate buffer for about 20 min to cool down and subsequently rinsed in Tris buffer/ 2 % milk for 5 min. Endogenous peroxidases were inactivated by incubating the sections with 100 µl of 3 % hydrogen peroxide for 5 min. Next, the sections were incubated with 100 µl of goat-serum diluted in PBS/BSA (1:5) for 20 min at room temperature before proceeding with the 100 µl of the primary antibody diluted in PBS/BSA. After an overnight incubation at 4°C, the sections were washed with Tris buffer/2 % milk and incubated with 100 µl of bridging antibody, i.e. biotinylated secondary antibody (Dako) for 10 min. They were then rinsed with Tris buffer/2 % milk and probed with 100 µl of tertiary antibody, i.e. Horseradish Peroxidase streptavidin complex (Dako), by incubating the sections for 10 min. They were then rinsed with the Tris buffer and incubated with 100 µl of DAB for 10 min. Finally, the sections were rinsed twice with dH_2O for 5 min each and counterstained for 30 sec with haematoxylin following the steps until mounting (section 3.2.6.3). The enzymatic reaction between the HRP and DAB yielded a very a stable brown precipitate that was visualized under the microscope (section 3.2.7).

3.2.6.5 May-Giemsa

The sections were processed as above (section 3.2.6.3) until rehydration. They were then washed twice shortly in 100 % methanol before incubating with the staining solution for 30 min. The sections were then washed shortly with dH_2O before being incubated with

the Giemsa solution for 30 min. After a short wash with dH_2O, the sections were dipped in 1 % acetic acid, washed with dH_2O and dehydrated as mentioned above (section 3.2.6.3).

3.2.6.6 Luxol-Fast-Blue and 'nuclear fast red'

The sections were processed as above (section 3.2.6.3) until rehydration. They were then incubated overnight in the LFB solution at 56°C. After cooling down, the sections were washed briefly with 96 % ethanol, then dH_2O before incubating in 0.1 % lithium carbonate. After a brief wash in 70 % ethanol and dH_2O, the sections were incubated for 5 min in the 'nuclear fast red' solution and then washed with dH_2O. The sections were subsequently dehydrated and mounted as mentioned above (section 3.2.6.3).

3.2.6.7 Semithin sections

The mice were anaesthetized and perfused with Karlsson-Schultz solution as mentioned above (section 3.2.6.1). The spinal cords were removed and post-fixed in 4% PFA for 16 hrs and further contrasted with osmium tetraoxide before being embedded in epoxy resin (Serva). Semithin sections (0.5 μm) were cut at comparable levels using a microtome (Leica, RM 2155) with a diamond knife (Histo HI 4317, Diatome). The sections were then stained with methylene blue-Azur II for 1 min at 60°C and mounted with Eukitt.

3.2.7 Light and Fluorescent Microscopy

The light and fluorescent microscopic observation was performed with an oil immersion 100x, 63x and 40x lenses and air 20x lenses (Leica, DMRXA) in the different experiments and the microscope was equipped with a ProgResC14 camera system (Jenoptic, Jena, Germany). The images were digitalized, analyzed and processed using Image J software (http://rsbweb.nih.gov/ij) and Photoshop 7.0.1.

3.2.8 Two-photon laser scanning in vivo microscopy

3.2.8.1 Anaesthesia and surgery

The experiments (n>3 per genotype) were carried out with 12-16-week-old mice. A general anaesthesia was initiated by injecting 77 mg pentobarbital sodium i.p. (dissolved in 0.9 % NaCl solution) per kg of body weight. The anaesthesia was continued with 40-60 mg per kg and methohexital sodium (Brevimytal Lilly). The mice were supported by artificial ventilation. The spinal cord segments L4 and L5 were exposed by a

laminectomy of the L1 and L2 spines for the imaging of the dorsal white columns. The animals were paralyzed with pancuronium bromide (Pancuronium Organon) to avoid any movement induced by active respiration during imaging. The spinal column was rigidly fixed with custom-made clamps. In all experiments, the exposed spinal cord was continuously superfused by ACSF. The body temperature was measured rectally and maintained between 36 and 38°C by a heated support.

3.2.8.2 Two-photon laser scanning microscopy and image acquisition

A two-photon laser scanning microscope (2P-LSM, Zeiss Axiocope 2 with LSM510 NLO scanhead) equipped with an infrared fs-pulsed Ti:Sa laser (Mira 900/10 W Verdi; Coherent, Glasgow, UK) and a 40x (NA 0.8) or 20x (NA 1.0) water immersion objective was used for the acquisition of high resolution images. The laser was set at 895±5 nm for the simultaneous excitation of EGFP and EYFP. The emitted light was split by a 520 nm longpass dichroic mirror (Semrock, Rochester, USA) and collected by photo-multiplier tubes (Hamamatsu, Japan) through two bandpass filters, a 500±12 nm and a 542±27 nm, respectively (Semrock). Parallel, uniformly spaced (1.5 to 2 μm) planes of 400*400 to 600*600 μm^2 regions of the dorsal columns were recorded, digitized and processed to obtain z-stacks of images. The total acquisition time for a stack of 16 to 24 images was approximately 30-60 s. Several stacks were taken continuously to obtain a time-lapse series of microglial movement.

3.2.8.3 Image processing and analysis

The images were processed and the analysis was performed using the Zeiss LSM software and the ImageJ software. Prior to any analysis, the time series of the image stacks were corrected for the shifts in the horizontal and vertical directions by using an autocorrelation based custom-made software written in Matlab (v.7). In the majority of images, the median filter of ImageJ was used to remove any speckle-like noise. The EGFP and EYFP signals could be separated by choosing the right filter sets that permitted an unambiguous discernment of EGFP-expressing microglia from EYFP-expressing neurons. These cell types were also distinguished by the differences in their morphology.

4. Results

4.1 Microglial cells and myelin-associated inhibitors

4.1.1 Microglial cells express the Nogo-66 receptors and co-receptors

The myelin-associated inhibitors, i.e. MAG, Nogo-A and OMgp, bind to the same neuronal receptor, NgR1 (Liu et al., 2006). Additionally, it was shown that MAG also binds to the NgR2 and NgR3 receptor (Venkatesh et al., 2005). The expression of these receptors and the co-receptors that mediate myelin-associated inhibition has not been previously shown in isolated microglial cells. To test the expression of these receptors in microglia, microglial cells were purified from postnatal transgenic mice that express the enhanced green fluorescent protein (EGFP) under the microglial CX3CR1 promoter (Jung et al., 2000) (Fig.7A). The FACS isolated EGFP-positive microglia were analyzed with quantitative RT-PCR for the expression of the receptor complex that is known to mediate the inhibition by myelin in neurons (Fig.7B). Indeed, at the mRNA level the isolated microglia expressed all three homologues of the Nogo-66 receptor, i.e. NgR1, NgR2 and NgR3. Additionally, microglia expressed the co-receptors Lingo-1, EGFR and Troy, but not the low-affinity neurotrophin receptor p75. At the protein level, lysates from microglia cultured for 24 hrs were positive for the NgR1 (Fig.7C). These results show for the first time that the receptors and co-receptors involved in the myelin-associated axonal inhibition are also expressed in microglia and are in agreement with previous studies showing the presence of some of these receptors at the histological level in microglia (Satoh et al., 2005; 2007) and in macrophages, their counterparts in the PNS (Fry et al., 2007).

Microglia can be categorized based on their functional state in: i) 'resting', displaying a ramified morphology and weakly expressing molecules such as MHC II antigens, CD11c, CD40 and CD80 co-stimulatory molecules; or ii) 'activated', displaying a more round proliferative morphology and exhibiting regulation in the expression of these and other molecules (Ponomarev et al., 2005). Therefore, I examined whether the expression of these receptors is regulated dependent on the functional state of microglia. To this end, microglia were stimulated with lipopolysaccharide (LPS), a substance in the Gram-negative bacterial cell wall that is known to activate microglia both *in vivo* and *in vitro* (Häusler et al., 2002; Kloss et al., 2001). Microglial cells were plated for 24 hrs before

being stimulated with LPS (0.1 ng/ml) for another 24 hrs. The microglia were then stained with Mac-1, a marker raised against the α chain of the complement receptor 3 (CR3). The staining revealed the presence of 'resting' microglia that exhibited a ramified morphology with long and thin processes extending from their relatively small somata under non-stimulatory conditions (Fig.8Aa). After LPS stimulation, microglia were activated showing a more flat, round morphology with less and shorter extending processes and an increase in their soma size (Fig.8Ab). The mRNA expression profile analysis revealed an up-regulation of NgR1 and Lingo-1 expression, a down-regulation of NgR3, Troy, p75 and EGFR, and no change in the NgR2 expression (Fig.8B). These data show a regulation of the receptor complex expression in the different functional states of microglia.
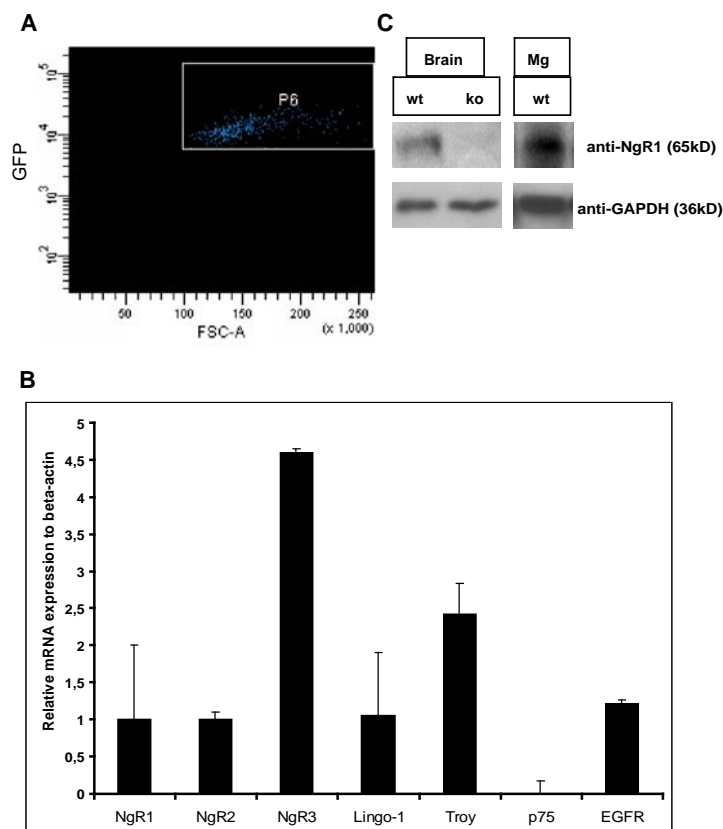
Figure 7. Microglial expression of the Nogo-66 receptors (NgRs) and co-receptors

A) Newborn P8-P10 heterozygous transgenic CX3CR1-EGFP mice were employed for FACS to isolate brain microglia in high purity. The EGFP-positive microglia could be clearly distinguished and isolated (window P6) from the total brain lysate.

B) The RNA from the FACS-sorted microglia was isolated, reversely transcribed, and the resulting cDNA was used for the quantitative RT-PCR expression profile of the NgRs and co-receptors. Beta-actin was used for standardization. Microglia expressed the NgR1 and the two homologues NgR2 and NgR3. The co-receptors Lingo-1, Troy and EGFR were also detected at the mRNA level but not the low-affinity

neurotrophin receptor p75. Mac-1 expression served as a microglial marker. The data represent the mean ± SEM of triplicates.

C) Mouse brain microglia (Mg) were cultured for 24 hrs and a western blotting analysis revealed the expression of the NgR1 at the protein level. Total brain lysates from wild-type and NgR1-deficient mice were used as positive and negative controls.

A

B
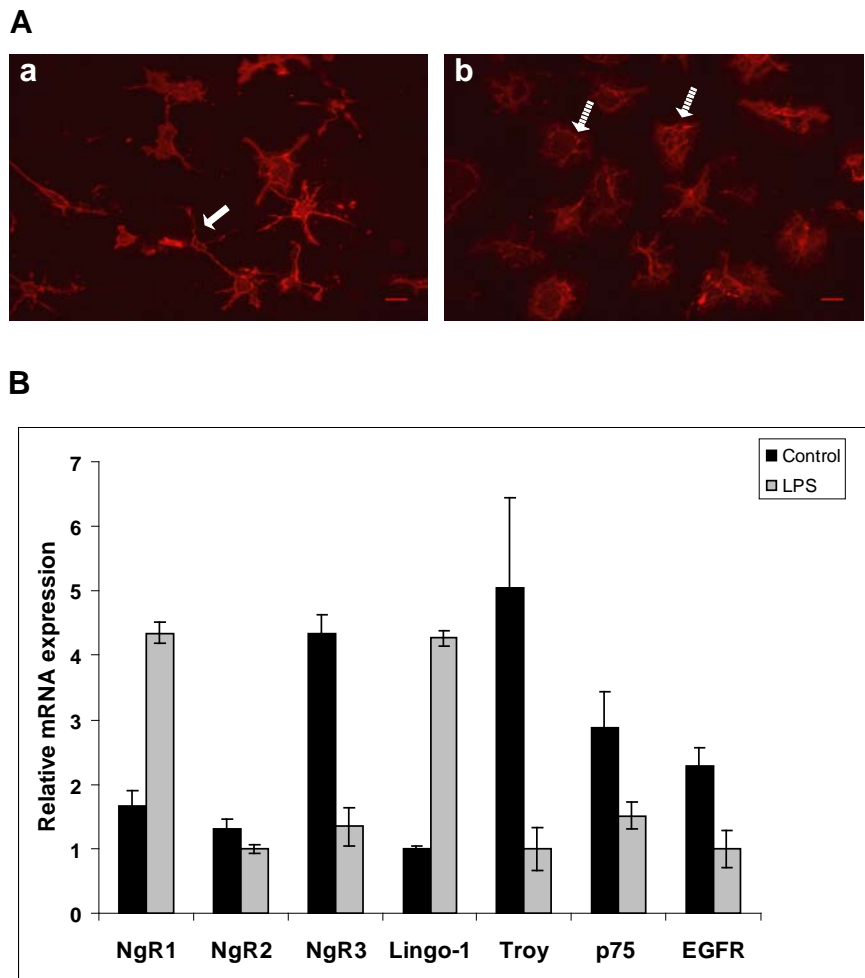
Figure 8. Microglial expression of the Nogo receptor complex after LPS stimulation

A) Mouse brain microglia cultured for 24 hrs on poly-L-lysine were visualized with immunoreactivity for the mouse $\alpha_M\beta_2$ integrin using the species-specific monoclonal antibody Mac-1. After 24 hrs, the microglia had several thin processes (arrows) and were ramified (a). A 1-day stimulation with LPS (0.1 ng/ml) led to microglial activation and a change in their morphology. Most of the microglia had shorter and thicker processes, while others adopted a round flat shape (dashed arrows) (b). Scale bars, 10 μm.

B) Quantitative RT-PCR expression analysis of the NgRs and co-receptors in the absence or presence of LPS stimulation revealed differences between the two culture conditions. There was an up-regulation of NgR1 and Lingo-1 and down-regulation of NgR3, Troy, p75 and EGFR. The expression of Ngr2 was not altered. The data represent mean values ± SEM.

4.1.2 Microglial process outgrowth is inhibited by MAG

The expression of the Nogo receptor complex in microglia implies a potential impact of the myelin-associated inhibitors on microglia. To test this hypothesis, an assay similar to the 'neurite outgrowth assay' described for neurons was employed (Mukhoparadhyay et al., 1994). Briefly, monolayers of CHO cells stably expressing MAG at the surface (Fig.9B), control-CHO cells, and Nogo-A-expressing 3T3 cells were established before plating microglia on top of these layers (Fig.9A).
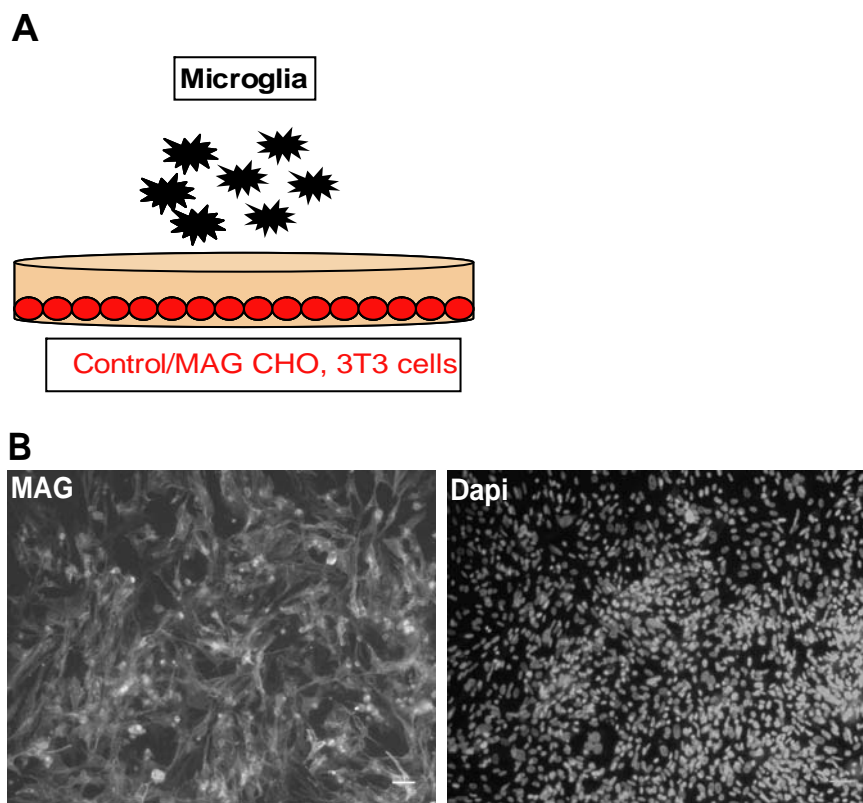
Figure 9. Microglial process outgrowth assay

A) A schematic figure of the microglial process outgrowth assay. Control and MAG-expressing CHO cells or Nogo-A-expressing 3T3 cell monolayers were established overnight. Microglia were plated on the monolayers and, after 4 hrs or 24 hrs, the co-cultures were fixed and stained.

B) Epifluorescence micrographs of MAG-expressing cell layers stained with anti-MAG and the nuclear marker Dapi. Scale bars, 20 μm.

Microglia isolated from wild-type mice were plated for 24 hrs on confluent monolayers of CHO and 3T3 cells. Microglia on top of control-CHO cells had a bipolar and often bore more processes (processed morphology), while, when cultured on the MAG-CHO cell layer, they were more round and with fewer processes (Fig.10A).

A

B

C
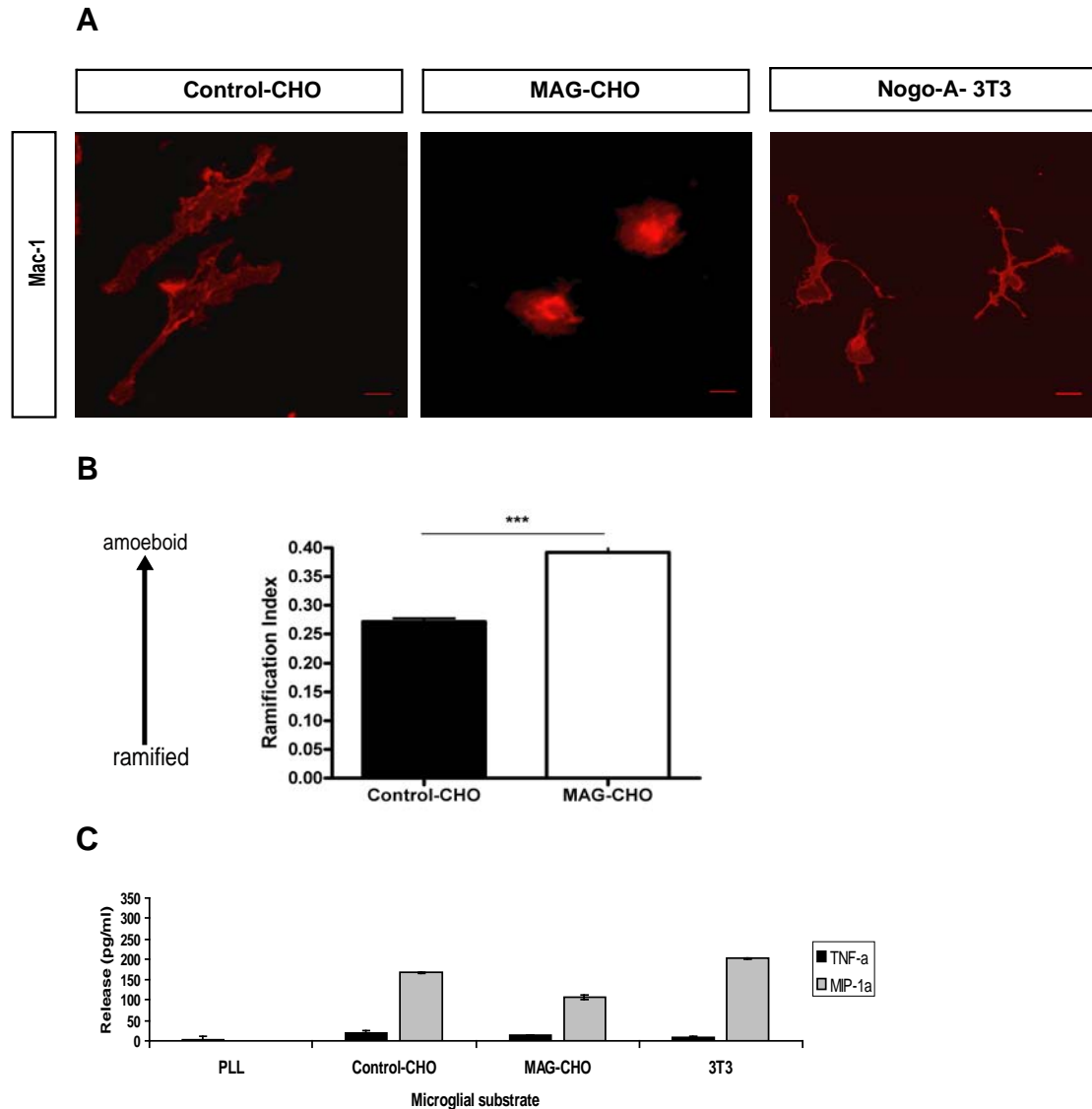
Figure 10. Microglial process outgrowth inhibition by myelin-associated glycoprotein

A) Microglia isolated from wild type P0-P2 mixed glial cultures were cultured on confluent monolayers of control or MAG-expressing CHO cells and Nogo-A-expressing 3T3 cells. The co-cultures were fixed after 24 hrs and stained for the $\alpha_M\beta_2$ integrin using the species-specific monoclonal antibody Mac-1. Microglia had a ramified and bipolar morphology when cultured on control-CHO cells, while they became more round and less processed when cultured on MAG-CHO cells. The microglial processes were not inhibited in the presence of Nogo-A-expressing 3T3 cells. Scale bars, 10 μm.

B) The microglial morphology was determined using the ramification index (RI=4π (cell area/cell perimeter^2)). This equation gives a value closer to 0 when the microglial cells bear more processes (more ramified) and values closer to 1 when the cells have fewer processes (more amoeboid). Microglial processes were inhibited by MAG, as microglial cells had a significantly higher RI on MAG-CHO cells (0.39±0.009) than on control-CHO cells (0.27±0.006). All the results represent the mean ramification index (±SEM) for 300-350 microglial cells from at least three independent experiments. A Student's *t-test* was applied (***P<0.0001).

C)   The supernatants of the microglial-CHO and microglial-3T3 co-cultures were analyzed with ELISA for chemokines and cytokines and compared with microglial cells plated on poly-L-lysine (PLL). There was no release of IL-6 and low release of MIP-1α and TNF-α, which is not a sign of microglial activation. The data represent mean values ± SEM of technical triplicates. Similar results were acquired from 3 independent experiments.

Interestingly, microglia had a ramified morphology when co-cultured with the Nogo-A-expressing 3T3 cells, indicating that Nogo-A does not or only partially inhibits microglial process outgrowth. Notably, microglia were more ramified on top of the 3T3 cells compared to the control-CHO cells (Fig.10A), suggesting that other molecules expressed at the surface of these cell lines might influence the microglial morphology and status. The microglial morphological changes were quantified by the ramification index (RI); this is a ratio between the cell surface area and the cell perimeter, giving a value between 0 and 1 dependent on whether they have more processes (more processed morphology) or they are more round (less processed morphology) respectively. Microglia plated on MAG-CHO cells had a significantly increased mean RI (0.39±0.009) compared to control-CHO co-cultures (0.27±0.006), indicating a less processed morphology (Fig.10B). In order to exclude the possibility that microglial process retraction was due to MAG-mediated microglial activation, the supernatants of the co-cultures were tested for cytokine and chemokine release (Fig.10C). Microglia plated on poly-L-lysine were used as a control. The profile of TNF-a, IL-6 and MIP-1a revealed a release that was undetectable or in low amounts, supporting the lack of microglial activation when co-cultured with CHO or 3T3 cells. Taken together, these data illustrate that MAG and not Nogo-A act as an inhibitor of microglial process outgrowth *in vitro*.

4.1.3 MAG-mediated microglial process inhibition is NgR1 and Rho-A dependent

The molecular mechanism, which leads to neuronal growth cone collapse after encountering MAG, involves the binding to the NgR1 receptor and the co-receptors and downstream activation of RhoA signalling (Fournier et al., 2003; Mahta et al., 2007; Vinson et al., 2001). Therefore, I examined whether NgR1 and RhoA are involved in MAG-mediated microglial process inhibition. Microglia were isolated from NgR1-deficient mice and plated on control or MAG-expressing CHO feeder layers for 24 hrs.

Interestingly, microglial cells cultured on MAG-CHO cells had a less processed morphology compared to those cultured on control-CHO cells (Fig.11A).

A

B
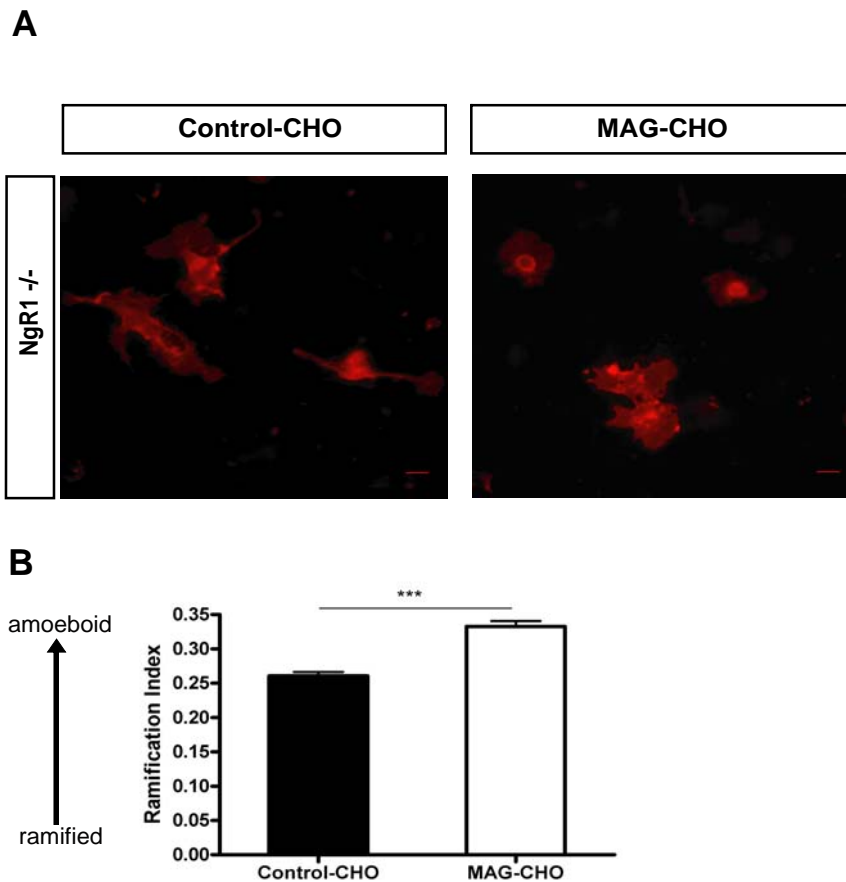
Figure 11. MAG-mediated microglial process inhibition is partially NgR1-dependent

A) Microglia isolated from NgR1-deficient P0-P2 mixed glial cultures were cultured on confluent monolayers of control or MAG-expressing CHO cells. The co-cultures were fixed after 24 hrs and stained for Mac-1. Microglia had a ramified and often bipolar morphology when cultured on control-CHO cells, while they become more round and less processed when cultured on MAG-CHO cells. Scale bars, 10 μm.

B) The microglial morphology was determined by the ramification index (RI). NgR1-deficient microglia had a significantly higher RI on MAG-CHO cells (0.33 ± 0.008) than on control-CHO cells (0.26 ± 0.006). All results represent the mean RI±SEM for 300-350 microglial cells from at least three independent experiments. A Student's *t-test* was applied (***$P<0.0001$).

The quantification of the microglial ramification index (RI) revealed that NgR1-deficient microglia on MAG-CHO cells were significantly more ramified (0.33 ± 0.008) compared to microglia on control-CHO cells (0.26 ± 0.006) (Fig.11B), but this was significantly reduced compared to the ramification index of wild-type microglia plated on MAG-CHO

cells (0.39±0.009) (Fig.10B). These results suggest that MAG-elicited inhibition is partially NgR1-dependent and that other receptors might be involved additionally.
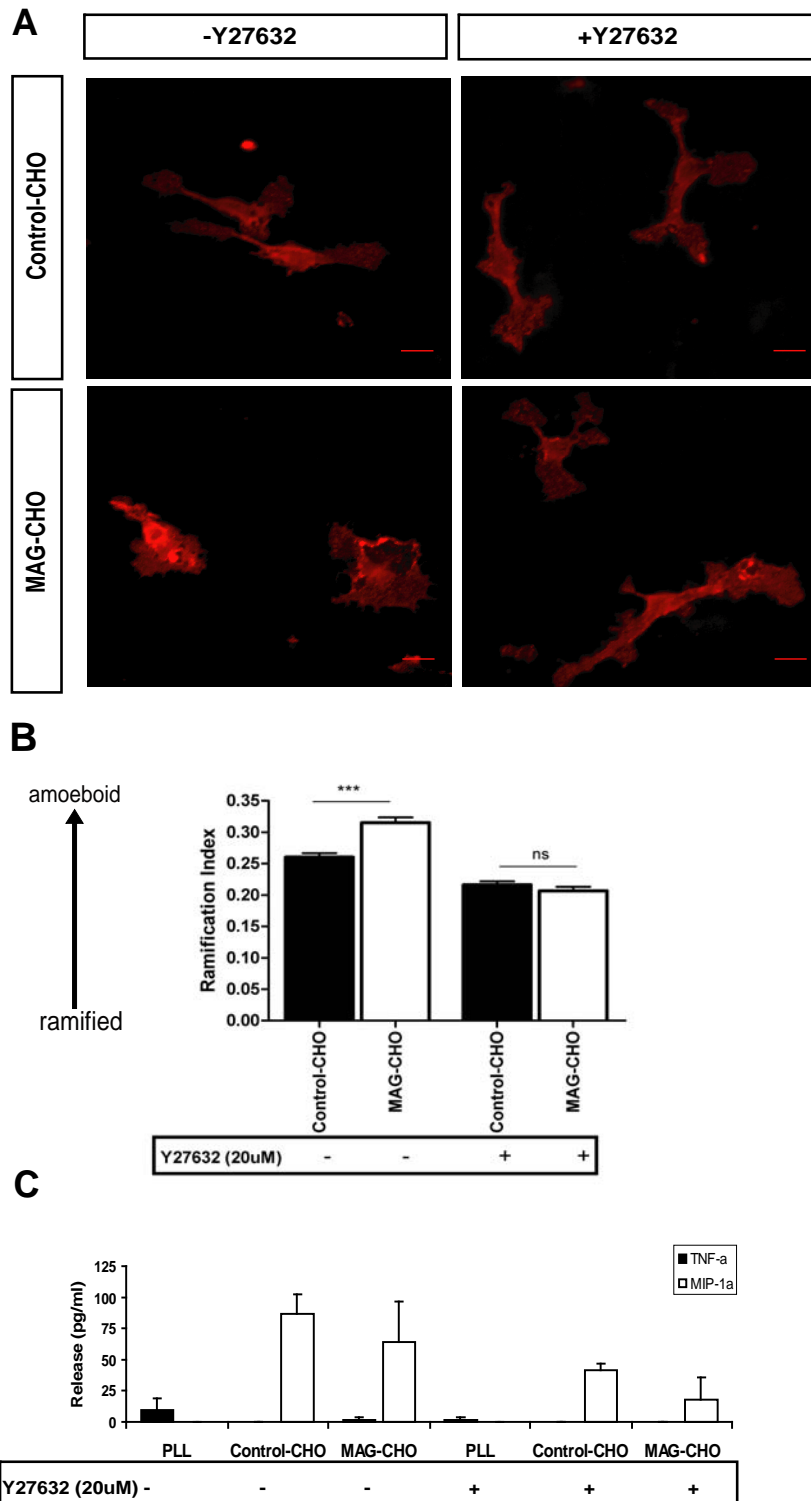
Figure 12. MAG-induced microglial inhibition involves the activation of RhoA

A) Microglia isolated from wild type P0-P2 mixed glial cultures were cultured on confluent monolayers of control or MAG-expressing CHO cells, in the presence or absence of the Rho-associated kinase inhibitor,

Y27632 (20 μM). The co-cultures were fixed after 4 hrs and stained for Mac-1. Microglia had a ramified morphology when cultured on control-CHO cells, while they become more round and less processed when cultured on MAG-CHO cells. In the presence of the Rho kinase inhibitor, Y27632, the MAG-elicited microglial process inhibition was blocked and the cells had a more processed morphology. Scale bars, 10 μm.

B) The microglial morphology was determined by the ramification index (RI=4π (cell area/cell perimeter^2)). This quantification revealed that microglial cells had significantly smaller RI on control-CHO cells (0.26±0.007) than on MAG-CHO cells (0.32±0.008). Additionally, this inhibition was blocked in the presence of the Y27632 inhibitor, as there was no significant difference between the RI of microglial cells cultured on MAG or control- CHO cells (0.20±0.007 and 0.21±0.006 respectively). All results represent the mean RI ±SEM for 300-350 microglial cells from at least three independent experiments. A Student's *t-test* was applied (***$P<0.0001$).

C) The supernatants of the microglial-CHO co-cultures in the absence (-) or presence (+) of the Rho-associated kinase inhibitor Y27632, were analyzed with ELISA for chemokine and cytokine release and compared with microglial cells plated on poly-L-lysine (PLL). There was no release of TNF-α and low release of MIP-1α excluding the possibility of microglial activation in these culturing conditions. The data represent mean values ± SEM of technical triplicates. Similar results were acquired from at least 3 independent experiments.

To assess whether the downstream cascade from all receptors involved leads to RhoA activation, the microglial/CHO co-cultures were incubated with Y27632, a Rho-associated kinase (ROCK) inhibitor. Microglial cells isolated from wild-type mice were plated on confluent monolayers of MAG-CHO or control-CHO cells for 4 hrs. Under control conditions, even for as short a period as 4 hrs, microglia displayed an elongated and processed morphology (Fig.12A). Notably, microglial process outgrowth was strongly inhibited on MAG-CHO cells and microglia showed an amoeboid morphology. In the presence of the ROCK inhibitor, MAG-elicited microglial inhibition was fully reversed (Fig.12A). The quantification of the ramification index (RI) revealed that microglia plated on MAG-CHO cells had a significantly increased mean RI (0.32±0.008) compared to control-CHO co-cultures (0.26±0.007), indicating a less processed morphology. Interestingly, MAG-mediated microglial process inhibition was reversed in the presence of the Rho-associated kinase inhibitor Y27632 and was not significantly different from the control condition (change from 0.21±0.006 in the control-CHO to 0.20±0.007 in the presence of MAG) (Fig.12B). To exclude any microglial effects of the CHO cells in the presence or absence of the ROCK inhibitor, the supernatants of the co-

cultures were tested for cytokine and chemokine release. The ELISA analysis of the supernatants showed no signs of microglial activation compared to microglia plated on PLL (Fig.12C). Taken together, these data suggest that the downstream signalling cascade that leads to microglial process inhibition after encountering MAG involves the activation of the Rho-associated kinase.

4.1.4 Microglia avoid myelin-associated glycoprotein as a substrate in a stripe assay

As an independent approach, a substrate stripe assay was employed to assess the repulsive influence of MAG on microglia in more detail and without the influence of other molecules expressed at the surface of CHO cells. Recombinant proteins containing only the extracellular domain of MAG (full length Ig domains 1-5 or "truncated" containing only the Ig domains 1-3) were purified from CHO cells (Fig.13). The fully glycosylated protein (MAG d1-5) was purified from wild-type CHO cells and the proteins lacking N-glycans were purified in mutant CHO cells (MAG d1-5L and MAGd1-3L). These proteins were further used as soluble proteins or as a substrate for culturing microglia.
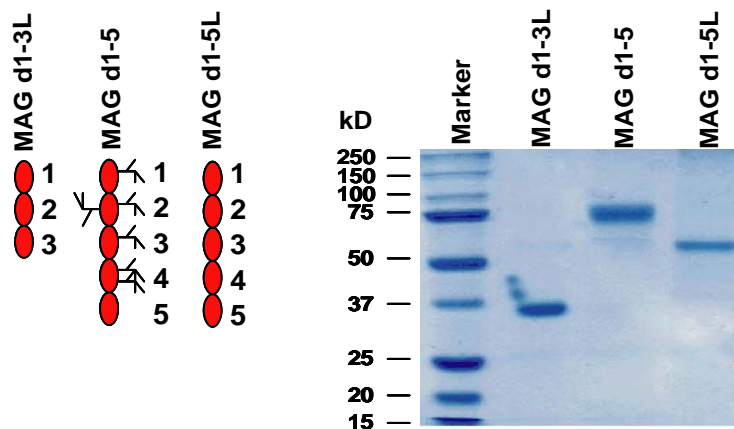
Figure 13. Recombinant MAG proteins

The full length of the extracellular domain of MAG d 1-5, as well as a mutant form comprising the Ig-like domains 1-3, was purified in CHO cells. CHO cells stably expressing wild type MAG were used to purify fully glycosylated recombinant proteins (MAG d1-5, ~80kDa), while CHO cells lacking glycosylation enzymes and stably expressing mutant MAG were used for purification of proteins lacking N-glycans and sialic acid (MAG d1-5L, ~65kDa or MAG d1-3L, ~40kDa).

In the stripe assay, the entire coverslip was pre-coated with poly-L-Lysine (PLL) and additional stripes of MAG were used to test its inhibitory activity. This assay could reflect the *in vivo* situation where microglial processes can grow near to or avoid MAG. The microglial processes displayed a clear preference for the PLL-lanes, avoiding the MAG-coated lanes (Fig.14A). Interestingly, microglia aligned their processes near the MAG stripes without crossing, suggesting that MAG is not permissive but rather gives a direction to microglial process outgrowth. As previously shown in neurons, MAG-elicited neurite outgrowth inhibition does not depend on the sialic acid binding and the inhibitory site on MAG is localized within the Ig domain 5 (Tang et al., 1997; Cao et al., 2007). In order to assess which MAG domains are responsible for microglial inhibition, a shortened form of MAG lacking the domains 4 and 5 (MAG d1-3) was employed (Fig.14B). This recombinant protein was expressed in a mutant CHO cell line and therefore lacked any N-linked carbohydrates and sialic acid. Interestingly, the microglial cells were repelled by MAG, even in the absence of N-glycosylation and sialic acid and the absence of the Ig domains 4/5. In order to confirm the role of NgR1 in MAG-mediated microglial process inhibition, the same assay was repeated with NgR1-deficient microglial cells (Fig.14C). Quantification of the microglial cells growing or avoiding the MAG stripes revealed that the full length MAG (MAG d1-5) was not permissive for wild-type microglial process outgrowth (86.2±2.5% of total cells on PLL), while a small number of microglial cells grew completely or partially on MAG stripes (13.8±2.5% of total cells) (Fig.14E). The absence of N-glycosylation and the Ig domains 4/5 did not lead to an increase of microglial growth on the MAG lanes (88.3±2.2% of total cells on PLL and 11.8±2.2% on MAG). Quantification of the NgR1-deficient microglial cells growing in or crossing the MAG d1-5 stripes revealed a significant increase in the number of cells compared to wild-type microglia (35±0.9% of total cells and 13.8±2.5% respectively), but there was significantly more avoidance of the MAG stripes compared to PLL (35±0.9% of total cells on MAG compared to 65±0.9% on PLL) (Fig.14E). To make sure that these differences were not due to technical handling, FITC-conjugated streptavidin was used as a control (Fig.14D). Indeed, 69.8±3.4% of the total number cells grow (19.5±2.7%) or cross (50.3±1%) the streptavidin stripes. Taken together, these results confirm the MAG-elicited microglial process inhibition and show that this is dependent on the MAG Ig domains 1-3 and partially dependent on the microglial NgR1.
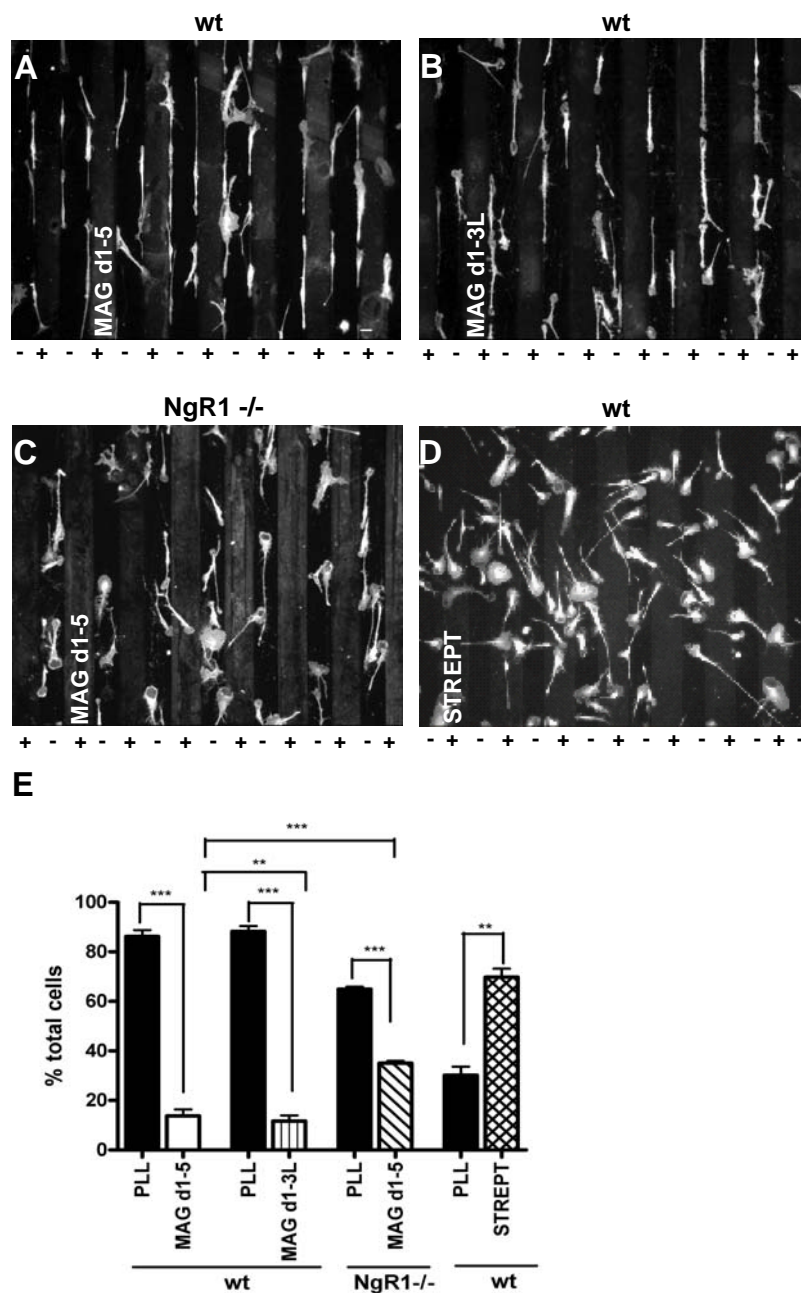
Figure 14. MAG is an inhibitory substrate for microglial cells

Coverslips were precoated with poly-L-Lysine (PLL). Full-length MAG (d1-5) (A,C), mutant MAG (d1-3) (B) or FITC-conjugated streptavidin (D) was added in a stripe pattern. Wild-type (A,B,D) and NgR1-deficient (C) microglial cells were plated for 24 hrs and coverslips were fixed and stained for Mac-1 and MAG.

A-D) Microglial cells were plated on alternating stripes of PLL/MAG d1-5 (+) or PLL (-) stripes. Note that microglial processes aligned themselves along the MAG stripes but avoid crossing them (A). In the absence of the MAG Ig-like domains 4 and 5, microglial cells avoided the MAG stripes and preferred the PLL lanes (B). The majority of NgR1-deficient microglia avoided MAG d1-5 lanes, but there was an increased

number of microglia growing on or crossing the MAG stripes (C). As a control for the microglial growth behaviour in a stripe pattern of substrates, FITC-conjugated streptavidin was applied. Microglia were not inhibited by streptavidin (D). Scale bars, 20 μm.

E) The quantification of microglial process outgrowth on the different substrates reveals that there was a significantly lower number of microglia growing on or crossing MAG stripes (13.8±2.5%) compared to PLL (86.2±2.5%) and this repellence depended on the Ig domains 1-3 (88.3±2.2% on PLL). Additionally, the absence of NgR1 led to a partial improvement of the MAG inhibition, but was still significantly different from the PLL stripes (65±0.9% of total cells on PLL and 35±0.9% growing or crossing MAG stripes). In the control, streptavidin allowed the outgrowth of microglial processes. The results represent the mean percentage of the total cell number ± SEM for more than 200 microglial cells per experiment and at least four independent experiments. Student's *t*-test was applied (***P<0.0001, **P=0.0012).

4.1.5 Soluble myelin-associated glycoprotein induces microglial inflammatory response.

MAG does not only exist as a transmembrane protein, but also as a soluble MAG fragment solely consisting of the extracellular domain, termed dMAG, previously identified in the CSF of normal humans and patients with demyelinating diseases (Yanagisawa et al., 1985). It was additionally shown *in vitro* that soluble MAG fragments can be released during myelin preparation and that this retains its neurite inhibitory properties (Tang et al., 1997). Therefore, the microglial response to soluble dMAG was further assessed. Primary microglial cells were treated with different concentrations of the soluble full-length MAG d1-5 (Fig.15A,D,G,J), the non N-glycosylated full length MAG d1-5L (Fig.15B,E,H,K), or the mutant form of MAG d1-3L (Fig.15C,F,I,L). The secretion of cytokines and chemokines, such as interleukin-6 (IL-6), tumor necrosis factor (TNF-α), KC (murine equivalent of growth regulatory oncogene-α (GROα)) and macrophage inflammatory protein-1α (MIP-1α), was assessed in the supernatants after 20 hrs. Surprisingly, the incubation of primary microglia with soluble dMAG resulted in a dose-dependent release of different cytokines and chemokines. Untreated cultures were devoid of any measurable cytokine or chemokine release (data not shown) and lipopolysaccharide (LPS) (1ng/ml) stimulation was used as a reference for known microglial responses. The MAG-elicited cytokine and chemokine release was normalized to the LPS-induced release and presented as a percentage. Interestingly, the microglia showed a maximum response after 1 μg/ml dMAG exposure and this release was not dependent on the glycosylation, sialic-acid binding or the Ig domains 4/5 of MAG. These

results suggest that soluble dMAG has a novel role, namely that of inducing a strong microglial inflammatory response when presented in high concentrations and this effect is dependent on the Ig domains 1-3.
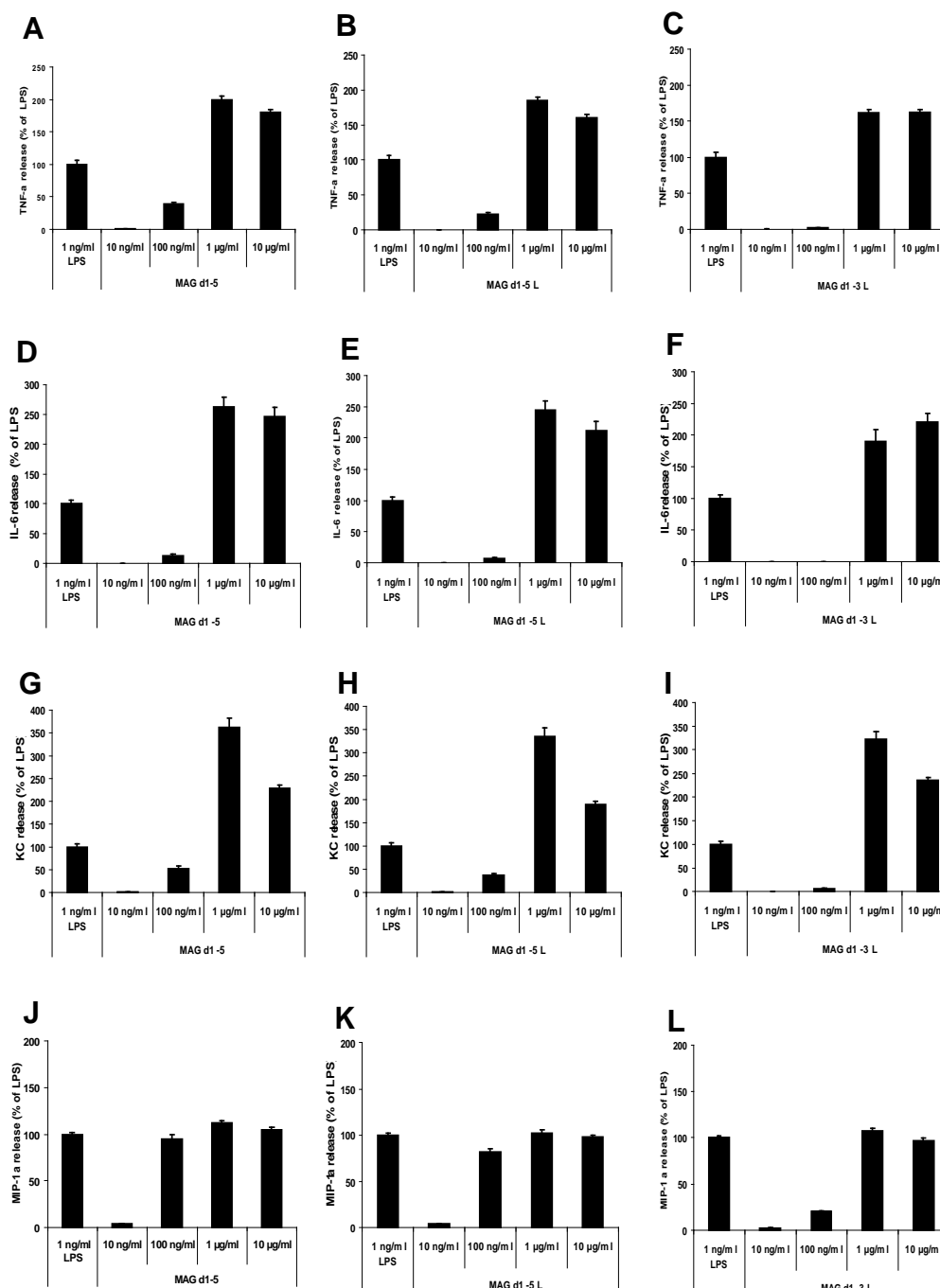
Figure 15. Effects of soluble dMAG in primary microglial cytokine and chemokine release
Primary microglial cells were plated for 24 hrs and then incubated with different concentrations of recombinant glycosylated full-length MAG d1-5 (A,D,G,J), non- glycosylated full-length MAG d1-5L (B,E,H,K), or mutant MAG d1-3L (C,F,I,L). After 20 hrs, the supernatants were collected and tested for

cytokines and chemokines. Lipopolysaccharide (LPS)-induced microglial stimulation was used as an internal control. There was a dose-dependent response of microglia to different concentrations of soluble dMAG. The microglial response to soluble MAG did not depend on N-glycosylation or the Ig-like domains 1-3 and it occurred in a dose-dependent manner. The data is normalized to control (LPS) and expressed as mean ± SEM (n ≥ 12, at least three experiments).
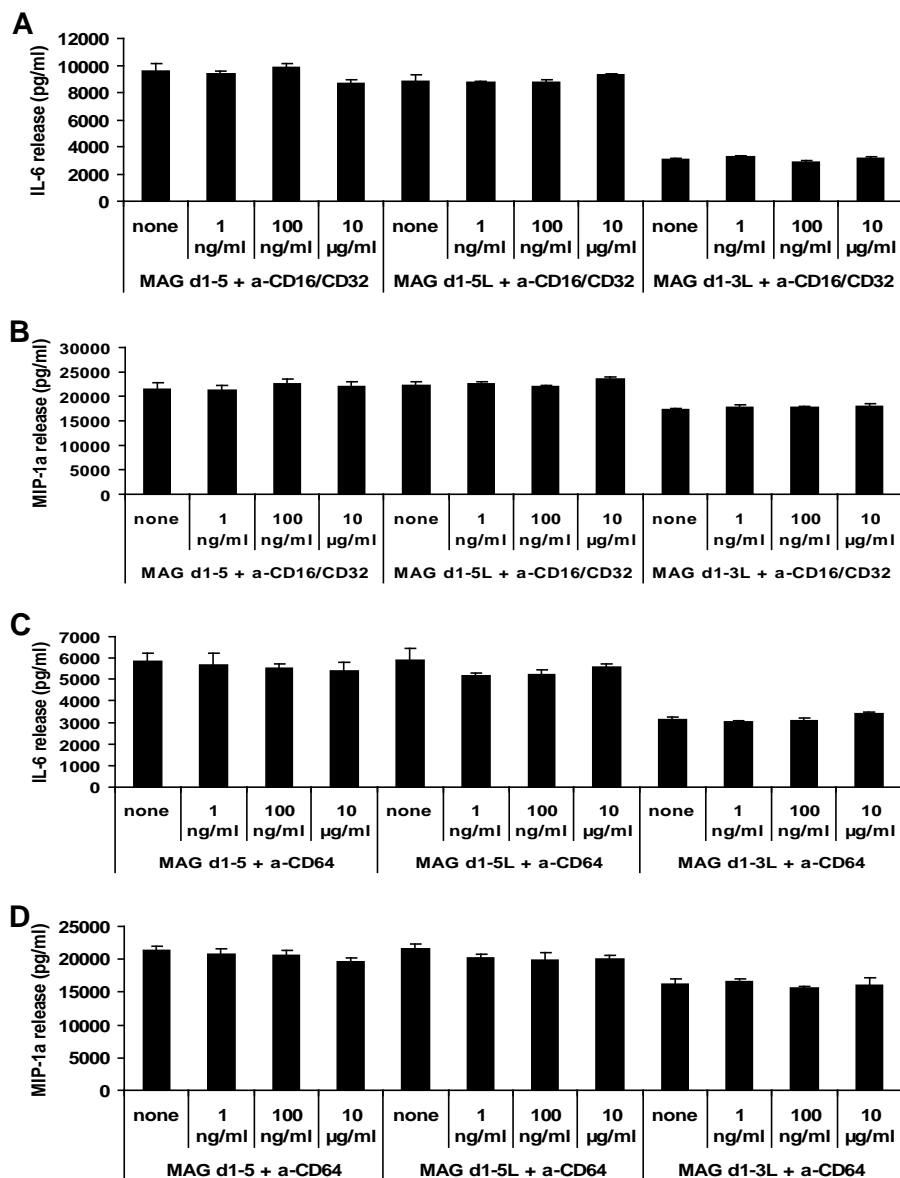
Figure 16. Blocking the Fcγ receptors does not alter the microglial inflammatory response to soluble MAG

Primary microglial cells were plated for 24 hrs and then incubated shortly with different concentrations of Fcγ receptor blocking antibodies before plating in the presence of 1 μg/ml of recombinant MAG and different concentrations of the blocking antibodies. The supernatants were collected after 20 hrs and analyzed for cytokine and chemokine release. Blocking the Fcγ receptors II and III (CD32/CD16) did not alter the inflammatory response of microglia in the presence of the soluble MAG proteins (A,B).

Additionally, blocking the Fcγ receptor I (CD64) in the presence of the soluble MAG proteins did not modify the release of IL-6 or MIP-1a (C,D). The data is expressed as mean ± SEM (n ≥ 6, at least two experiments).

The recombinant MAG proteins were purified as Fc-chimeras and then the Fc-tag was removed by enzymatic digestion with a 3C protease. To test whether any Fc-portion was uncleaved or co-purified with these proteins, western blot analysis was performed using an antibody directed against the Fc and did not reveal any traces of Fc (data not shown). In order to exclude any possibility that there might be low, uneasily detectable amounts of Fc as impurities that could trigger the microglial inflammatory response, all three Fcγ receptors were blocked by incubating with the specific antibodies (Fig.16).

In vivo, microglial cells express at least three Fc receptors, namely FcγRI (CD64), II (CD32) and III (CD16), and these receptors mediate phagocytosis and cytotoxicity *in vitro* (Ulvestad et al., 1994). The microglia exhibited the maximum inflammatory release when 1 μg/ml of recombinant MAG proteins was used (Fig.15). Therefore, this amount (1 μg/ml) and different concentrations of the blocking antibodies were used to test whether the inflammatory response would be altered. Blocking the FcγRII and FcγRIII did not lead to any change in the MAG-mediated microglial inflammatory response (Fig.16A,B). Additionally, blocking the FcγRI did not change the MAG-induced microglial inflammatory response (Fig.16C,D). These results show that there is no interference from any Fc-portions possibly co-purified with the recombinant MAG in the soluble MAG-elicited microglial inflammatory response and that the Fc receptors are not involved in the MAG-microglial signalling.

4.1.6 Surface-presented MAG-mediated microglial response does not interfere with the TLR pathways

Twelve mouse toll-like receptors (TLRs) have been identified that are important for the front-line defence against pathogens, even in the brain (Hanisch et al., 2008). Recent studies have shown that these receptors might not only signal in the presence of pathogens, but also due to endogenous signals that indicate threats to the brain's

structural and functional integrity (Larsen et al., 2007). Consequently, I set about testing whether the function of surface-presented MAG is not only restricted to microglial process outgrowth, but might interfere with other pathways by providing anti-inflammatory signals. To test whether the MAG-elicited microglial signalling interferes with the TLR pathways, known TLR agonists for the toll-like receptors 1, 2, 4 and 6 were used. Microglia were cultured on control and MAG-CHO layers and stimulated with Pam3SK4 (a TLR 1/2 agonist), LPS (a TLR4 agonist) and MALP-2 (a TLR 2/6 agonist) (Fig.17). In the absence of TLR agonists, there was no microglial inflammatory response, as measured for TNF-α (Fig.17A), KC (Fig.17B), MIP-1α (Fig.17C) and IL-6 (data not shown). Surprisingly, the addition of Pam3SK4 and LPS did not stimulate an inflammatory response in the microglia (Fig.17), suggesting that other molecules expressed on the surface of the CHO cells might suppress this activity. On the other hand, MALP-2 led to a low KC release and increased MIP-1α release but without any difference between the control and MAG-CHO/microglia co-cultures. These data suggest that there might be an involvement of the MAG-mediated pathway with the TLR 2 and 6-related pathways.
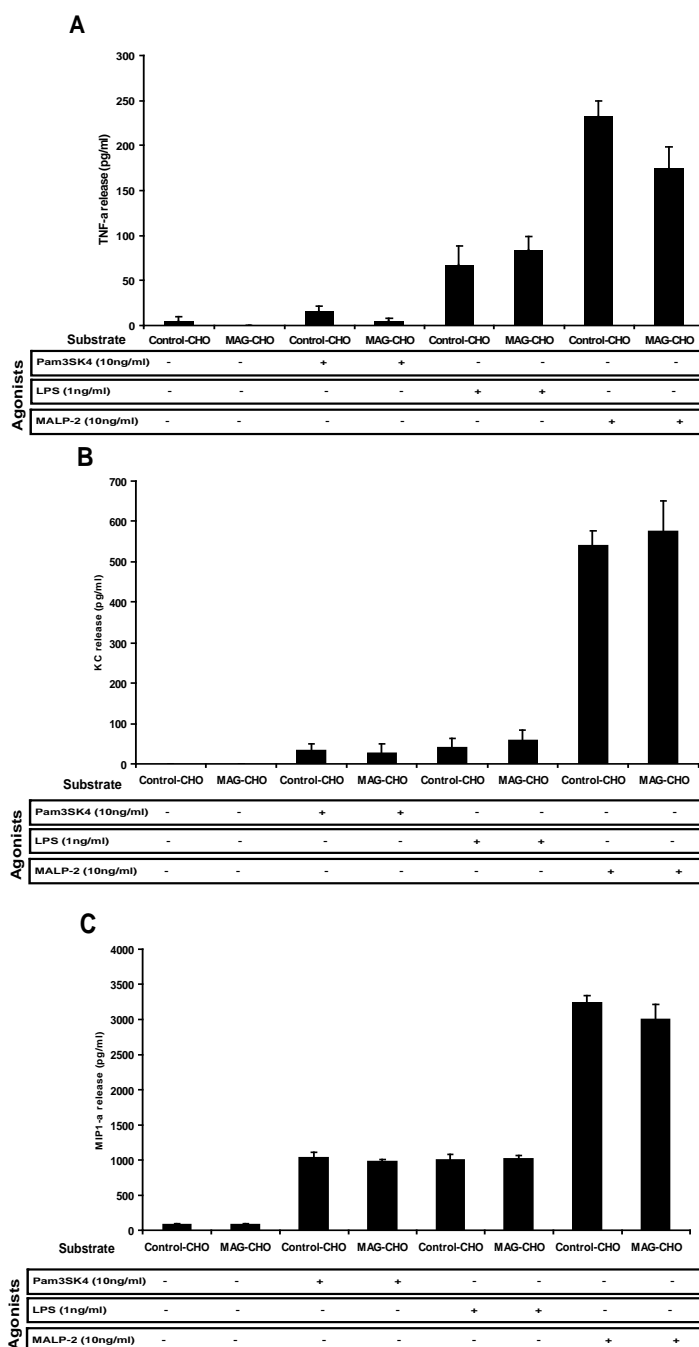
Figure 17. Surface presented MAG does not involve common pathways with the toll-like receptors (TLRs) in microglia

Primary microglial cells were plated for 24 hrs on confluent monolayers of control and MAG-expressing CHO cells in the absence or presence of the toll-like receptors (TLRs) agonists Pam3SK4 (TLR 1/2), LPS (TLR 4) and MALP-2 (TLR 2/6). The analysis for TNF-α (A), KC (B) and MIP-1α (C) release revealed a general suppressive effect of other surface-expressed molecules on CHO cells for the Pam3SK4 and LPS stimulation. In case of the MALP-2 stimulation, there was no difference in the microglial response in the presence of the agonist and in the presence or absence of MAG. The data is expressed as mean ± SEM (n ≥ 6, at least three independent experiments).

A

Substrate	PLL	MAG	PLL	MAG	PLL	MAG	PLL	MAG
Pam3SK4 (10ng/ml)	-	-	+	+	-	-	-	-
LPS (1ng/ml)	-	-	-	-	+	+	-	-
MALP-2 (10ng/ml)	-	-	-	-	-	-	+	+

B

Substrate	PLL	MAG	PLL	MAG	PLL	MAG	PLL	MAG
Pam3SK4 (10ng/ml)	-	-	+	+	-	-	-	-
LPS (1ng/ml)	-	-	-	-	+	+	-	-
MALP-2 (10ng/ml)	-	-	-	-	-	-	+	+

C

Substrate	PLL	MAG	PLL	MAG	PLL	MAG	PLL	MAG
Pam3SK4 (10ng/ml)	-	-	+	+	-	-	-	-
LPS (1ng/ml)	-	-	-	-	+	+	-	-
MALP-2 (10ng/ml)	-	-	-	-	-	-	+	+
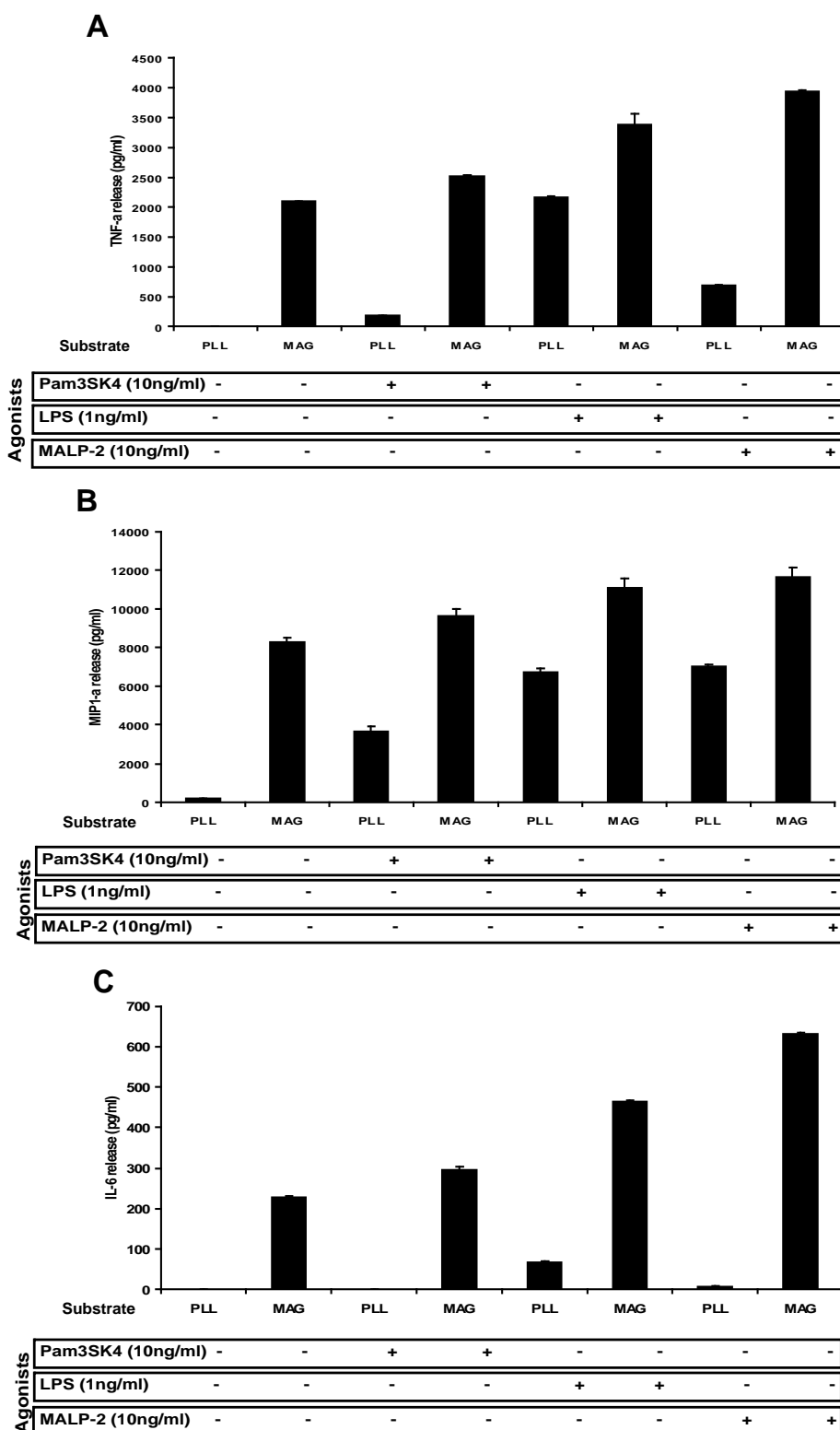
Figure 18. MAG-elicited microglial response does not involve common pathways with the toll-like receptors (TLRs)

Primary microglial cells were plated for 24 hrs on poly-L-lysine (PLL) and MAG or only PLL-coated coverslips in the absence or presence of the toll-like receptors (TLRs) agonists Pam3SK4 (TLR 1/2), LPS (TLR 4) and MALP-2 (TLR 2/6). The analysis for TNF-α (A), MIP-1α (B) and IL-6 (C) release showed a

71

distinct microglial response in the presence of the TLR agonists independent of the presence of MAG. The data is expressed as mean ± SEM (n ≥ 6, at least three independent experiments).

To better assess the involvement of the TLR 1, 2, 4 and 6 pathways by using TLR agonist stimulation, such as Pam3SK4, LPS and MALP-2, without the influence of the CHO cells, the recombinant MAG protein (MAG d1-5) was employed. Coverslips coated with PLL and MAG or PLL only were used as substrates for microglia in the presence of the TLR agonists (Fig.18). Surprisingly, there was an inflammatory response when the microglia were cultured on MAG, even in the absence of any TLR agonist, probably due to an amount of unbound soluble protein that can elicit such an effect. Taking this into account, I analyzed whether the addition of the TLR agonists would have an additive effect on the chemokine and cytokine release. The results of this study show that the MAG-microglial interaction probably does not involve common receptors or downstream signalling with the toll-like receptor 1, 2, 4 and 6-related pathways.

4.1.7 In vivo imaging of the microglial behaviour reveals changes in the absence of MAG

To further investigate whether MAG acts as an inhibitor of microglia *in vivo*, two-photon laser scanning microscopy was employed in the dorsal column of the spinal cord of anaesthetized mice. To study microglial behaviour in the living mice, wild-type and MAG-deficient mice were crossed with transgenic mice in which microglia express the enhanced green fluorescent protein (EGFP) and neurons express the enhanced yellow fluorescent protein (EYFP) (Jung et al., 2000; Winter et al., 2007). Microglia, as previously shown (Davalos et al., 2005), had very motile processes in the normal brain and this movement was adjusted in the case of 'danger signals'. Based on the working hypothesis MAG acts as an inhibitor of microglial process outgrowth, so the overall microglial process outgrowth should be altered in the absence of MAG. This change would not be due to microglial activation, as it was previously shown that the absence of MAG in young animals does not lead to microglial activation (Loers et al., 2004).
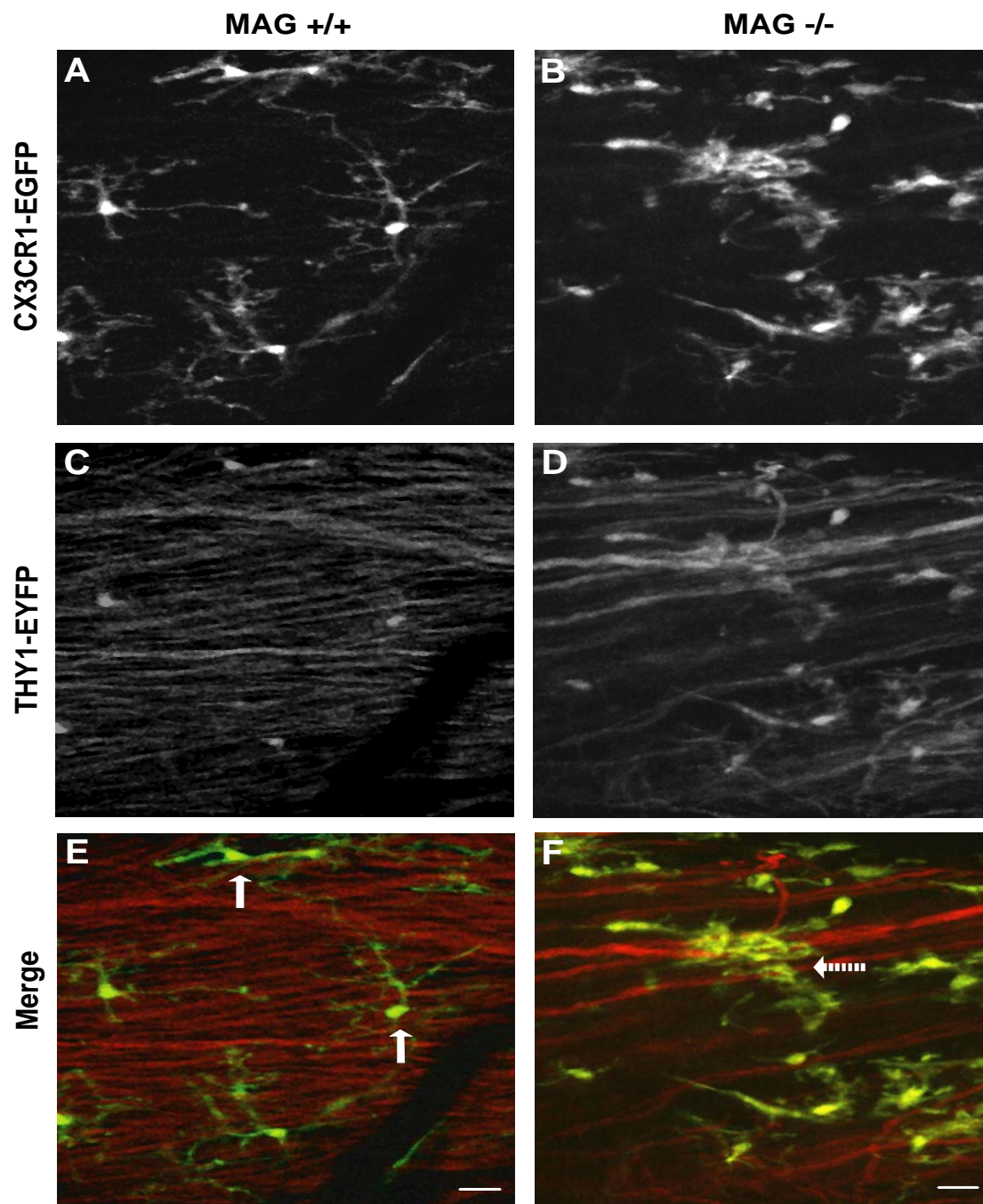
Figure 19. Altered microglial morphology in the absence of MAG in the spinal cord of anaesthetized mice

In vivo imaging of GFP-positive microglial cells and YFP-positive axons in the spinal cord of wild type (A, C, E) or MAG-deficient mice (B, D, F) revealed differences in the microglial morphology.

A, C, E. Microglial cells had small somata and a large number of thin and extremely ramified processes that extend along the myelinated axons in a distinct spatial pattern (arrows).

B, D, F. Microglia changed their morphology in the absence of MAG. There was a loss of microglial process ramification and the microglia somata were in closer proximity. It is notable that an increased number of microglial processes associates with the neighbouring axons (dashed arrow). Scale bars, 20 µm.

Indeed, there was a striking difference in the overall pattern of microglial process distribution in the absence of MAG. In contrast, the microglial somata and main branches remained morphologically stable over the period of observation independently of the presence or absence of MAG, and there was no obvious difference in the overall microglial process movement (data not shown). In the wild-type mice, thin and ramified microglial processes were extended along the myelinated axons (arrows) displaying a distinct cell-to-cell territorial distribution (Fig. 19A, C, E). Strikingly, in the absence of MAG, microglial processes lost this distribution pattern and they were apposed to neurons (dashed arrow) in an increased density (Fig. 19B, D, F). This data suggests that *in vivo* surface-presented MAG and/or low amounts of soluble MAG that is possibly shed from the membrane act as an inhibitor of microglial process outgrowth, which also determines their distribution.

4.1.8 Activation of microglial cells leads to myelin 'attack' in the absence of MAG

Next, an *in vivo* model where microglia are activated was used to investigate whether MAG-mediated microglial process inhibition has a physiological role in a disease situation. In adult PLP-deficient mice, an increased number of axonal swellings is present and accompanied by microglial activation (Griffiths et al., 1998). In a previous study, young MAG-deficient mice showed no signs of microglial activation as revealed by Mac-3 staining, a marker of microglial activation (Loers et al., 2004). In the same study, the number of Mac-3-positive activated microglia was significantly higher in aged MAG-deficient mice than in the wild-type controls. Therefore, PLP-deficient mice were crossed with MAG-deficient mice to yield double mutants and to assess the role of MAG with respect to microglial behavior in a disease model. In a previous study, the early onset of axonal degeneration in MAG*PLP double mutants was reported (Uschkureit et al., 2000). In order to assess the microglial status in this double-deficient mouse model ('resting' versus 'activated' microglia) paraffin-embedded tissue was stained with Mac-3 (Fig.20). In the current study, low microglial activation was observed in the single PLP- (b) or MAG-deficient mice (c), and strong Mac-3 immunoreactivity in MAG*PLP double mutants (a). Interestingly, the microglial activation observed in the double mutants was much stronger than the additive activation in PLP- or MAG- single mutants.

| MAG -/- PLP -/Y | MAG +/- PLP -/Y | MAG -/- PLP +/Y |
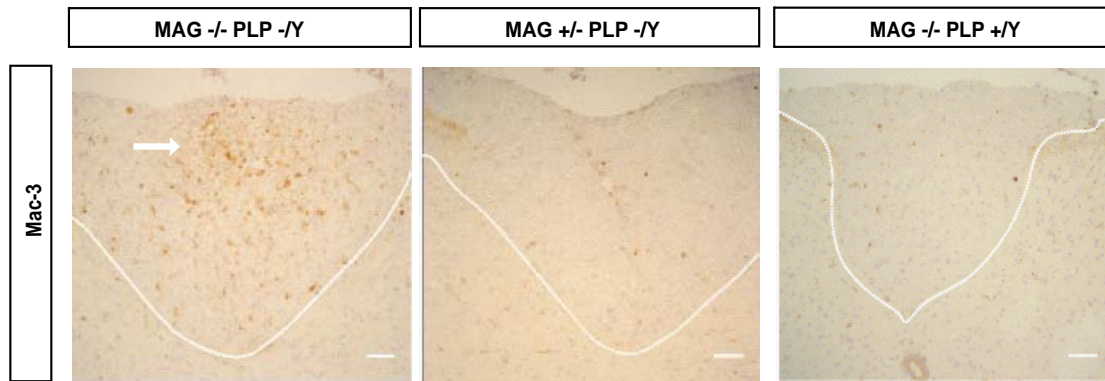
Figure 20. Increased microglial activation in the MAG*PLP double mutant mice

Paraffin-embedded tissue from MAG*PLP double-deficient (a), PLP -deficient (b) and MAG-deficient mutant mice (c) at the age of 13 months was immunostained for Mac-3 and examined by light microscopy. There was an increased immunoreactivity in the dorsal column of the spinal cord of the MAG*PLP double mutants (a) (arrow), while there were only a few Mac-3 positive cells in any of the single mutants (b,c). Scale bars, 25 μm.

To further assess the interaction of the myelin sheath with microglia, the mice were processed for electron microscopy. An earlier study of MAG*PLP double mutants in our lab (unpublished data) revealed the presence of microglial cells invading the periaxonal space although there was no prior report of such a case in any of the single mutants or other myelin protein mutants. Additionally, these mice had a short life span of 6 months. In the current study, the mice lived >12 months. For the present analysis, PLP-deficient mice heterozygous for the *mag* allele were used; it was previously suggested that there are no differences between mag+/- and mag-/- mice with respect to myelin abnormalities (Fujita et al., 1998). Interestingly, an increased number of large lipid-laden microglia/macrophages was observed in semithin sections of the MAG*PLP double mutants (Fig.21Aa) but in neither of the single mutants (Fig. 21Ab,c) at the age of 13 months. As previously described (Griffiths et al., 1998), demyelination and an increase in the number of microglial nuclei (Fig. 21Ab), a sign of microgliosis, were observed in PLP-deficient mice. The MAG-deficient mice did not show any increase in the number of microglial nuclei in the semithin level and the myelin sheath was intact (Fig.21Ac). In order to confirm these results with another method, paraffin-embedded tissue was used and processed with May-Giemsa staining (Fig.21B). As expected, there were cells with a light blue irregular foamy cytoplasm, much vacuolated in MAG*PLP double mutant mice

(a), but not in the PLP or MAG single deficient mice (b and c respectively). Taken together, these results show that due to PLP-deficiency activated microglia attack and ingest enormous amounts of myelin in the absence of MAG. This finding suggests that MAG acts as an inhibitor in the myelin sheath against activated microglia, supporting the inhibitory role of MAG, even under pathological conditions.
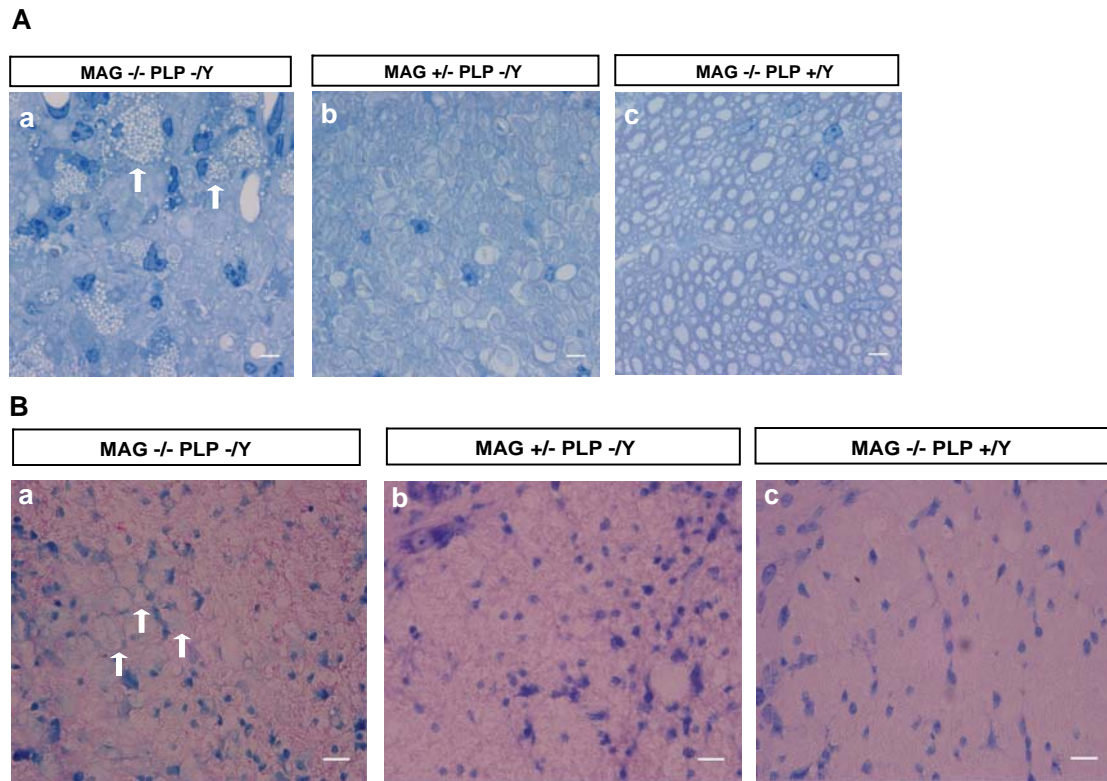
Figure 21. Activated microglia attack the myelin sheath in the absence of MAG *in vivo*

A)   Semithin cross sections from the dorsal column of the spinal cord of MAG*PLP double-deficient (a), PLP-deficient (b) and MAG-deficient (c) mutant mice were examined by light microscopy. These animals were at the age of 13 months. The presence of foamy macrophages/microglia attacking the myelin sheath (white lipid droplets) (arrows) were only present in the MAG*PLP double mutants (a) and not in any of the single mutants (b,c). The absence of PLP caused microglial activation, seen at this level as an increase in the microglial nuclei (b). The integrity of myelin and the presence of microglia cells were normal in the MAG-deficient mice (c). Scale bars, 5 μm.

B)   Paraffin-embedded tissue from MAG*PLP double-deficient mutants (a) and the respective PLP (b) and MAG (c) single-deficient mutants was stained with May-Giemsa. Cells with light blue vacuolated cytoplasm (arrows) were only present in the double mutants (a) and not in the PLP or MAG single deficient mice. Scale bars, 10 μm.

4.1.9 The role of MAG in LPS treated mice

Microglial cells are key components of the brain's defence mechanism in various pathologies, such as injury, autoimmune and neurodegenerative diseases and infections (Kreutzberg, 1996). Therefore, I wanted to assess whether the MAG-mediated signalling to microglia plays a role in pathology in a different model to the one described above using myelin mutant mice. A model that can mimic systemic inflammation in mice is the administration of lipopolysaccharide (LPS), a component of the Gram-negative bacterial cell wall (Andersson et al., 1992; Hauss-Wegrzyniak et al., 1998). Although it has long been believed that the brain is an immune-privileged organ, it was shown that even the intraperitoneal injection of LPS could lead to microglial activation in the brain (Kloss et al., 2001). Therefore, 2-3-month-old wild-type and MAG-deficient mice were injected intraperitoneally with 15 mg LPS/kg of body weight and sacrificed at various time points (Fig.22). To investigate the effect on microglia, the tissue was embedded in paraffin and the cerebellum was analyzed with Mac-3 immunoreactivity. At this age, the non-injected wild type and MAG-deficient mice exhibited very few, almost undetectable numbers of Mac-3-positive cells (Fig.22A,B). After LPS stimulation and after only 12 hrs, the number of Mac-3-positive cells increased with a more prominent population in the MAG-deficient mice (Fig.22C,D). The next 12 hrs of LPS stimulation, did not lead to additional microglial activation in the MAG mutant mice (Fig.22F), but there was an increase in the wild-type mice (Fig.22E). The peak of microglial activation and the maximum difference between the genotypes was reached after 48 hrs (Fig.22G,H). After a further 48 hrs, there was a small decrease in the population of Mac-3 positive cells in both genotypes (Fig.22I,J). Interestingly, a number of MAG-deficient mice died 72 hrs after LPS administration while wild-type mice did not show any signs of sickness. It is important to consider that intraperitoneal LPS administration not only affects the immune system of the brain, but also the peripheral immune system. Nevertheless, these results show a difference in the microglial response after LPS administration dependent on the genotype, which suggests that MAG might play a role in the myelin-microglial interaction even under pathological conditions.
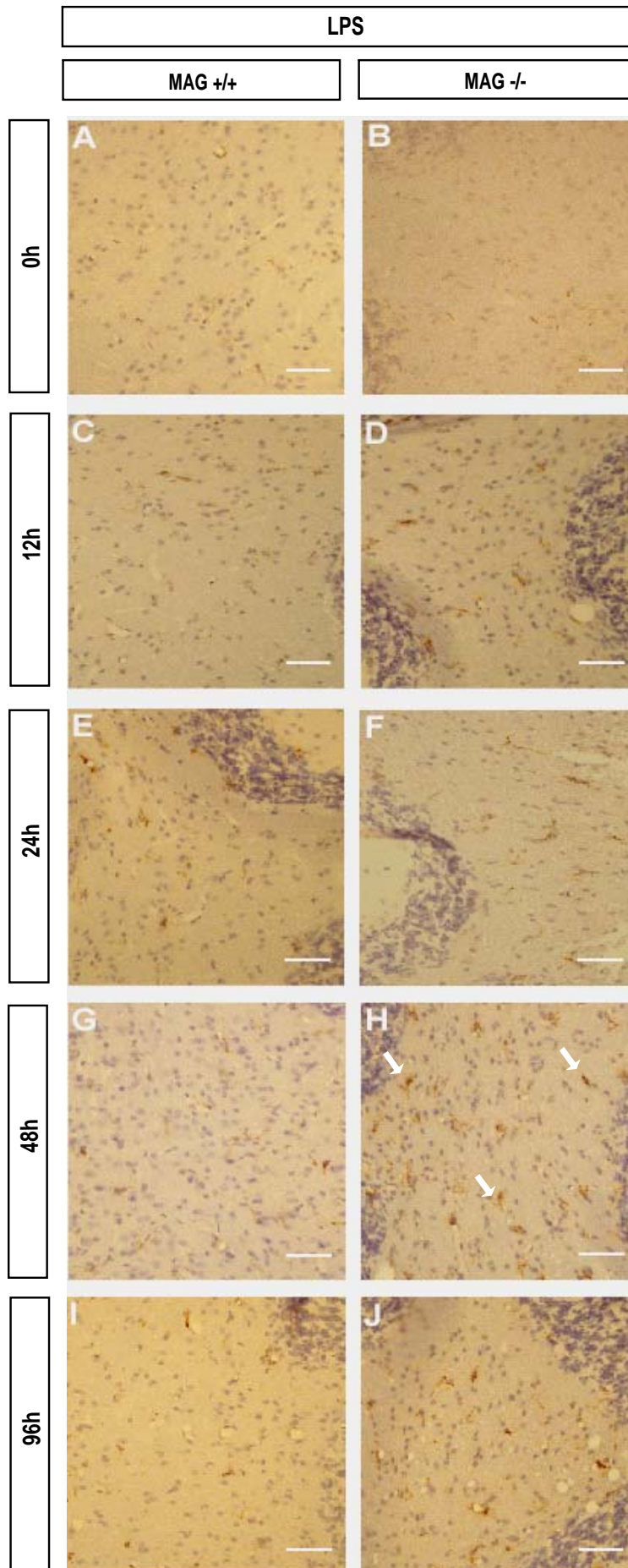
Figure 22. Persistent microglial activation in LPS treated mice in the absence of MAG

Light micrographs of the cerebellum of control (A,B), after 12 hrs (C,D), 24 hrs (E,F), 48 hrs (G,H) and 96 hrs (I,J) of the lipopolysaccharide (LPS) intraperitoneal injection of wild-type (A,C,E,G,I) and MAG-deficient mice (B,D,F,H,J). Sections were immunostained with the Mac-3 antibody, a microglial activation marker. There was almost no immunoreactivity in the control wild-type (A) and MAG-deficient mice at the age of 3-4 months (B). LPS stimulation led to increased microglial activation in MAG-deficient compared to wild-type mice at all different time points. Note that the peak of microglial activation was after 48 hrs in the MAG-deficient mice (arrows), although there was already strong Mac-3 immunoreactivity even at 12 hrs post injection. Scale bars, 25 μm.

4.1.10 The role of MAG in EAE mice

Multiple sclerosis (MS) is a widespread inflammatory disease of the central nervous system (CNS) that results in progressive demyelination and axonal loss (Bruck and Stadelmann, 2005; Trapp and Nave, 2008). Rodent models of experimental autoimmune encephalomyelitis (EAE) have been widely used to examine the mechanism of MS and the preclinical efficacy of mainly immunomodulatory drugs. The number of EAE models is large, each reflecting aspects of the subtypes of pathologies observed in the CNS of MS patients. One can achieve a range of pathological and temporal outcomes using a combination of different strains of mice, rats, or other mammals and different epitopes for immunization (peptides, whole proteins, or complex mixtures like spinal cord homogenate (Stromnes and Goverman, 2006).

To further assess the potential role of the MAG-microglial interaction in a strong inflammatory disease, EAE-induced mice from a wild-type and MAG-deficient background were analyzed. First, the extent of demyelination and cellular infiltration was evaluated; therefore, the spinal cords were removed and embedded at different time points after immunization and stained for Luxol-fast blue and counterstained for 'nuclear red' (Fig.23). This staining allows the identification of demyelinating areas and the cellular infiltration from the periphery (T-cells and macrophages). Behavioural signs of EAE rarely started earlier than 10-12 days post-immunization (Stromnes and Goverman, 2006). There was no obvious demyelination and cell infiltration in the dorsal column of the wild-type mice 1dpi (day post immunization), but there was a subtle infiltration in the MAG-deficient mice (Fig.23A,B). The demyelination and cellular infiltration proceeded without any obvious differences between the wild-type and MAG-deficient mice at 12 and 30 days post-immunization, revealing a peak at 30 d.p.i (Fig.23C-F). The degree of demyelination and possibly remyelination was assessed at 5 months p.i, showing an intense LFB signal in the wild-type mice (Fig.23G), but a focal loss of the signal in disperse areas of the dorsal column in MAG-deficient mice (Fig.23H). Collectively, these results revealed a difference in the extent of demyelination and cellular infiltration between the two genotypes, suggesting the involvement of MAG in the onset and progression of the disease.
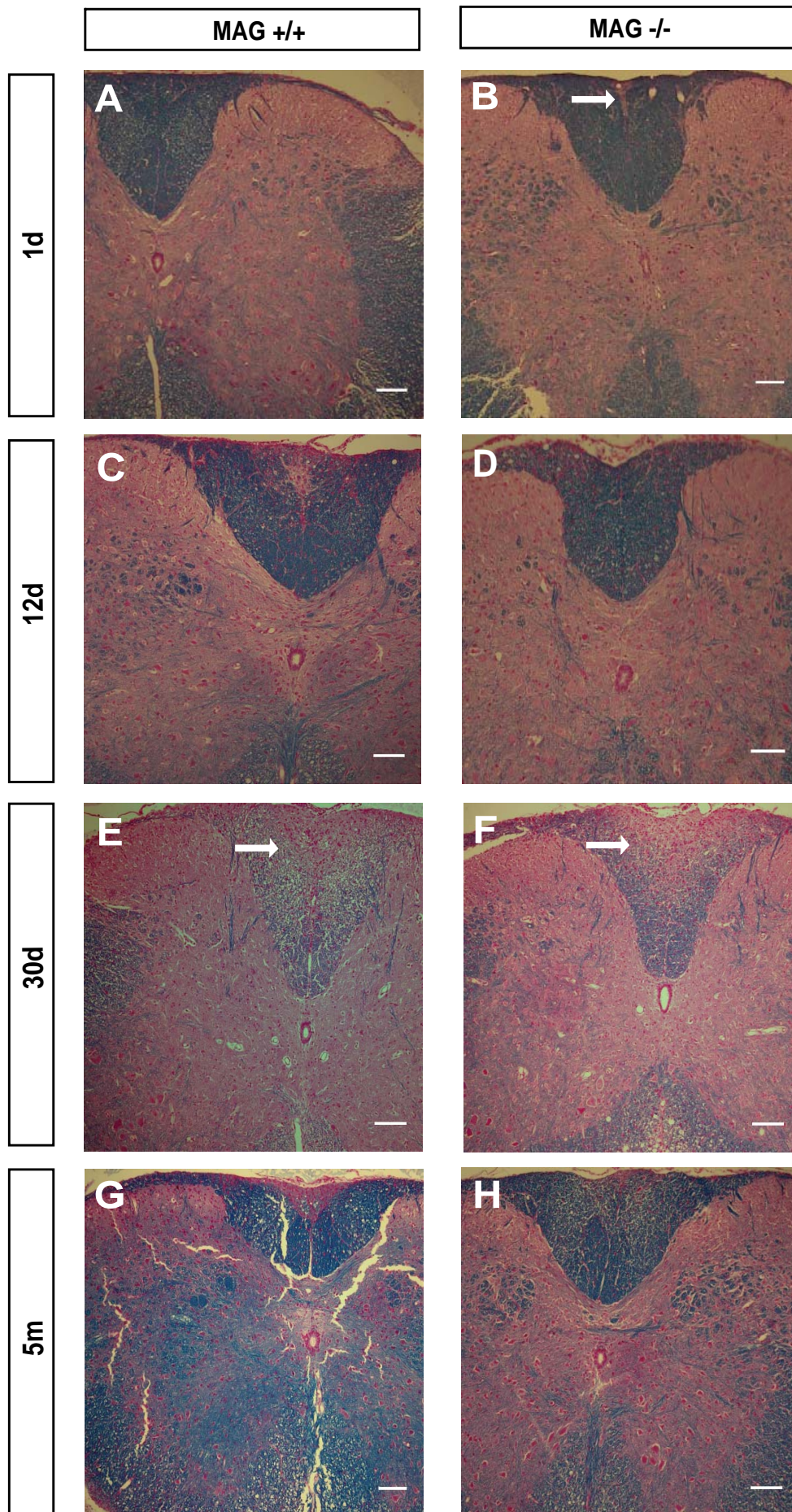
Figure 23. Histological analysis of CNS tissue from EAE wild-type and MAG-deficient mice

Spinal cords from wild-type (A,C,E,G) and MAG-deficient (B,D,F,H) mice were isolated at 1d, 12d, 30d and 5m post-immunization and embedded in paraffin. Sections were analyzed for demyelination and cell infiltration using a combined Luxol-fast blue (LFB) with 'nuclear red' staining. There was an early onset of cellular infiltration in the MAG-deficient mice (arrow) (B) compared to control (A). The extent of demyelination and cellular infiltration between the different genotypes was indistinguishable at 12 d.p.i (C,D), when the behavioural sickness of the animals actually starts. The peak of the demyelination and cellular infiltration was similar for both wild-type and MAG-deficient mice at 30 d.p.i (arrows) (E,F). At later stages, such as 5 m.p.i, the extent of demyelination in the wild-type mice was no longer so obvious (G), while there are dispersed demyelinating areas in the MAG-deficient mice (H). Scale bars, 50 µm.

To further examine the microglial/macrophage behaviour during the different stages of the disease and with regard to the two different genotypes, the paraffin sections were stained with Mac-3 (Fig.24). There was dispersed microglial activation in the dorsal column of MAG-deficient mice as early as 1 d.p.i (Fig.24B), but there was no obvious immunoreactivity in the wild-type animals (Fig.24A) at the same time point. The microglial/macrophage activation proceeded at day 12 p.i. in the wild-type mice compared to MAG-deficient mice (Fig.24C,D) and remained persistent after 30 d.p.i. (Fig.24E,F). Contrary to the LFB results, there was persistent immunoreactivity in the wild-type mice (Fig.24G) after 5 months post-immunization, while no obvious Mac-3-positive cells were evident in the MAG-deficient mice (Fig.24H). Taken together, these data suggest that MAG is involved in regulating the microglial/macrophage behavior under strong inflammatory conditions, such as the EAE model.
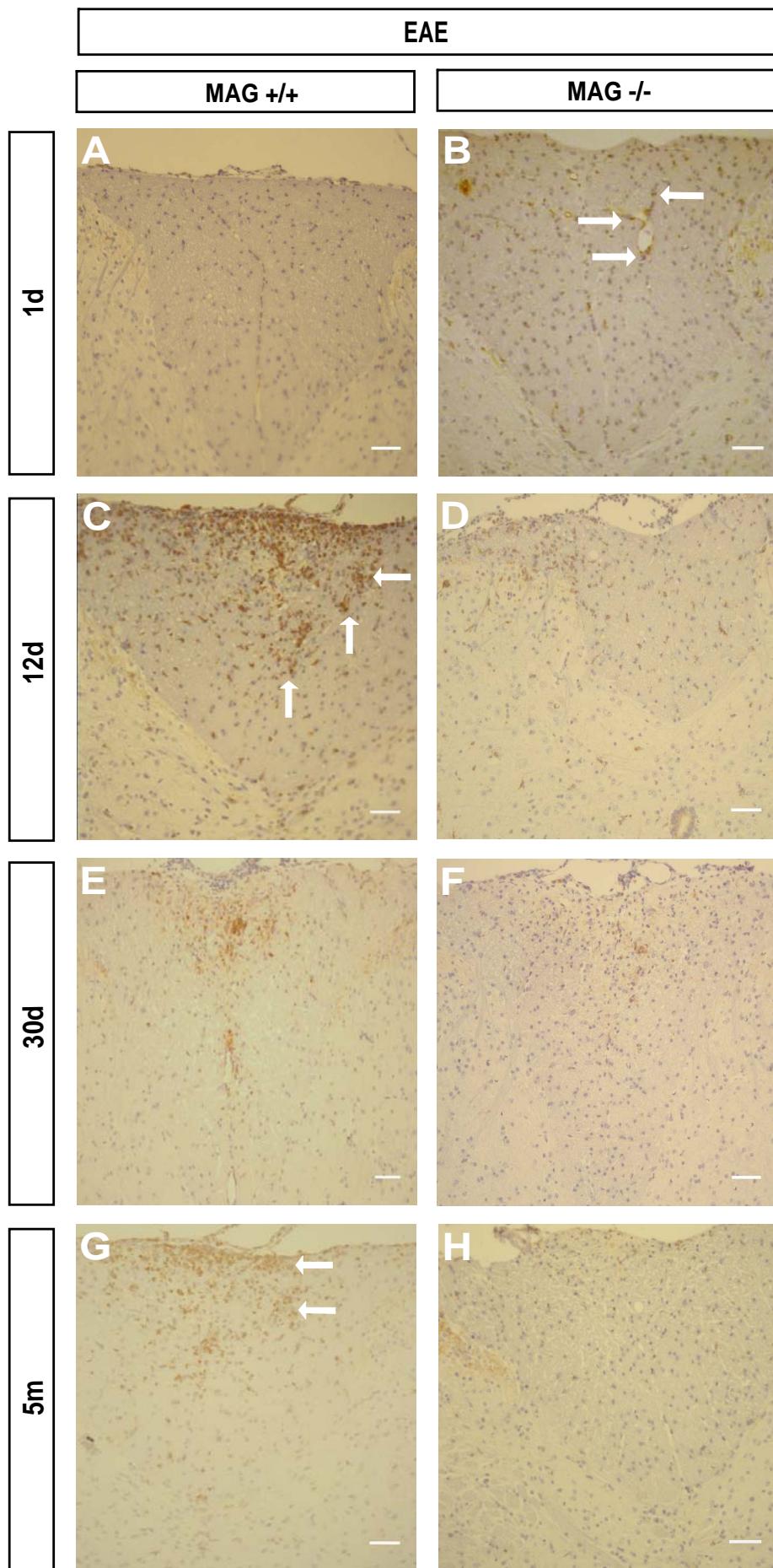
Figure 24. Histopathology of CNS tissue from EAE wild-type and MAG-deficient mice

Paraffin embedded spinal cords from wild-type (A,C,E,G) and MAG-deficient (B,D,F,H) mice at 1d, 12d, 30d and 5m post-immunization were immunostained with Mac-3, a microglial/macrophage marker. There was an early onset of microglial activation and the presence of macrophages in the MAG-deficient mice (arrows) (B) compared to control (A). In the wild-type mice, the presence of microglia/macrophages peaks at 12 d.p.i (arrows) and was persistent after 30 days and 5 months post-immunization. In contrast, in MAG-deficient mice the presence of microglial/macrophages in the dorsal column was reduced over time. Scale bars, 25 μm

4.2 Astrocytes and myelin-associated inhibitors

4.2.1 Astrocytes express the Nogo-66 receptors and co-receptors

Astrocytes are also reactive glial cells with motile processes as shown *in vivo* (Hirrlinger et al., 2004). Therefore, the same myelin-associated inhibitory mechanism might also take place against the astrocytes. First, the astrocytic expression of the receptors and the co-receptors known to bind the myelin-associated inhibitors in neurons was assessed. Astrocytes were purified from postnatal transgenic mice that express the enhanced green fluorescent protein (EGFP) under the astrocytic glial fibrillary acidic protein (GFAP) promoter (Nolte et al., 2001) (Fig.25A). The FACS-isolated EGFP-positive astrocytes were analyzed by quantitative RT-PCR (Fig.25B) for the expression of the receptor complex that is known to mediate the myelin-mediated inhibition in neurons and based on our results in microglia. Indeed, at the mRNA level the isolated astrocytes expressed all three homologues of Nogo-66 receptor, namely NgR1, NgR2 and NgR3. Additionally, astrocytes expressed the co-receptors Lingo-1, EGFR and the low-affinity neurotrophin receptor p75. They additionally expressed the Troy and EGF receptor in relatively high amounts when compared to beta-actin. The expression of GFAP was used as an astrocytic control. These results show for the first time that isolated astrocytes express the receptors and co-receptors known to bind the myelin-associated inhibitors and support previous studies showing the presence of these receptors in astrocytes *in vivo* (Satoh et al., 2005; 2007).

A) Newborn heterozygous transgenic GFAP-EGFP mice were employed to isolate highly pure brain astrocytes. The EGFP-positive astrocytes could be distinguished clearly and isolated (window P6) from the total brain cellular population.

B) RNA from the FACS sorted astrocytes was isolated and processed for quantitative RT-PCR expression profile analysis. Beta-actin was used as a standard. Astrocytes expressed the NgR1 and the two homologues NgR2 and NgR3 and the co-receptors Lingo-1 and p75. Additionally, the relative expression of Troy and EGFR was high. The glial fibrillary acidic protein (GFAP) expression served as an astrocytic marker. Data represent mean ± SEM of triplicates.

Figure 25. Astrocytic expression of the Nogo-66 receptors (NgRs) and co-receptors

4.2.2 Astrocytic processes are inhibited by MAG

The next question addressed was whether the myelin-associated inhibitors have an effect on astrocytes. Therefore, the same co-culture CHO or 3T3/astrocyte assay (Fig.9) was employed. Astrocytes were isolated from wild-type mixed glial cultures after shaking off the microglia and an additional mild trypsinisation step. These were plated for 24 hrs on confluent monolayers of control and MAG-expressing CHO and Nogo-A-expressing 3T3 cells. Interestingly, astrocytes on top of control-CHO cells often had a bipolar and elongated morphology, while the length of their processes was decreased and there was

an increase in the number of 'flattened' astrocytes when cultured on the MAG-CHO monolayer (Fig.26). On the other hand, astrocytes had a bipolar and often multipolar morphology when cultured onto the Nogo-A-expressing 3T3 cell layer, indicating that Nogo-A does not inhibit the astrocytic processes. Interestingly, astrocytes were more multipolar on top of the 3T3 cells compared to the control-CHO cells, suggesting that other molecules expressed at the surface of these cell lines might influence the astrocytic morphology. Taken together, these preliminary data show that, *in vitro,* MAG but not Nogo-A may act as an inhibitor of astrocytic process outgrowth.
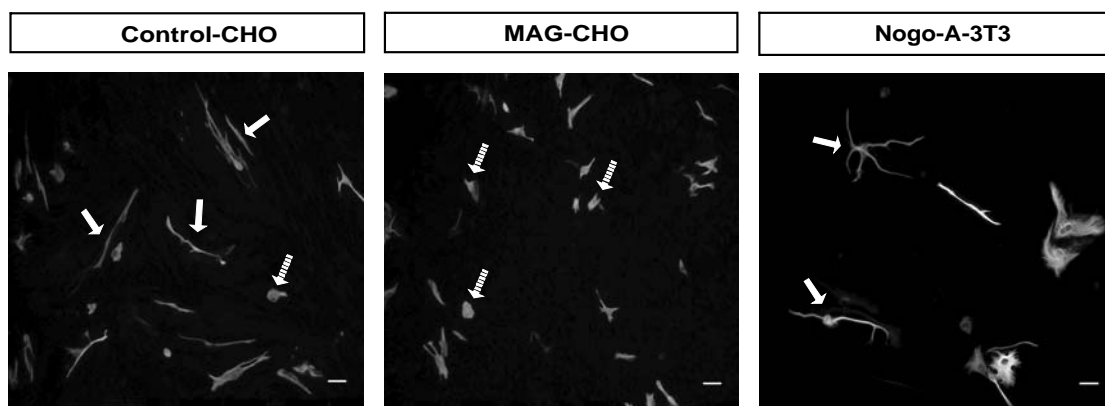
Figure 26. Astrocytes are inhibited by myelin-associated glycoprotein

Astrocytes isolated from wild type P0-P2 mixed glial cultures after shaking off the microglia were cultured on confluent monolayers of control or MAG-expressing CHO cells and Nogo-A-expressing 3T3 cells. The co-cultures were fixed after 24 hrs and stained for the glial fibrillary acidic protein (GFAP) using a species-specific polyclonal antibody. Astrocytes had an elongated morphology when cultured on control-CHO cells, while their processes became shorter when cultured on MAG-CHO cells. The astrocytic processes were elongated in the presence of Nogo-A-expressing 3T3 cells. Scale bars, 20 μm.

4.2.3 Astrogliosis in EAE mice

In the diseased central nervous system, microglial activation is accompanied by astrogliosis. Major reactive changes of astrocytes *in vivo* include among others the up-regulation of the glial fibrillary acidic protein (GFAP) accompanied by cellular hypertrophy. Astrocytes respond to "danger" signals in the CNS as well as the microglial cells. An example of such a response is multiple sclerosis, where astrocytes become reactive and form a glial scar (Holley et al., 2003).
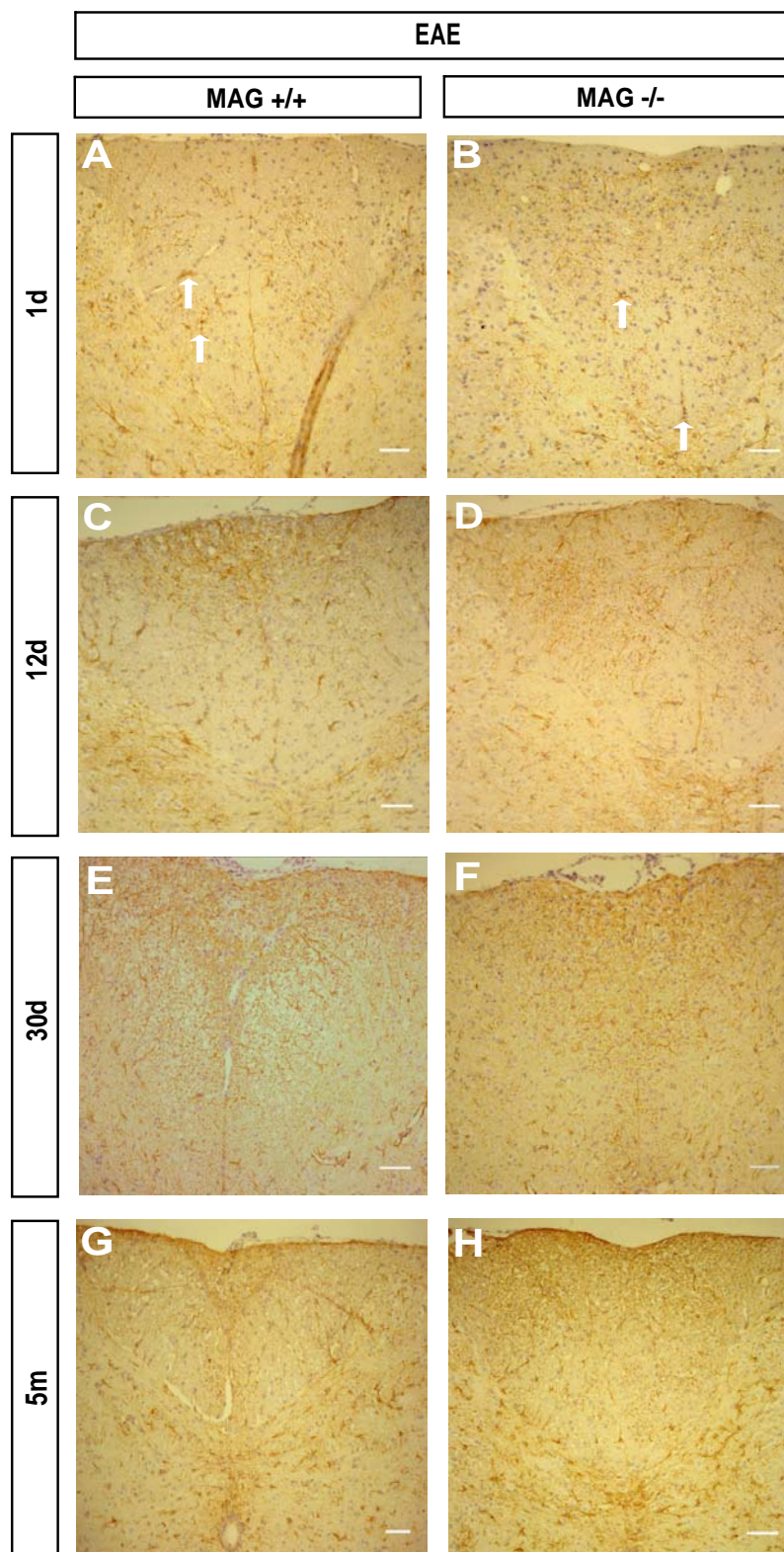
Figure 27. Astrogliosis in EAE mice

Light micrographs of spinal cords from wild-type (A,C,E,G) and MAG-deficient (B,D,F,H) mice 1d, 12d, 30d or 5m post-immunization. Sections were immunostained with the GFAP antibody, an astrocytic marker (arrows). There is no difference in the extent of the astrogliosis between the wild-type and MAG-deficient mice at any of the time points examined. Scale bars, 25 μm.

Therefore, I asked whether the MAG-mediated signalling to astrocytes plays a role *in vivo* under a pathological condition. Hence, the rodent EAE model was employed to assess the astrocytic response in wild-type versus MAG-deficient mice. The mice were sacrificed at different time points and the activation of astrocytes was evaluated as the immunoreactivity of GFAP (Fig.27). There was a strong astroglial response even after 1 day post immunization (d.p.i.), but no difference between the two genotypes (Fig.27A,B). The same observations were made by comparing the extent of astrogliosis in the different genetic backgrounds at 12 d.p.i, 30 d.p.i and 5 months after immunization (Fig.27C-H). Collectively, these results show that the inhibitory role of MAG in the astrocytic process outgrowth found *in vitro* cannot be directly translated into the regulation of the astrocytic response in a strong inflammatory condition, such as the EAE model.

5. Discussion

In higher vertebrates, the central nervous system (CNS) is one of the tissues that has limited regeneration capability. One of the obstacles known to limit axonal regeneration is the myelin sheath (Berry, 1982). In the last decade, extensive research has been carried out in the field of axonal regeneration to identify the myelin-associated inhibitors and underlying molecular pathways involved (Filbin, 2003; Liu et al., 2006; Yiu and He, 2006). These inhibitors, i.e. MAG, Nogo and OMgp, act through the same neuronal receptor complex, composed by Ngr1/Lingo-1/p75 or Troy, which leads to neurite outgrowth inhibition. Nevertheless, the physiological role of these inhibitory mechanisms under non-pathological conditions has been neglected. Based on the hypothesis of this study these inhibitors might be directed towards the resident glial cells of the CNS, such as microglia and astrocytes, as the emergence of reduced regenerative ability in higher vertebrates coincides with the increasing complexity of the innate immune system and the appearance of the adaptive immune system (Popovich and Longbrake, 2008).

5.1 Microglia express the repertoire of receptors and co-receptors known to bind the myelin-associated inhibitors

The involvement of the Nogo-66 receptors and the co-receptors in myelin-mediated neurite outgrowth inhibition has been shown both *in vitro* and *in vivo* (Xie and Zheng, 2008). As a first step to approach the present working hypothesis, I tested whether microglia also express this receptor complex. FACS-highly purified microglia from CX3CR1-EGFP transgenic mouse brains (Fig.7a) (Jung et al., 2000) were used and tested for the expression of these receptors at the mRNA level. Indeed, in this study it was shown that microglia express NgR1, NgR2, NgR3, Lingo-1, Troy and EGFR, though not the p75 neurotrophin receptor (Fig.7B). Additionally, the expression of NgR1 could be also confirmed at the protein level (Fig.7C). These results are in agreement with previous studies showing the expression of some of these receptors in microglia at the histological level in human tissues (Satoh et al., 2005; 2007). Furthermore, it was recently shown that these receptors are expressed in the counterpart cells of microglia in the PNS, the macrophages (Fry et al., 2007). Taken together, microglia express the molecular machinery known to bind the myelin-associated inhibitors and transduce the inhibitory signal to neurons.

5.2 A novel role of MAG in inhibiting microglial process outgrowth

The next logical step to test my hypothesis was to assess whether microglia respond to the presence of the myelin inhibitors. Interestingly, a recent study revealed that the inhibitory role of myelin through the NgR receptor complex is extended in non-neuronal cells, such as macrophages (Fry et al., 2007). Employing an "outgrowth assay" previously described for neurons (Mukhopadhyay et al., 1994) with some modifications, microglia were co-cultured with CHO cells in the presence or absence of MAG. Here, microglial process outgrowth was inhibited by surface-presented MAG *in vitro* (Fig.10A,B). Microglial cells had fewer and shorter processes when cultured on MAG-CHO feeder cells compared to control-CHO cells, and this change was independent of microglial activation (Fig.10C). However, to confirm the influence of MAG on microglial morphology, a stripe pattern of recombinant MAG was used as a substrate for microglia (Fig.14). In this assay, the inhibitory properties of MAG on microglial process outgrowth were reconfirmed as microglial cells avoided crossing the MAG-lanes. These data are the first to show that the inhibitory effect of MAG is not merely restricted to axons, but also targets the microglial cells in the CNS. On the other hand, Nogo-A-expressing 3T3 fibroblasts did not lead to microglial process inhibition (Fig.10A), suggesting that Nogo-A is not inhibitory for microglia. It cannot be formally excluded, however, that this preliminary observation might be due to other molecules expressed at the cell surface of the 3T3 cells, which might promote process outgrowth and thus suppress the inhibitory properties of Nogo-A. Therefore, further experiments with Nogo-A-knock down 3T3 cells are needed to elucidate the effect of Nogo-A on microglial morphology. Finally, it would be interesting to test whether microglial processes are specifically inhibited by MAG or they also respond to oligodendrocyte-myelin glycoprotein (OMgp).

It is known that MAG not only binds to NgR1, but also NgR2 and gangliosides (Mehta et al., 2007). The binding of MAG to the neuronal NgR1 receptor complex or gangliosides leads to RhoA and downstream molecules such as Rho kinase (ROCK) activation and subsequently growth cone collapse (Vinson et al., 2001; Fournier et al., 2003; Mahta et al., 2007). Furthermore, microglia express the Nogo-66 receptors, as well as the co-receptors Troy and Lingo-1 (Fig.7). I therefore tested whether MAG-mediated microglial inhibition is NgR1- and RhoA-dependent. Using NgR1-deficient mice and the Rho-

asociated kinase inhibitor Y27632, I found that the MAG-mediated microglial process inhibition is only partly NgR1-dependent (Fig.11) but could be completely reversed by blocking the ROCK in the CHO/microglial co-cultures (Fig.12). The partial involvement of NgR1 in the MAG-elicited microglial avoidance was additionally verified in the stripe assay (Fig.14). These results suggest that microglial receptors of the myelin-associated inhibitors probably involve more than the NgR1, but all of the receptor signalling converts to RhoA activation. Additional to NgR2, which could not be experimentally tested as null-mutant mice have not been available for this study, novel receptors must be taken into account. Interestingly, the novel axonal receptor PirB (Atwal et al., 2008), which is unrelated to NgRs, has been very recently described to play an important role in myelin-associated inhibition. Its presence in glial cells at present is only speculative.

Focusing on the inhibitory properties related to the molecular structure of MAG, this glycoprotein contains five extracellular immunoglobulin (Ig)-like domains with eight glycosylation sites and additional sialic acid charge in Ig domain 1 (Quarles, 2007). Furthermore, it was previously shown that MAG binds to neurons in a sialic acid-dependent mechanism, but this is distinct from the inhibitory domain of MAG that resides within the Ig domain 5 (Kelm et al., 1994; Cao et al., 2007). Therefore, the domain specificity of MAG-elicited microglial inhibition was investigated by employing a truncated recombinant MAG (MAG Ig domain 1-3) in the stripe assay (Fig.14B). Here, it was shown that the domain of MAG inhibiting the microglial process outgrowth is located within the Ig domains 1-3. Additionally, it was shown that the N-glycosylation and the sialic acid charge of MAG do not play a role in the microglial inhibition. These results show that the inhibitory domain of MAG is different regarding the cell type that is targeted, namely neurons or microglia, suggesting that different recognition mechanisms might be involved in the two cell types. This is not surprising, as MAG is a member of the siglec protein family that are known to mediate cis- and trans-interactions with other members of the same family and are mainly expressed in immune cells (Crocker et al., 2007). Therefore, MAG might interact with other siglecs residing at the microglial membrane. Further analysis regarding of other siglec members would shed some light on their potential involvement as binding partners of MAG. Taken together, microglial processes are repelled by MAG *in vitro* and this inhibition partly involves the NgR1 receptor, while the downstream signalling leads to RhoA activation. Finally, the

important domains of MAG inhibiting the microglial process outgrowth are the Ig domains 1-3.

5.3 MAG as a signal for microglial activation

Apart from the MAG isoform as a type I transmembrane protein, a soluble proteolytic fragment of MAG, namely dMAG, was found *in vivo* (Sato et al., 1984; Yim and Quarles, 1992; Moller, 1996). This extracellular domain of MAG retained its neurite inhibitory properties (Tang et al., 1997). Moreover, it was shown that there was an increased amount of dMAG in patients with multiple sclerosis compared to healthy controls (Moller et al., 1987). In a recent *in vitro* study, it was shown that specific matrix metalloproteinases (MMPs), such as MMP-2, MMP-7 and MMP-9, mediate the cleavage of cell surface-presented MAG, as well as recombinant MAG-Fc chimera (Milward et al., 2008). The expression of these metalloproteinases is upregulated in the MS (Yong et al., 2007; Scarisbrick et al., 2008). I therefore hypothesized that, as a sign of myelin destruction, soluble dMAG might play a different role when presented to microglia. Consequently, the response of microglial cells was tested in the presence of soluble dMAG in different concentrations (Fig.15). These data revealed that the microglia responded to soluble dMAG in a dose-dependent manner by releasing cytokines and chemokines. Furthermore, as shown for the surface-presented MAG, this release was not dependent on the Ig domains 4/5. Interestingly, the cyto- and chemokine microglial release by MAG did not involve the Fc receptors, as demonstrated by blocking the receptors with specific antibodies (Fig.16). Finally, it would be interesting to investigate the effect of soluble MAG on microglia *in vivo*. For that reason, the soluble recombinant extracellular domain of MAG could be applied externally in the MAG-deficient mice and the microglial behaviour monitored using two-photon *in vivo* imaging. Taken together, microglia respond to the soluble extracellular domain of MAG in a dose-dependent manner and this inflammatory response is independent of N-glycosylation, sialic-acid moieties and the Ig domains 4/5.

The present data suggest that MAG plays a dual role in microglial behaviour. When MAG is presented at the cell surface, it repels microglial processes while cleavage of MAG from the membrane, a sign of myelin destruction, leads to microglial activation

when presented in high amounts. Interestingly, in case of multiple sclerosis, the levels of MMPs are increased (Yong et al., 2007; Scarisbrick et al., 2008); this could lead to increased proteolytic cleavage and the release of dMAG, a pathological sign that could be "sensed" further by microglia and trigger their activation. Additionally, some of these MMPs are expressed by microglia and are upregulated in pathology, such as MS or LPS stimulation *in vitro* (Gottschall et al., 1995; Cossins et al., 1997). Therefore, it is conceivable that there is a feed back loop, where the increased shedding of MAG leads to microglial activation and the further upregulation of MMPs and subsequently an increased release of MAG. Consequently, one could think that the blocking of MMPs with some inhibitors could stop the activation signalling to microglia. This approach would be rather complex, as MMPs seem to play a detrimental and a beneficial role in the pathophysiology of the CNS (Yong, 2005). However, it would be interesting to assess the involvement of metalloproteinases in regulating the MAG-microglial signalling. Nevertheless, these results are the first to show that a single myelin protein can trigger a microglial inflammatory response when presented in a non-physiological context.

5.4 *In vivo* relevance of MAG in regulating microglial behaviour

The conditions under which the microglial cells are in a resting or activated state have been studied extensively (Raivich et al., 1999; van Rossum and Hanisch, 2004). Changes in the microglial status from quiescent to activated in neuropathological cases such as laser-induced brain injury are often accompanied by microglial movement towards the lesion site (Nimmerjahn et al., 2005). However, having remarkably motile processes, even under healthy conditions, microglial cells are able to control the status of the CNS environment (Davalos et al., 2005; 2008; Nimmerjahn et al., 2005). This microglial process outgrowth should be controlled and restricted in terms of space, as any abnormal signalling to microglia would lead to the activation and further response of the adaptive immune system (Aloisi, 2001). Based on the working hypothesis MAG plays a spatially inhibitory role in microglial process outgrowth by restricting their access to the axon-myelin unit. Therefore, anaesthetized CXCR-EGFP transgenic mice (Jung et al., 2000) were used to visualize the motility of microglia in the spinal cord (Fig.19). Monitoring the microglial behaviour with reference to YFP-expressing neurons *in vivo* (Winter et al., 2007), the microglial behaviour was altered in the absence of MAG compared to the

wild-type controls. Interestingly, there was a high number of microglia with fewer processes and in close association with the axons (Fig.19F). Additionally, the spatial distribution of microglial cells and their processes was altered in the absence of MAG. More precisely, there are many microglia that contact each other in the MAG-deficient mice, a feature that is only observed under pathological stimuli, such as laser-induced lesion, in the wild-type mice (data not shown). Therefore, I have hypothesized that the lack of the inhibitor (MAG) *in vivo* leads to the exposure of molecules that "attract" the microglial somata and/or processes. These "attractants" that I resemble to "hot glue", are possibly more exposed due to the lack of the inhibitor in the MAG-deficient mice and as a result the microglial process distribution is altered in the MAG-deficient mice.

Regarding the *in vivo* data presented in this work as a whole, I suggest that, as a surface presented molecule or in low amounts shed from the membrane, MAG plays an inhibitory-repellent role in restricting the microglial processes from perturbing the axon-myelin unit. This "control mechanism" is important, as any interference would lead 1) to the loss of neuronal function and 2) possibly to further microglial signalling to the adaptive immune system. Thus, I suggest that the MAG-microglial signalling is important for restricting the microglial process outgrowth and additionally might act as a signal to microglia that the integrity of the CNS tissue is normal. According to the current knowledge, this study is the first to show that the microglial behaviour is affected in young MAG-deficient mice.

5.5 The significance of MAG in the microglial behaviour in pathology

Is microglial-MAG signalling involved in pathology? I first investigated whether the receptor complex known to mediate the myelin-elicited inhibition and shown in this study to be expressed in microglia is regulated at the transcriptional level upon an activation signal. For that purpose, microglia were cultured and stimulated with LPS (Fig.8), a substance of the Gram-negative bacterial cell wall that activates microglia both *in vitro* and *in vivo* (Kloss et al., 2001). Interestingly, the Nogo-66 receptor complex was regulated upon activation; NgR1 and Lingo-1 were upregulated, no change regarding the NgR2 expression, while the rest of the receptors were downregulated (Fig.8B). This regulation is partially in agreement with the regulation of the NgR, Troy and Lingo-1 protein expression in the case of MS (Satoh et al., 2005; 2007). In this study, all three

proteins were upregulated in MS tissue and compared to healthy patients. The apparent difference regarding the regulation of Troy between this study and the studies mentioned above might be due to differences in 1) the nature of the activation signal and microglial response: LPS versus strong autoimmune response, 2) the organisms analyzed: mice versus humans, 3) the level of analysis: mRNA versus protein and 4) the material used for the analysis: microglia in culture versus brain tissue. Taken together, the current experiment showed that microglia responded to LPS and the transcription of the Nogo receptor complex was regulated upon activation.

Microglia respond to a number of stimuli in order to protect the CNS tissue (van Rossum and Hanisch, 2004). In this study it was also shown that there is a microglial response regarding the expression of the Nogo receptor complex upon activation. Thus, I asked whether MAG-microglial signalling interferes with, i.e. ameliorates or antagonizes other activating pathways such as the Toll-like receptor (TLR) pathways. Consequently, different TLR agonists, such as the Pam3SK4 (a TLR1/2 agonist), the LPS (a TLR4 agonist) and the MALP-2 (a TLR2/6 agonist) that involve different TLRs, were applied to the microglia/CHO co-cultures and the supernatants were analyzed for the release of cyto- and chemokines (Fig.17). This system failed to yield any concrete results, as there was no LPS- or Pam3SK4- mediated microglial activation, suggesting that there might be other molecules expressed at the surface of the CHO cells that interfere with the signalling. Although MALP-2 induced a microglial response, there was no obvious difference between the presence and absence of MAG. Consequently, the same experiment was repeated in the absence of the interfering "background" of the CHO cells by using the recombinant extracellular domain of MAG as a substrate (Fig.18). Surprisingly, microglia cultured on the MAG substrate showed an inflammatory response even in the absence of any stimulus. This might have been due to traces of unbound soluble MAG, which is now known (Fig.16) that it can lead to microglial inflammatory responses when presented in critical amounts. Nevertheless, the addition of the TLR agonists LPS, MALP-2 and Pam3SK4 in the presence or absence of MAG led to an additive microglial response. These results suggest that the MAG-microglial signalling probably does not interfere with the TLR 1, 2, 4 and 6 pathways *in vitro*.

The possible involvement of the MAG-mediating microglial signalling under pathological conditions was assessed *in vivo*. One such case in the CNS is the Wallerian

degeneration (WD) (Vargas and Barres, 2008). This term describes the progressive degeneration of the distal part of the nerve after transection. The slower rate of WD in the CNS compared to PNS has been attributed to poor myelin removal (Vargas and Barres, 2007). Microglia phagocytose CNS myelin at a slower rate than macrophages phagocytose PNS myelin, suggesting that local factors affect their phagocytic performance (Kuhlmann et al., 2002). Therefore, the microglial behaviour was tested in the absence of MAG in a model of WD. In mice lacking PLP, the main myelin protein of the CNS myelin WD and microglial activation was previously shown (Griffiths et al., 1998). In this work, it was shown that the absence of MAG triggered the formation of foamy microglial cells, indicating abnormal myelin phagocytosis (Fig.21A). These results suggest that MAG acts as an inhibitor and, in the case of activation signals, such as WD, the absence of MAG may facilitate the removal of myelin by activated microglia.

Another common pathological situation in the CNS where microglia participate in the first defence line is the presence of bacteria. The model used experimentally to study the pathways involved is the administration of LPS (Aravalli et al., 2007). Even the intraperitoneal injection of LPS in mice can lead to microglial activation in the brain (Kloss et al., 2001). Therefore, LPS was injected intraperitoneally in MAG-deficient and wild-type mice and the microglial response was analyzed at different time points. Indeed, as ascertained by Mac-3 staining, there was a difference between the MAG-deficient and wild-type mice in terms of their microglial response, a marker of microglial activation (Fig.22). Overall, the LPS-injected MAG-deficient mice had a higher number of Mac-3 positive cells in the white matter of the cerebellum compared to the LPS-injected wild-type mice. Additionally, a number of LPS-injected MAG-deficient mice became sick and died after 72 hrs, although the number of animals analyzed was not sufficient to draw any conclusions. The intraperitoneal administration could lead to the response of the peripheral immune system, such as the macrophages (Forestier et al., 1999). Additionally it is known that MAG signals to macrophages (Fry et al., 2007). Therefore, the sickness and, indirectly, the microglial response observed after LPS administration in the MAG-deficient mice might also be due in part to mechanisms and signalling that involve the macrophages. Nevertheless, these preliminary results suggest that the presence of MAG might play an important role in regulating the microglial response under pathological conditions, such as inflammation, as the absence of MAG led to enhanced microglial activation and to severe clinical symptoms of the mice.

Multiple sclerosis is another pathological condition in the central nervous system, where microglia have a detrimental and a beneficial role (McQualter and Bernard, 2007). One of the features of multiple sclerosis is myelin destruction. Therefore, based on the working hypothesis, the myelin-associated inhibitors are more exposed and, additionally, the upregulation of MMPs (see above) might lead to the increased exposure of dMAG. Therefore, the impact of MAG-microglial signalling was investigated in the MS model in rodents, i.e. experimental allergic encephalomyelitis (EAE). Wild-type and MAG-deficient mice were subjected to EAE (material kindly provided by P.Calabresi) and analyzed at different time points after immunization. One of the drawbacks of this model is that multiple sclerosis symptoms, such as demyelination and cellular infiltration, are only developed in the spinal cord. David and colleagues proposed that the MAG/NgR pathway might be involved in the valuable spatial restriction of microglia/macrophages in the lesion site in the case of MS (David et al., 2008). Therefore, the microglial activation was analyzed in the spinal cord of immunized mice of both genotypes. As this model leads to microglial activation and macrophage infiltration, and it is difficult to distinguish between the two cell types, the analysis involved both cell types. Thus, first the distribution of cell infiltration was examined with reference to myelinating areas, as ascertained using Luxol-fast blue staining. It was striking that there were signs of cellular infiltration in the MAG-deficient mice as early as 1d.p.i (Fig.23), while the clinical symptoms did not start earlier than 10-12 d.p.i with this model. Another interesting observation was that there was only a persistent loss of myelin 5 months post-immunization in the MAG-deficient mice. These results, although preliminary, suggest that the MAG-microglial signalling is indeed important and might indirectly regulate the response of the adaptive immune system.

The overall microglial activation in the EAE model was examined and surprisingly, this was different between the two genotypes. There was an early microglial response in the absence of MAG at 1d.p.i (Fig.24B), while later on massive microglial activation was observed only in the EAE-induced wild-type mice (Fig.24). One of the drawbacks of the EAE model is that there is a great variability between the animals induced, therefore a larger number of animals should be analyzed. It is also necessary to stain with other microglial/macrophage markers, as well as with T cell markers, in order to obtain a complete picture of the importance of MAG signalling in the context of pathology and its

effect on the different cell types. Taken together, these preliminary results suggest that the MAG signalling plays a role in regulating the microglial activity.

### 5.6 Astrocytes and myelin-associated inhibitors

Astrocytes also have numerous processes (Nedergaard et al., 2003) that may potentially interfere with important structures such as the axon-myelin unit. Consequently, the possibility that myelin-associated inhibitors might also target astrocytes was examined in this study. An approach similar to the one used for microglia was adopted. First, the expression of the Nogo receptors and co-receptors was assessed in purified astrocytes. Using FACS-sorted astrocytes from transgenic GFAP-EGFP mouse brains (Nolte et al., 2001), the expression of the entire Nogo receptor complex was detected at the mRNA level (Fig.25). These results support previous studies, showing the protein expression of NgR, Troy and Lingo-1 in astrocytes in human tissue (Satoh et al., 2005; 2007). Therefore, the role of MAG and Nogo-A in regulating the astrocytic morphology was further assessed by using MAG-expressing CHO cells and Nogo-A-expressing 3T3 cells co-cultured with astrocytes. Indeed, the astrocytes had fewer and shorter processes and the protoplasmic type was the dominant type when co-cultured with MAG-CHO cells. However, in the case of the Nogo-A-expressing cells, additional Nogo-A-negative contol-3T3 cells would be needed before firmly stating the absence of any other protein effect on astrocytic process outgrowth. In contrast, there was no obvious effect in the astrocytic morphology induced by Nogo-A (Fig.26). Taken together, these preliminary results showed an inhibitory effect of MAG on astrocytes. MAG signalling leads to RhoA activation in neurons (Niederost et al., 2002), in macrophages (Fry et al., 2007) and in microglia, as shown in this study. The astrocytic morphology is also regulated by the small GTPase Rho (Holtje et al., 2005), therefore it is possible that the same intracellular pathways related to the myelin-associated inhibitors are involved in astrocytes.

To test whether there is an effect of the potential MAG-astrocytic signalling *in vivo*, the EAE-induced mice were analyzed for reactive astrogliosis. There was no difference in the extent of the reactive astrogliosis between the wild-type and MAG-deficient mice (Fig.27). The physiological role of this interaction, however, may become more obvious *in vivo* in different models than EAE, which causes strong inflammatory responses, and therefore other signalling cascades might overrule the MAG-astrocytic signalling.

5.7 What is the impact of this study for the neuronal regeneration?

The *in vitro* and *in vivo* data presented in this study support the notion of a novel role of MAG in inhibiting and controlling microglial process outgrowth and possibly the microglial status. Surface-presented MAG and small amounts of dMAG shed from the membrane prevents the microglial processes from interfering with the axon-myelin unit (Fig.28A). In the case of pathology, such as inflammation caused by LPS or autoimmune responses, MAG can be more exposed either because of myelin destruction or the elevation of metalloproteinases that shed MAG from the membrane leading to microglial activation (Fig.28B).

The preliminary results presented in this work suggest that the presence of MAG seems to control the microglial response as, in the absence of MAG in the Wallerian degeneration model of PLP-deficient mice, activated microglia were found to "attack" the myelin sheath and to invade the periaxonal space (Ian Griffiths, unpublished data) (Fig.28C). Further investigation is necessary to test whether this role is also applicable to other disease models, such as injury. Interestingly, in this study there was no effect of Nogo-A on microglia, suggesting principle differences compared to the molecules involved in inhibiting neurons. In this respect, it would be also interesting to assess the function of other myelin-associated inhibitors, such as oligodendrocyte-myelin glycoprotein and ephrins to name but a few, in regulating microglial physiology and pathophysiology.
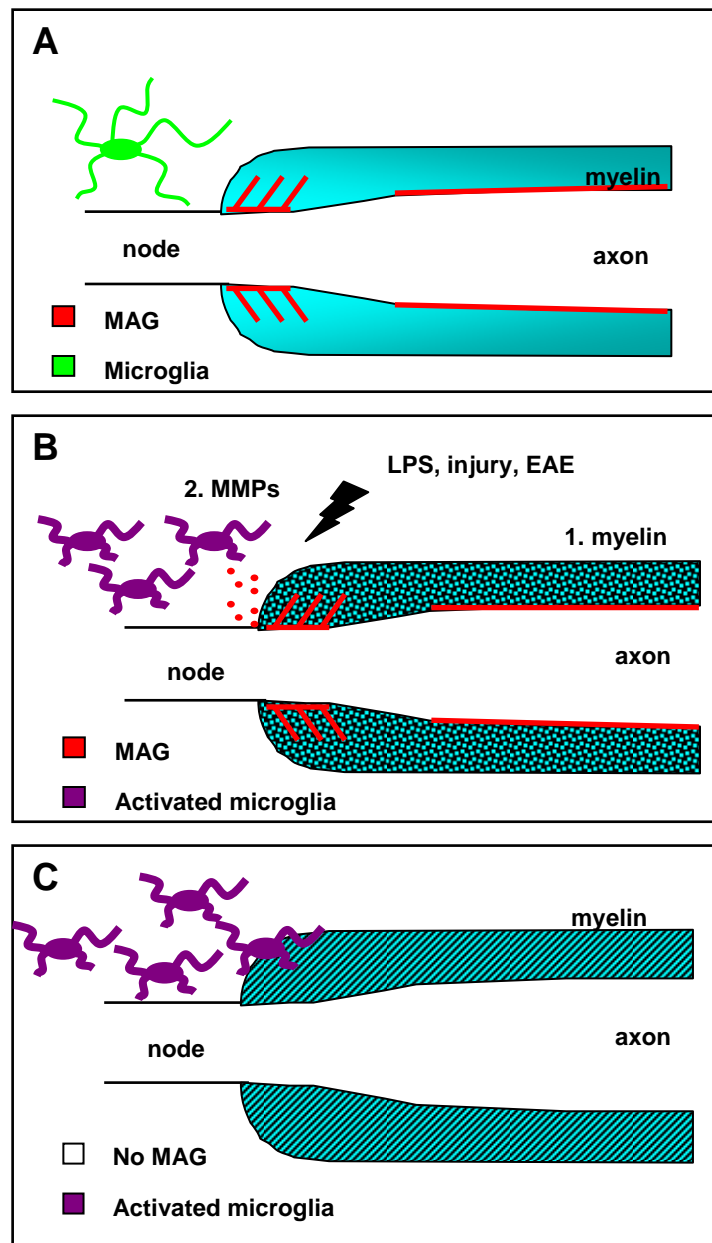
Figure 28. Model of the MAG-to-microglial signalling in the healthy and diseased CNS

MAG, and possibly other myelin-associated inhibitors, either surface presented or shed from the membrane by matrix metalloproteinases (MMPs), prevents microglial processes from interfering with the axon-myelin unit (A). In case of pathological stimuli, such as injury, LPS infection, Wallerian degeneration, PLP-deficiency or EAE that lead either to myelin degeneration or elevation of MMPs, more shed or surface-presented MAG are exposed to microglia leading to their activation (B). In the absence of MAG, microglia attack the myelin sheath and invade the periaxonal space (C).

One important approach to promote regeneration in the CNS after injury is to block the ligand/NgR complex (Grandpre et al., 2002) or the downstream RhoA signalling pathway (Dergham et al., 2002; Fournier et al., 2003). It is now known that this mechanism also regulates the microglial physiology; therefore, the beneficial effect for axonal regeneration might be detrimental to the microglial response. In another case of pathology, such as Wallerian degeneration, MAG and possibly the other myelin-associated inhibitors might restrict the microglial phagocytosis, which suggests that an overlapping but non-identical sort of inhibitors might be responsible for the slow CNS

99

myelin removal after injury. Consequently, blocking the inhibitors with, for example, synthetic peptides might increase the phagocytosing abilities of microglia.

The function of MAG and the other myelin-associated inhibitors in the CNS was only considered with respect to their negative effect on axonal outgrowth. Overcoming this inhibition and promoting axonal regeneration has been the main focus of many studies (Yiu and He, 2006; Chaudhry and Filbin, 2007). The involvement of this mechanism in the macrophage efflux from the basal lamina in the PNS (Fry et al., 2007) very recently extended the potential of this molecular machinery to non-neuronal cells. This study yielded new evidence that supports the notion that the myelin-associated inhibitory effect is beneficial in preventing the remarkably motile microglial processes from perturbing the axon-myelin unit under healthy conditions.

In conclusion, this study suggests that the evolutionary emergence of myelin-associated inhibitors was beneficial for the protection of the axon-myelin unit in the complex nervous system of higher vertebrates that also possess a complex immune system. As this mechanism regulates both axonal regeneration and microglial activity, it is essential that we consider these effects are considered in planning the current and future regeneration and neuroprotective strategies to avoid any interference with the immune system that might lead to increased inflammation.

6. Summary and Conclusions

Myelin-associated growth inhibitors, such as Nogo, MAG and OMgp, cause neuronal growth cone collapse and prevent the regeneration of CNS axons. In recent decades, a great amount of research has elicited the molecular mechanisms involved in neurite inhibition but little is known about the physiological function of these myelin-associated inhibitors. The working hypothesis was that the glial cells in the CNS might also be responsive to myelin inhibitors.

I first assessed the expression of the Nogo receptors and co-receptors in FACS-isolated brain microglia and astrocytes. For this experiment, transgenic mice that express the enhanced green fluorescent protein (EGFP) under a specific microglial (CX3CR1) or astrocytic (GFAP) promoter were employed. This analysis revealed that most of the key-players involved in myelin-associated inhibition are expressed in microglia and astrocytes.

Furthermore, the effect of MAG and Nogo-A on microglia and astrocytes *in vitro* was assessed by using MAG expressing CHO cells and Nogo-A-expressing 3T3 cells as feeder layers. Indeed, the microglial and the astrocytic processes were inhibited in the presence of MAG, but not Nogo-A. In addition, NgR1-deficient microglia and the Rho-associated kinase inhibitor Y27632 were used in the same assay to evaluate the involvement of NgR1 and RhoA in the MAG-microglial signalling. In these experiments, I showed that NgR1 is partially involved, while the inhibition of the RhoA could rescue the microglial process inhibition completely.

To confirm these results, a stripe assay was used where recombinant MAG lanes were alternated with PLL stripes as a substrate for microglial growth. This experiment confirmed the inhibitory role of MAG in microglia and the partial involvement of the NgR1. Additionally, using the same assay with a shorter mutant form of MAG, I could show that the MAG domain responsible for the microglial process inhibition lies within the Ig domain 1-3. Furthermore, I demonstrated that dMAG, the extracellular domain of MAG that serves as a sign of myelin destruction, has a different role when presented in high amounts in the medium by acting as a signal that leads to microglial activation.

By using two-photon *in vivo* microscopy under physiological conditions, the roaming behaviour of microglia was observed. Surprisingly, the absence of MAG led to an altered microglial process distribution and increased microglial association with the axons. When the CNS tissue was challenged, either by the absence of the major myelin proteolipid protein or by inflammation stimuli, such as the lipopolysaccharide administration or the EAE, the microglial response was altered in the absence of MAG, supporting the idea that MAG might be important in signalling to microglia even under pathological conditions.

7. References

Aloisi, F. (2001). Immune function of microglia. *Glia* **36**(2): 165-79.

Andersson, J., L. Bjork, C. A. Dinarello, H. Towbin and U. Andersson (1992). Lipopolysaccharide induces human interleukin-1 receptor antagonist and interleukin-1 production in the same cell. *Eur J Immunol* **22**(10): 2617-23.

Aravalli, R. N., P. K. Peterson and J. R. Lokensgard (2007). Toll-like receptors in defense and damage of the central nervous system. *J Neuroimmune Pharmacol* **2**(4): 297-312.

Arquint, M., J. Roder, L. S. Chia, J. Down, D. Wilkinson, H. Bayley, P. Braun and R. Dunn (1987). Molecular cloning and primary structure of myelin-associated glycoprotein. *Proc Natl Acad Sci U S A* **84**(2): 600-4.

Arroyo, E. J. and S. S. Scherer (2000). On the molecular architecture of myelinated fibers. *Histochem Cell Biol* **113**(1): 1-18.

Atwal, J. K., J. Pinkston-Gosse, J. Syken, S. Stawicki, Y. Wu, C. Shatz and M. Tessier-Lavigne (2008). PirB is a functional receptor for myelin inhibitors of axonal regeneration. *Science* **322**(5903): 967-70.

Berry, M. (1982). Post-injury myelin-breakdown products inhibit axonal growth: an hypothesis to explain the failure of axonal regeneration in the mammalian central nervous system. *Bibl Anat*(23): 1-11.

Bruck, W. and C. Stadelmann (2005). The spectrum of multiple sclerosis: new lessons from pathology. *Curr Opin Neurol* **18**(3): 221-4.

Cai, D., Y. Shen, M. De Bellard, S. Tang and M. T. Filbin (1999). Prior exposure to neurotrophins blocks inhibition of axonal regeneration by MAG and myelin via a cAMP-dependent mechanism. *Neuron* **22**(1): 89-101.

Cao, Z., J. Qiu, M. Domeniconi, J. Hou, J. B. Bryson, W. Mellado and M. T. Filbin (2007). The inhibition site on myelin-associated glycoprotein is within Ig-domain 5 and is distinct from the sialic acid binding site. *J Neurosci* **27**(34): 9146-54.

Cardona, A. E., E. P. Pioro, M. E. Sasse, V. Kostenko, S. M. Cardona, I. M. Dijkstra, D. Huang, G. Kidd, S. Dombrowski, R. Dutta, J. C. Lee, D. N. Cook, S. Jung, S. A. Lira, D. R. Littman and R. M. Ransohoff (2006). Control of microglial neurotoxicity by the fractalkine receptor. *Nat Neurosci* **9**(7): 917-24.

Caroni, P. and M. E. Schwab (1988a). Antibody against myelin-associated inhibitor of neurite growth neutralizes nonpermissive substrate properties of CNS white matter. *Neuron* **1**(1): 85-96.

Caroni, P. and M. E. Schwab (1988b). Two membrane protein fractions from rat central myelin with inhibitory properties for neurite growth and fibroblast spreading. *J*

Cell Biol **106**(4): 1281-8.

Chan, W. Y., S. Kohsaka and P. Rezaie (2007). The origin and cell lineage of microglia: new concepts. *Brain Res Rev* **53**(2): 344-54.

Chaudhry, N. and M. T. Filbin (2007). Myelin-associated inhibitory signaling and strategies to overcome inhibition. *J Cereb Blood Flow Metab* **27**(6): 1096-107.

Chen, M. S., A. B. Huber, M. E. van der Haar, M. Frank, L. Schnell, A. A. Spillmann, F. Christ and M. E. Schwab (2000). Nogo-A is a myelin-associated neurite outgrowth inhibitor and an antigen for monoclonal antibody IN-1. *Nature* **403**(6768): 434-9.

Chivatakarn, O., S. Kaneko, Z. He, M. Tessier-Lavigne and R. J. Giger (2007). The Nogo-66 receptor NgR1 is required only for the acute growth cone-collapsing but not the chronic growth-inhibitory actions of myelin inhibitors. *J Neurosci* **27**(27): 7117-24.

Cossins, J. A., J. M. Clements, J. Ford, K. M. Miller, R. Pigott, W. Vos, P. Van der Valk and C. J. De Groot (1997). Enhanced expression of MMP-7 and MMP-9 in demyelinating multiple sclerosis lesions. *Acta Neuropathol* **94**(6): 590-8.

Crocker, P. R., J. C. Paulson and A. Varki (2007). Siglecs and their roles in the immune system. *Nat Rev Immunol* **7**(4): 255-66.

Davalos, D., J. Grutzendler, G. Yang, J. V. Kim, Y. Zuo, S. Jung, D. R. Littman, M. L. Dustin and W. B. Gan (2005). ATP mediates rapid microglial response to local brain injury in vivo. *Nat Neurosci* **8**(6): 752-8.

Davalos, D., J. K. Lee, W. B. Smith, B. Brinkman, M. H. Ellisman, B. Zheng and K. Akassoglou (2008). Stable in vivo imaging of densely populated glia, axons and blood vessels in the mouse spinal cord using two-photon microscopy. *J Neurosci Methods* **169**(1): 1-7.

David, S. and A. J. Aguayo (1981). Axonal elongation into peripheral nervous system "bridges" after central nervous system injury in adult rats. *Science* **214**(4523): 931-3.

David, S., E. J. Fry and R. Lopez-Vales (2008). Novel roles for Nogo receptor in inflammation and disease. *Trends Neurosci* **31**(5): 221-6.

Dergham, P., B. Ellezam, C. Essagian, H. Avedissian, W. D. Lubell and L. McKerracher (2002). Rho signaling pathway targeted to promote spinal cord repair. *J Neurosci* **22**(15): 6570-7.

Dodd, D. A., B. Niederoest, S. Bloechlinger, L. Dupuis, J. P. Loeffler and M. E. Schwab (2005). Nogo-A, -B, and -C are found on the cell surface and interact together in many different cell types. *J Biol Chem* **280**(13): 12494-502.

Domeniconi, M., Z. Cao, T. Spencer, R. Sivasankaran, K. Wang, E. Nikulina, N. Kimura, H. Cai, K. Deng, Y. Gao, Z. He and M. Filbin (2002). Myelin-associated glycoprotein interacts with the Nogo66 receptor to inhibit neurite outgrowth. *Neuron* **35**(2): 283-90.

Dong, Y. and E. N. Benveniste (2001). Immune function of astrocytes. *Glia* **36**(2): 180-90.

Dreyfus, C. F., X. Dai, L. D. Lercher, B. R. Racey, W. J. Friedman and I. B. Black (1999). Expression of neurotrophins in the adult spinal cord in vivo. *J Neurosci Res* **56**(1): 1-7.

Filbin, M. T. (2003). Myelin-associated inhibitors of axonal regeneration in the adult mammalian CNS. *Nat Rev Neurosci* **4**(9): 703-13.

Fischer, D., Z. He and L. I. Benowitz (2004). Counteracting the Nogo receptor enhances optic nerve regeneration if retinal ganglion cells are in an active growth state. *J Neurosci* **24**(7): 1646-51.

Fitch, M. T. and J. Silver (2008). CNS injury, glial scars, and inflammation: Inhibitory extracellular matrices and regeneration failure. *Exp Neurol* **209**(2): 294-301.

Forestier, C., E. Moreno, J. Pizarro-Cerda and J. P. Gorvel (1999). Lysosomal accumulation and recycling of lipopolysaccharide to the cell surface of murine macrophages, an in vitro and in vivo study. *J Immunol* **162**(11): 6784-91.

Fournier, A. E., T. GrandPre and S. M. Strittmatter (2001). Identification of a receptor mediating Nogo-66 inhibition of axonal regeneration. *Nature* **409**(6818): 341-6.

Fournier, A. E., G. C. Gould, B. P. Liu and S. M. Strittmatter (2002). Truncated soluble Nogo receptor binds Nogo-66 and blocks inhibition of axon growth by myelin. *J Neurosci* **22**(20): 8876-83.

Fournier, A. E., B. T. Takizawa and S. M. Strittmatter (2003). Rho kinase inhibition enhances axonal regeneration in the injured CNS. *J Neurosci* **23**(4): 1416-23.

Fry, E. J., C. Ho and S. David (2007). A role for Nogo receptor in macrophage clearance from injured peripheral nerve. *Neuron* **53**(5): 649-62.

Fujita, N., A. Kemper, J. Dupree, H. Nakayasu, U. Bartsch, M. Schachner, N. Maeda, K. Suzuki and B. Popko (1998). The cytoplasmic domain of the large myelin-associated glycoprotein isoform is needed for proper CNS but not peripheral nervous system myelination. *J Neurosci* **18**(6): 1970-8.

Gao, H. M. and J. S. Hong (2008). Why neurodegenerative diseases are progressive: uncontrolled inflammation drives disease progression. *Trends Immunol* **29**(8): 357-65.

Giulian, D. and T. J. Baker (1986). Characterization of ameboid microglia isolated from developing mammalian brain. *J Neurosci* **6**(8): 2163-78.

Gottschall, P. E., X. Yu and B. Bing (1995). Increased production of gelatinase B (matrix metalloproteinase-9) and interleukin-6 by activated rat microglia in culture. *J Neurosci Res* **42**(3): 335-42.

GrandPre, T., F. Nakamura, T. Vartanian and S. M. Strittmatter (2000). Identification of the Nogo inhibitor of axon regeneration as a Reticulon protein. *Nature* **403**(6768): 439-44.

GrandPre, T., S. Li and S. M. Strittmatter (2002). Nogo-66 receptor antagonist peptide promotes axonal regeneration. *Nature* **417**(6888): 547-51.

Griffiths, I., M. Klugmann, T. Anderson, D. Yool, C. Thomson, M. H. Schwab, A. Schneider, F. Zimmermann, M. McCulloch, N. Nadon and K. A. Nave (1998). Axonal swellings and degeneration in mice lacking the major proteolipid of myelin. *Science* **280**(5369): 1610-3.

Habib, A. A., L. S. Marton, B. Allwardt, J. R. Gulcher, D. D. Mikol, T. Hognason, N. Chattopadhyay and K. Stefansson (1998). Expression of the oligodendrocyte-myelin glycoprotein by neurons in the mouse central nervous system. *J Neurochem* **70**(4): 1704-11.

Hanisch, U. K. and H. Kettenmann (2007). Microglia: active sensor and versatile effector cells in the normal and pathologic brain. *Nat Neurosci* **10**(11): 1387-94.

Hanisch, U. K., T. V. Johnson and J. Kipnis (2008). Toll-like receptors: roles in neuroprotection? *Trends Neurosci* **31**(4): 176-82.

Hartline, D. K. and D. R. Colman (2007). Rapid conduction and the evolution of giant axons and myelinated fibers. *Curr Biol* **17**(1): R29-35.

Hausler, K. G., M. Prinz, C. Nolte, J. R. Weber, R. R. Schumann, H. Kettenmann and U. K. Hanisch (2002). Interferon-gamma differentially modulates the release of cytokines and chemokines in lipopolysaccharide- and pneumococcal cell wall-stimulated mouse microglia and macrophages. *Eur J Neurosci* **16**(11): 2113-22.

Hauss-Wegrzyniak, B., L. Lukovic, M. Bigaud and M. E. Stoeckel (1998). Brain inflammatory response induced by intracerebroventricular infusion of lipopolysaccharide: an immunohistochemical study. *Brain Res* **794**(2): 211-24.

He, F. and Y. E. Sun (2007). Glial cells more than support cells? *Int J Biochem Cell Biol* **39**(4): 661-5.

Hirrlinger J, S. Hülsmann, F. Kirchhoff (2004). Astroglial processes show spontaneous motility at active synaptic terminals in situ. *Eur J Neurosci.* **20**(8):2235-9.

Hoek, R. M., S. R. Ruuls, C. A. Murphy, G. J. Wright, R. Goddard, S. M. Zurawski, B. Blom, M. E. Homola, W. J. Streit, M. H. Brown, A. N. Barclay and J. D. Sedgwick (2000). Down-regulation of the macrophage lineage through interaction with OX2 (CD200). *Science* **290**(5497): 1768-71.

Holley, J. E., D. Gveric, J. Newcombe, M. L. Cuzner and N. J. Gutowski (2003). Astrocyte characterization in the multiple sclerosis glial scar. *Neuropathol Appl Neurobiol* **29**(5): 434-44.

Holtje, M., A. Hoffmann, F. Hofmann, C. Mucke, G. Grosse, N. Van Rooijen, H. Kettenmann, I. Just and G. Ahnert-Hilger (2005). Role of Rho GTPase in astrocyte morphology and migratory response during in vitro wound healing. *J Neurochem* **95**(5): 1237-48.

Horner, P. J. and T. D. Palmer (2003). New roles for astrocytes: the nightlife of an 'astrocyte'. La vida loca! *Trends Neurosci* **26**(11): 597-603.

Huang, J. K., G. R. Phillips, A. D. Roth, L. Pedraza, W. Shan, W. Belkaid, S. Mi, A. Fex-Svenningsen, L. Florens, J. R. Yates, 3rd and D. R. Colman (2005). Glial membranes at the node of Ranvier prevent neurite outgrowth. *Science* **310**(5755): 1813-7.

Huber, A. B., O. Weinmann, C. Brosamle, T. Oertle and M. E. Schwab (2002). Patterns of Nogo mRNA and protein expression in the developing and adult rat and after CNS lesions. *J Neurosci* **22**(9): 3553-67.

Jaramillo, M. L., D. E. Afar, G. Almazan and J. C. Bell (1994). Identification of tyrosine 620 as the major phosphorylation site of myelin-associated glycoprotein and its implication in interacting with signaling molecules. *J Biol Chem* **269**(44): 27240-5.

Ji, B., L. C. Case, K. Liu, Z. Shao, X. Lee, Z. Yang, J. Wang, T. Tian, S. Shulga-Morskaya, M. Scott, Z. He, J. K. Relton and S. Mi (2008). Assessment of functional recovery and axonal sprouting in oligodendrocyte-myelin glycoprotein (OMgp) null mice after spinal cord injury. *Mol Cell Neurosci* **39**(2): 258-67.

Jung, S., J. Aliberti, P. Graemmel, M. J. Sunshine, G. W. Kreutzberg, A. Sher and D. R. Littman (2000). Analysis of fractalkine receptor CX(3)CR1 function by targeted deletion and green fluorescent protein reporter gene insertion. *Mol Cell Biol* **20**(11): 4106-14.

Kelm, S., A. Pelz, R. Schauer, M. T. Filbin, S. Tang, M. E. de Bellard, R. L. Schnaar, J. A. Mahoney, A. Hartnell, P. Bradfield and et al. (1994). Sialoadhesin, myelin-associated glycoprotein and CD22 define a new family of sialic acid-dependent adhesion molecules of the immunoglobulin superfamily. *Curr Biol* **4**(11): 965-72.

Kettenmann, H. (2007).Neuroscience: the brain's garbage men.*Nature* **446**(7139):987-9.

Kim, J. E., S. Li, T. GrandPre, D. Qiu and S. M. Strittmatter (2003). Axon regeneration in young adult mice lacking Nogo-A/B. *Neuron* **38**(2): 187-99.

Kim, J. E., B. P. Liu, J. H. Park and S. M. Strittmatter (2004). Nogo-66 receptor prevents raphespinal and rubrospinal axon regeneration and limits functional recovery from spinal cord injury. *Neuron* **44**(3): 439-51.

Kloss, C. U., M. Bohatschek, G. W. Kreutzberg and G. Raivich (2001). Effect of lipopolysaccharide on the morphology and integrin immunoreactivity of ramified microglia in the mouse brain and in cell culture. *Exp Neurol* **168**(1): 32-46.

Klugmann, M., M. H. Schwab, A. Puhlhofer, A. Schneider, F. Zimmermann, I. R. Griffiths and K. A. Nave (1997). Assembly of CNS myelin in the absence of proteolipid protein. *Neuron* **18**(1): 59-70.

Koprivica, V., K. S. Cho, J. B. Park, G. Yiu, J. Atwal, B. Gore, J. A. Kim, E. Lin, M. Tessier-Lavigne, D. F. Chen and Z. He (2005). EGFR activation mediates inhibition of axon regeneration by myelin and chondroitin sulfate proteoglycans. *Science* **310**(5745): 106-10.

Kramer, E. M., A. Schardt and K. A. Nave (2001). Membrane traffic in myelinating oligodendrocytes. *Microsc Res Tech* **52**(6): 656-71.

Kreutzberg, G. W. (1996). Microglia: a sensor for pathological events in the CNS. *Trends Neurosci* **19**(8): 312-8.

Kuhlmann, T., U. Wendling, C. Nolte, F. Zipp, B. Maruschak, C. Stadelmann, H. Siebert and W. Bruck (2002). Differential regulation of myelin phagocytosis by macrophages/microglia, involvement of target myelin, Fc receptors and activation by intravenous immunoglobulins. *J Neurosci Res* **67**(2): 185-90.

Lappe-Siefke, C., S. Goebbels, M. Gravel, E. Nicksch, J. Lee, P. E. Braun, I. R. Griffiths and K. A. Nave (2003). Disruption of Cnp1 uncouples oligodendroglial functions in axonal support and myelination. *Nat Genet* **33**(3): 366-74.

Larsen, P. H., T. H. Holm and T. Owens (2007). Toll-like receptors in brain development and homeostasis. *Sci STKE* **2007**(402): pe47.

Lassmann, H. (2008). Models of multiple sclerosis: new insights into pathophysiology and repair. *Curr Opin Neurol* **21**(3): 242-7.

Lauren, J., M. S. Airaksinen, M. Saarma and T. Timmusk (2003). Two novel mammalian Nogo receptor homologs differentially expressed in the central and peripheral nervous systems. *Mol Cell Neurosci* **24**(3): 581-94.

Lehmann, M., A. Fournier, I. Selles-Navarro, P. Dergham, A. Sebok, N. Leclerc, G. Tigyi and L. McKerracher (1999). Inactivation of Rho signaling pathway promotes CNS axon regeneration. *J Neurosci* **19**(17): 7537-47.

Li, C., M. B. Tropak, R. Gerlai, S. Clapoff, W. Abramow-Newerly, B. Trapp, A. Peterson and J. Roder (1994). Myelination in the absence of myelin-associated glycoprotein. *Nature* **369**(6483): 747-50.

Li, S. and S. M. Strittmatter (2003). Delayed systemic Nogo-66 receptor antagonist promotes recovery from spinal cord injury. *J Neurosci* **23**(10): 4219-27.

Li, S., B. P. Liu, S. Budel, M. Li, B. Ji, L. Walus, W. Li, A. Jirik, S. Rabacchi, E. Choi, D. Worley, D. W. Sah, B. Pepinsky, D. Lee, J. Relton and S. M. Strittmatter (2004). Blockade of Nogo-66, myelin-associated glycoprotein, and oligodendrocyte myelin glycoprotein by soluble Nogo-66 receptor promotes axonal sprouting and recovery after spinal injury. *J Neurosci* **24**(46): 10511-20.

Li, S., J. E. Kim, S. Budel, T. G. Hampton and S. M. Strittmatter (2005). Transgenic inhibition of Nogo-66 receptor function allows axonal sprouting and improved locomotion after spinal injury. *Mol Cell Neurosci* **29**(1): 26-39.

Li, W., L. Walus, S. A. Rabacchi, A. Jirik, E. Chang, J. Schauer, B. H. Zheng, N. J. Benedetti, B. P. Liu, E. Choi, D. Worley, L. Silvian, W. Mo, C. Mullen, W. Yang, S. M. Strittmatter, D. W. Sah, B. Pepinsky and D. H. Lee (2004). A neutralizing anti-Nogo66 receptor monoclonal antibody reverses inhibition of neurite outgrowth by central nervous system myelin. *J Biol Chem* **279**(42): 43780-8.

Liebscher, T., L. Schnell, D. Schnell, J. Scholl, R. Schneider, M. Gullo, K. Fouad, A. Mir, M. Rausch, D. Kindler, F. P. Hamers and M. E. Schwab (2005). Nogo-A antibody improves regeneration and locomotion of spinal cord-injured rats. *Ann Neurol* **58**(5): 706-19.

Liedtke, W., W. Edelmann, P. L. Bieri, F. C. Chiu, N. J. Cowan, R. Kucherlapati and C. S. Raine (1996). GFAP is necessary for the integrity of CNS white matter architecture and long-term maintenance of myelination. *Neuron* **17**(4): 607-15.

Liu, B. P., A. Fournier, T. GrandPre and S. M. Strittmatter (2002). Myelin-associated glycoprotein as a functional ligand for the Nogo-66 receptor. *Science* **297**(5584): 1190-3.

Liu, B. P., W. B. Cafferty, S. O. Budel and S. M. Strittmatter (2006). Extracellular regulators of axonal growth in the adult central nervous system. *Philos Trans R Soc Lond B Biol Sci* **361**(1473): 1593-610.

Loers, G., F. Aboul-Enein, U. Bartsch, H. Lassmann and M. Schachner (2004). Comparison of myelin, axon, lipid, and immunopathology in the central nervous system of differentially myelin-compromised mutant mice: a morphological and biochemical study. *Mol Cell Neurosci* **27**(2): 175-89.

Lowry, O. H., N. J. Rosebrough, A. L. Farr and R. J. Randall (1951). Protein measurement with the Folin phenol reagent. *J Biol Chem* **193**(1): 265-75.

McKerracher, L., S. David, D. L. Jackson, V. Kottis, R. J. Dunn and P. E. Braun (1994). Identification of myelin-associated glycoprotein as a major myelin-derived inhibitor of neurite growth. *Neuron* **13**(4): 805-11.

Mehta, N. R., P. H. Lopez, A. A. Vyas and R. L. Schnaar (2007). Gangliosides and Nogo receptors independently mediate myelin-associated glycoprotein inhibition of neurite outgrowth in different nerve cells. *J Biol Chem* **282**(38): 27875-86.

Mi, S., X. Lee, Z. Shao, G. Thill, B. Ji, J. Relton, M. Levesque, N. Allaire, S. Perrin, B.

Sands, T. Crowell, R. L. Cate, J. M. McCoy and R. B. Pepinsky (2004). LINGO-1 is a component of the Nogo-66 receptor/p75 signaling complex. *Nat Neurosci* **7**(3): 221-8.

Milward, E., K. J. Kim, A. Szklarczyk, T. Nguyen, G. Melli, M. Nayak, D. Deshpande, C. Fitzsimmons, A. Hoke, D. Kerr, J. W. Griffin, P. A. Calabresi and K. Conant (2008). Cleavage of myelin associated glycoprotein by matrix metalloproteinases. *J Neuroimmunol* **193**(1-2): 140-8.

Moller, J. R. (1996). Rapid conversion of myelin-associated glycoprotein to a soluble derivative in primates. *Brain Res* **741**(1-2): 27-31.

Moller, J. R., K. Yanagisawa, R. O. Brady, W. W. Tourtellotte and R. H. Quarles (1987). Myelin-associated glycoprotein in multiple sclerosis lesions: a quantitative and qualitative analysis. *Ann Neurol* **22**(4): 469-74.

Montag, D., K. P. Giese, U. Bartsch, R. Martini, Y. Lang, H. Bluthmann, J. Karthigasan, D. A. Kirschner, E. S. Wintergerst, K. A. Nave and et al. (1994). Mice deficient for the myelin-associated glycoprotein show subtle abnormalities in myelin. *Neuron* **13**(1): 229-46.

Morell, P. and A. H. Ousley (1994). Metabolic turnover of myelin glycerophospholipids. *Neurochem Res* **19**(8): 967-74.

Mukhopadhyay, G., P. Doherty, F. S. Walsh, P. R. Crocker and M. T. Filbin (1994). A novel role for myelin-associated glycoprotein as an inhibitor of axonal regeneration. *Neuron* **13**(3): 757-67.

Myer, D. J., G. G. Gurkoff, S. M. Lee, D. A. Hovda and M. V. Sofroniew (2006). Essential protective roles of reactive astrocytes in traumatic brain injury. *Brain* **129**(Pt 10): 2761-72.

Nair, A., T. J. Frederick and S. D. Miller (2008). Astrocytes in multiple sclerosis: a product of their environment. *Cell Mol Life Sci* **65**(17): 2702-20.

Nave, K. A. and B. D. Trapp (2008). Axon-glial signaling and the glial support of axon function. *Annu Rev Neurosci* **31**: 535-61.

Nedergaard, M., B. Ransom and S. A. Goldman (2003). New roles for astrocytes: redefining the functional architecture of the brain. *Trends Neurosci* **26**(10): 523-30.

Niederost, B., T. Oertle, J. Fritsche, R. A. McKinney and C. E. Bandtlow (2002). Nogo-A and myelin-associated glycoprotein mediate neurite growth inhibition by antagonistic regulation of RhoA and Rac1. *J Neurosci* **22**(23): 10368-76.

Nimmerjahn, A., F. Kirchhoff and F. Helmchen (2005). Resting microglial cells are highly dynamic surveillants of brain parenchyma in vivo. *Science* **308**(5726): 1314-8.

Nolte, C., M. Matyash, T. Pivneva, C. G. Schipke, C. Ohlemeyer, U. K. Hanisch, F. Kirchhoff and H. Kettenmann (2001). GFAP promoter-controlled EGFP-expressing transgenic mice: a tool to visualize astrocytes and astrogliosis in living brain tissue. *Glia* **33**(1): 72-86.

Oertle, T., M. E. van der Haar, C. E. Bandtlow, A. Robeva, P. Burfeind, A. Buss, A. B. Huber, M. Simonen, L. Schnell, C. Brosamle, K. Kaupmann, R. Vallon and M. E. Schwab (2003). Nogo-A inhibits neurite outgrowth and cell spreading with three discrete regions. *J Neurosci* **23**(13): 5393-406.

Park, J. B., G. Yiu, S. Kaneko, J. Wang, J. Chang, X. L. He, K. C. Garcia and Z. He (2005). A TNF receptor family member, TROY, is a coreceptor with Nogo receptor in mediating the inhibitory activity of myelin inhibitors. *Neuron* **45**(3): 345-51.

Perry, V. H. and S. Gordon (1988). Macrophages and microglia in the nervous system. *Trends Neurosci* **11**(6): 273-7.

Pignot, V., A. E. Hein, C. Barske, C. Wiessner, A. R. Walmsley, K. Kaupmann, H. Mayeur, B. Sommer, A. K. Mir and S. Frentzel (2003). Characterization of two novel proteins, NgRH1 and NgRH2, structurally and biochemically homologous to the Nogo-66 receptor. *J Neurochem* **85**(3): 717-28.

Pocock, J. M. and H. Kettenmann (2007). Neurotransmitter receptors on microglia. *Trends Neurosci* **30**(10): 527-35.

Poliak, S. and E. Peles (2003). The local differentiation of myelinated axons at nodes of Ranvier. *Nat Rev Neurosci* **4**(12): 968-80.

Ponomarev, E. D., L. P. Shriver, K. Maresz and B. N. Dittel (2005). Microglial cell activation and proliferation precedes the onset of CNS autoimmunity. *J Neurosci Res* **81**(3): 374-89.

Popovich, P. G. and E. E. Longbrake (2008). Can the immune system be harnessed to repair the CNS? *Nat Rev Neurosci* **9**(6): 481-93.

Prinjha, R., S. E. Moore, M. Vinson, S. Blake, R. Morrow, G. Christie, D. Michalovich, D. L. Simmons and F. S. Walsh (2000). Inhibitor of neurite outgrowth in humans. *Nature* **403**(6768): 383-4.

Qiu, J., D. Cai, H. Dai, M. McAtee, P. N. Hoffman, B. S. Bregman and M. T. Filbin (2002). Spinal axon regeneration induced by elevation of cyclic AMP. *Neuron* **34**(6): 895-903.

Quarles, R. H., J. L. Everly and R. O. Brady (1972). Demonstration of a glycoprotein which is associated with a purified myelin fraction from rat brain. *Biochem Biophys Res Commun* **47**(2): 491-7.

Quarles, R. H. (2007). Myelin-associated glycoprotein (MAG): past, present and beyond. *J Neurochem* **100**(6): 1431-48.

Quarles, R. H. (2008). A Hypothesis About the Relationship of Myelin-Associated Glycoprotein's Function in Myelinated Axons to its Capacity to Inhibit Neurite Outgrowth. *Neurochem Res*.

Raisman, G. (2004). Myelin inhibitors: does NO mean GO? *Nat Rev Neurosci* **5**(2): 157-61.

Raivich, G., M. Bohatschek, C. U. Kloss, A. Werner, L. L. Jones and G. W. Kreutzberg (1999). Neuroglial activation repertoire in the injured brain: graded response, molecular mechanisms and cues to physiological function. *Brain Res Brain Res Rev* **30**(1): 77-105.

Raivich, G. (2005). Like cops on the beat: the active role of resting microglia. *Trends Neurosci* **28**(11): 571-3.

Rock, R. B., G. Gekker, S. Hu, W. S. Sheng, M. Cheeran, J. R. Lokensgard and P. K. Peterson (2004). Role of microglia in central nervous system infections. *Clin Microbiol Rev* **17**(4): 942-64, table of contents.

Sato, S., R. H. Quarles and R. O. Brady (1982). Susceptibility of the myelin-associated glycoprotein and basic protein to a neutral protease in highly purified myelin from human and rat brain. *J Neurochem* **39**(1): 97-105.

Satoh, J., H. Onoue, K. Arima and T. Yamamura (2005). Nogo-A and nogo receptor expression in demyelinating lesions of multiple sclerosis. *J Neuropathol Exp Neurol* **64**(2): 129-38.

Satoh, J., H. Tabunoki, T. Yamamura, K. Arima and H. Konno (2007). TROY and LINGO-1 expression in astrocytes and macrophages/microglia in multiple sclerosis lesions. *Neuropathol Appl Neurobiol* **33**(1): 99-107.

Scarisbrick, I. A. (2008). The multiple sclerosis degradome: enzymatic cascades in development and progression of central nervous system inflammatory disease. *Curr Top Microbiol Immunol* **318**: 133-75.

Scherer, S. S. and E. J. Arroyo (2002). Recent progress on the molecular organization of myelinated axons. *J Peripher Nerv Syst* **7**(1): 1-12.

Schnell, L. and M. E. Schwab (1990). Axonal regeneration in the rat spinal cord produced by an antibody against myelin-associated neurite growth inhibitors. *Nature* **343**(6255): 269-72.

Schwab, M. E. and H. Thoenen (1985). Dissociated neurons regenerate into sciatic but not optic nerve explants in culture irrespective of neurotrophic factors. *J Neurosci* **5**(9): 2415-23.

Schwartz, M., O. Butovsky, W. Bruck and U. K. Hanisch (2006). Microglial phenotype: is the commitment reversible? *Trends Neurosci* **29**(2): 68-74.

Shao, Z., J. L. Browning, X. Lee, M. L. Scott, S. Shulga-Morskaya, N. Allaire, G. Thill, M. Levesque, D. Sah, J. M. McCoy, B. Murray, V. Jung, R. B. Pepinsky and S. Mi (2005). TAJ/TROY, an orphan TNF receptor family member, binds Nogo-66 receptor 1 and regulates axonal regeneration. *Neuron* **45**(3): 353-9.

Simonen, M., V. Pedersen, O. Weinmann, L. Schnell, A. Buss, B. Ledermann, F. Christ, G. Sansig, H. van der Putten and M. E. Schwab (2003). Systemic deletion of the myelin-associated outgrowth inhibitor Nogo-A improves regenerative and plastic responses after spinal cord injury. *Neuron* **38**(2): 201-11.

Sivasankaran, R., J. Pei, K. C. Wang, Y. P. Zhang, C. B. Shields, X. M. Xu and Z. He (2004). PKC mediates inhibitory effects of myelin and chondroitin sulfate proteoglycans on axonal regeneration. *Nat Neurosci* **7**(3): 261-8.

Song, H., G. Ming, Z. He, M. Lehmann, L. McKerracher, M. Tessier-Lavigne and M. Poo (1998). Conversion of neuronal growth cone responses from repulsion to attraction by cyclic nucleotides. *Science* **281**(5382): 1515-8.

Stebbins, J. W., H. Jaffe, H. M. Fales and J. R. Moller (1997). Determination of a native proteolytic site in myelin-associated glycoprotein. *Biochemistry* **36**(8): 2221-6.

Streit, W. J. (2001). Microglia and macrophages in the developing CNS. *Neurotoxicology* **22**(5): 619-24.

Streit, W. J. (2002). Microglia as neuroprotective, immunocompetent cells of the CNS. *Glia* **40**(2): 133-9.

Stromnes, I. M. and J. M. Goverman (2006). Active induction of experimental allergic encephalomyelitis. *Nat Protoc* **1**(4): 1810-9.

Tang, S., Y. J. Shen, M. E. DeBellard, G. Mukhopadhyay, J. L. Salzer, P. R. Crocker and M. T. Filbin (1997a). Myelin-associated glycoprotein interacts with neurons via a sialic acid binding site at ARG118 and a distinct neurite inhibition site. *J Cell Biol* **138**(6): 1355-66.

Tang, S., R. W. Woodhall, Y. J. Shen, M. E. deBellard, J. L. Saffell, P. Doherty, F. S. Walsh and M. T. Filbin (1997b). Soluble myelin-associated glycoprotein (MAG) found in vivo inhibits axonal regeneration. *Mol Cell Neurosci* **9**(5-6): 333-46.

Tang, S., J. Qiu, E. Nikulina and M. T. Filbin (2001). Soluble myelin-associated glycoprotein released from damaged white matter inhibits axonal regeneration. *Mol Cell Neurosci* **18**(3): 259-69.

Towbin, H., T. Staehelin and J. Gordon (1979). Electrophoretic transfer of proteins from polyacrylamide gels to nitrocellulose sheets: procedure and some applications. *Proc Natl Acad Sci U S A* **76**(9): 4350-4.

Trapp, B. D. and K. A. Nave (2008). Multiple sclerosis: an immune or neurodegenerative disorder? *Annu Rev Neurosci* **31**: 247-69.

Tropak, M. B., P. W. Johnson, R. J. Dunn and J. C. Roder (1988). Differential splicing of MAG transcripts during CNS and PNS development. *Brain Res* **464**(2): 143-55.

Ulvestad, E., K. Williams, R. Matre, H. Nyland, A. Olivier and J. Antel (1994). Fc receptors for IgG on cultured human microglia mediate cytotoxicity and phagocytosis of antibody-coated targets. *J Neuropathol Exp Neurol* **53**(1): 27-36.

Umemori, H., S. Sato, T. Yagi, S. Aizawa and T. Yamamoto (1994). Initial events of myelination involve Fyn tyrosine kinase signalling. *Nature* **367**(6463): 572-6.

Uschkureit, T., O. Sporkel, J. Stracke, H. Bussow and W. Stoffel (2000). Early onset of axonal degeneration in double (plp-/-mag-/-) and hypomyelinosis in triple (plp-/-mbp-/-mag-/-) mutant mice. *J Neurosci* **20**(14): 5225-33.

van Rossum, D. and U. K. Hanisch (2004). Microglia. *Metab Brain Dis* **19**(3-4): 393-411.

Vargas, M. E. and B. A. Barres (2007). Why is Wallerian degeneration in the CNS so slow? *Annu Rev Neurosci* **30**: 153-79.

Venkatesh, K., O. Chivatakarn, H. Lee, P. S. Joshi, D. B. Kantor, B. A. Newman, R. Mage, C. Rader and R. J. Giger (2005). The Nogo-66 receptor homolog NgR2 is a sialic acid-dependent receptor selective for myelin-associated glycoprotein. *J Neurosci* **25**(4): 808-22.

Venkatesh, K., O. Chivatakarn, S. S. Sheu and R. J. Giger (2007). Molecular dissection of the myelin-associated glycoprotein receptor complex reveals cell type-specific mechanisms for neurite outgrowth inhibition. *J Cell Biol* **177**(3): 393-9.

Vielmetter, J., B. Stolze, F. Bonhoeffer and C. A. Stuermer (1990). In vitro assay to test differential substrate affinities of growing axons and migratory cells. *Exp Brain Res* **81**(2): 283-7.

Vinson, M., P. J. Strijbos, A. Rowles, L. Facci, S. E. Moore, D. L. Simmons and F. S. Walsh (2001). Myelin-associated glycoprotein interacts with ganglioside GT1b. A mechanism for neurite outgrowth inhibition. *J Biol Chem* **276**(23): 20280-5.

Vyas, A. A., H. V. Patel, S. E. Fromholt, M. Heffer-Lauc, K. A. Vyas, J. Dang, M. Schachner and R. L. Schnaar (2002). Gangliosides are functional nerve cell ligands for myelin-associated glycoprotein (MAG), an inhibitor of nerve regeneration. *Proc Natl Acad Sci U S A* **99**(12): 8412-7.

Wang, K. C., V. Koprivica, J. A. Kim, R. Sivasankaran, Y. Guo, R. L. Neve and Z. He (2002). Oligodendrocyte-myelin glycoprotein is a Nogo receptor ligand that inhibits neurite outgrowth. *Nature* **417**(6892): 941-4.

Wang, X., S. J. Chun, H. Treloar, T. Vartanian, C. A. Greer and S. M. Strittmatter (2002). Localization of Nogo-A and Nogo-66 receptor proteins at sites of axon-

myelin and synaptic contact. *J Neurosci* **22**(13): 5505-15.

Williams, A., G. Piaton and C. Lubetzki (2007). Astrocytes--friends or foes in multiple sclerosis? *Glia* **55**(13): 1300-12.

Wilms, H., D. Hartmann and J. Sievers (1997). Ramification of microglia, monocytes and macrophages in vitro: influences of various epithelial and mesenchymal cells and their conditioned media. *Cell Tissue Res* **287**(3): 447-58.

Winter, S. M., J. Hirrlinger, F. Kirchhoff and S. Hulsmann (2007). Transgenic expression of fluorescent proteins in respiratory neurons. *Respir Physiol Neurobiol* **159**(1): 108-14.

Wong, S. T., J. R. Henley, K. C. Kanning, K. H. Huang, M. Bothwell and M. M. Poo (2002). A p75(NTR) and Nogo receptor complex mediates repulsive signaling by myelin-associated glycoprotein. *Nat Neurosci* **5**(12): 1302-8.

Xie, F. and B. Zheng (2008). White matter inhibitors in CNS axon regeneration failure. *Exp Neurol* **209**(2): 302-12.

Yanagisawa, K., R. H. Quarles, D. Johnson, R. O. Brady and J. N. Whitaker (1985). A derivative of myelin-associated glycoprotein in cerebrospinal fluid of normal subjects and patients with neurological disease. *Ann Neurol* **18**(4): 464-9.

Yang, L. J., C. B. Zeller, N. L. Shaper, M. Kiso, A. Hasegawa, R. E. Shapiro and R. L. Schnaar (1996). Gangliosides are neuronal ligands for myelin-associated glycoprotein. *Proc Natl Acad Sci U S A* **93**(2): 814-8.

Yim, S. H. and R. H. Quarles (1992). Biosynthesis and expression of the myelin-associated glycoprotein in cultured oligodendrocytes from adult bovine brain. *J Neurosci Res* **33**(3): 370-8.

Yin, X., T. O. Crawford, J. W. Griffin, P. Tu, V. M. Lee, C. Li, J. Roder and B. D. Trapp (1998). Myelin-associated glycoprotein is a myelin signal that modulates the caliber of myelinated axons. *J Neurosci* **18**(6): 1953-62.

Yin, X., R. C. Baek, D. A. Kirschner, A. Peterson, Y. Fujii, K. A. Nave, W. B. Macklin and B. D. Trapp (2006). Evolution of a neuroprotective function of central nervous system myelin. *J Cell Biol* **172**(3): 469-78.

Yiu, G. and Z. He (2006). Glial inhibition of CNS axon regeneration. *Nat Rev Neurosci* **7**(8): 617-27.

Yong, V. W. (2005). Metalloproteinases: mediators of pathology and regeneration in the CNS. *Nat Rev Neurosci* **6**(12): 931-44.

Yong, V. W., R. K. Zabad, S. Agrawal, A. Goncalves Dasilva and L. M. Metz (2007). Elevation of matrix metalloproteinases (MMPs) in multiple sclerosis and impact of immunomodulators. *J Neurol Sci* **259**(1-2): 79-84.

Zheng, B., C. Ho, S. Li, H. Keirstead, O. Steward and M. Tessier-Lavigne (2003). Lack of enhanced spinal regeneration in Nogo-deficient mice. *Neuron* **38**(2): 213-24.

Zheng, B., J. Atwal, C. Ho, L. Case, X. L. He, K. C. Garcia, O. Steward and M. Tessier-Lavigne (2005). Genetic deletion of the Nogo receptor does not reduce neurite inhibition in vitro or promote corticospinal tract regeneration in vivo. *Proc Natl Acad Sci U S A* **102**(4): 1205-10.

Zurn, A. D. and C. E. Bandtlow (2006). Regeneration failure in the CNs: cellular and molecular mechanisms. *Adv Exp Med Biol* **557**: 54-76.

8. Curriculum vitae

Foteini Orfaniotou

Date of Birth: 29.07.78
Address: Hermann-Rein-Strasse 3, 37075, Goettingen, Germany
Telephone: +49 551 3899739 (work), +49 551 4886323 (home)
Nationality: Greek
E-mail: orfaniotou@em.mpg.de

EDUCATION

2005-current	**Max Planck Institute of Experimental Medicine, Goettingen** PhD, Dept. Neurogenetics Thesis: 'Interaction of myelin-associated proteins with glial cells'
2003-2005	**International Max Planck Research School (IMPRS) in Molecular Biology, Max-Planck Institute of Exp.Medicine, Goettingen, Germany** Selected from 500 applicants worldwide Master's in Molecular Biology, Grade: Very good (B) Thesis: 'Subcellular sorting of proteolipids: M6B as a cargo of the AP-1 complex'
1998-2003	**National and Kapodistrian University of Athens, Greece** Diploma in Biology, Grade: Very good (7.35/10) Thesis: 'Cloning, over-expression, purification and biophysical analysis of the DNA binding protein HU from the archaebacterium *T. volcanium.*'
1997-1998	**National and Kapodistrian University of Athens, Greece** Training in the Faculty of Primary education
1995-1996	**2nd Secondary school of Alimos, Athens, Greece** Subjects: physics, mathematics, biology and modern Greek Apolitirio Grade (A level equivalent): Excellent (19/20)

EXPERIENCE

Research

06/2005-current	**Graduate Researcher** Analyzed the interaction of myelin-associated proteins with microglia and astrocytes, their downstream signalling cascades and their role in neurodegenerative diseases, using *in vitro* and *in vivo* approaches. Proficiency attained in histology of mouse brain and spinal cord, primary glial cultures and cell lines, Fluorescent Activating Cell Sorting, ELISA, protein purification, western blotting, RNA isolation, cDNA synthesis, qPCR, transfection, immunostaining, confocal and electron microscopy.
11/2004-5/2005	**Research Assistant** Developed solid foundation in recombinant DNA technologies, mammalian cell culture, site-directed mutagenesis

immunostaining, immunoprecipitation, western blotting, electron and fluorescent microscopy.

01/2004-7/2004   **Lab rotation Research Assistant**
Gained experience in handling mammalian cell cultures, Biacore, western blotting, subcellular fractionation, screening of a λ phage cDNA expression library, immunoblotting.

4/2003-8/2003   **Research Assistant**
Analyzed protein expression in blood of ALS, Alzheimer and control patients.

7/2001-7/2002   **Undergraduate Researcher**
Extensive knowledge in recombinant DNA technologies, bacterial cultures and protein purification.

<u>**Teaching and Presentation**</u>

3/2006-5/2006   **Research Mentor**
Mentored an undergraduate student's study project; managed program and guided studies to successful completion.

1/2004-current   **Seminar Spokesperson**
Delivered presentations to large audiences at International and European meetings, the annual Max Planck of Experimental Medicine graduate retreat, the annual graduate retreat of the International Max Planck Research School in Molecular Biology and the department of Neurogenetics at the Max Planck of Experimental Medicine.

FELLOWSHIPS AND AWARDS

2004-2005   Graduate fellowship, Max Planck of Experimental Medicine, Goettingen
2003-2004   Graduate fellowship, IMPRS in Molecular Biology, Goettingen, Germany.
1991-1996   Annual distinction award for exceptional academic performance, 2nd Secondary school of Alimos, Athens, Greece

LANGUAGES

Greek (fluent), English (fluent, Michigan Certificate of Proficiency), German and French (basic).

COMPUTER SKILLS

Word, Excel, Outlook, PowerPoint, Photoshop, Illustrator, Image J, GraphPad Prism.

PERSONAL SKILLS

Strong communication skills developed through collaborations with Prof. U.K. Hanisch, University Hospital of Goettingen and Prof. S. Kelm, University of Bremen. Ability to work both independently and in a team (successful completion of individual and group projects).

HOBBIES AND INTERESTS

Travelling and exploring different cultures, playing and attending basketball games, gym, reading (primarily twentieth century fiction, books on travel).

PUBLICATIONS

Orfaniotou F, Nadrigny F, Regen T, Werner H.B, Kassmann C.M, Steffens H, Kelm S, Kirchhoff F, Hanisch U-K, Griffiths I.R, Nave K-A. Myelin-associated glycoprotein modulates the roaming behaviour of microglial cells (in preparation)

Orfaniotou F, Tzamalis P, Thanassoulas A, Stefanidi E, Zees A, Boutou E, Vlassi M, Nounesis G, Viorgias CE. (2008) The stability of the archaeal HU histone-like DNA-binding protein from Thermoplasma volcanium. *Extremophiles* (in press)

Poulopoulou C, Davaki P, Sgouropoulos P, Tsaltas E, Nikolaou C, **Orfaniotou F**, Vassilopoulos D (2008)Reduced RAGE mRNA in mononuclear blood cells of patients with probable Alzheimer's disease. *Neurology*; 70(17)

Werner HB, Kuhlmann K, Shen S, Uecker M, Schardt A, Dimova K, **Orfaniotou F**, Dhaunchak A, Brinkmann BG, Möbius W, Guarente L, Casaccia-Bonnefil P, Jahn O, Nave KA(2007). Proteolipid protein is required for transport of sirtuin 2 into CNS myelin. *J Neurosci.*; 27(29)

Denikus N, **Orfaniotou F**, Wulf G, Lehmann PF, Monod M, Reichard U (2005). Fungal antigens expressed during invasive aspergillosis. *Infect Immun.*; 73(8)

ORAL PRESENTATIONS

Foteini Orfaniotou. Myelin-Associated Glycoprotein (MAG) as an inhibitor of microglial process outgrowth. *Cold Spring Harbor Laboratory (CSHL), Glia in Health and Disease, NY, USA* (2008).

Foteini Orfaniotou. Myelin-Associated Glycoprotein (MAG) as an inhibitor of microglial process outgrowth. *European Conference of Neuropathology, Athens, Greece* (2008).

Foteini Orfaniotou. Myelin-associated glycoprotein (MAG) as inhibitor of microglial cells. *Annual PhD seminar of IMPRS* (2007).

Foteini Orfaniotou. Interaction of glial cells with myelin-associated proteins. *Annual PhD seminar of IMPRS* (2006).

Foteini Orfaniotou. Interaction of glial cells with myelin-associated proteins. *Annual PhD retreat of Max Planck of Experimental Medicine* (2005).

MEETING ABSTRACTS

Foteini Orfaniotou, Nadrigny F, Kassmann C, Werner H, Nave K-A. Myelin-Associated Glycoprotein (MAG) as an inhibitor of microglial process outgrowth. *European Conference of Neuropathology, Athens, Greece* (2008)